

Abstract

This report is about construction and testing of the gravity boom for the Norwegian CubeSat NCube. It describes the design and testing phase of the boom and on its way explores vacuum labs, freezing cold tunnels and even the absurdities of a zero-g environment. It concludes that a boom of 1.5 meters made of measuring tape is rigid enough to deploy in space.

Contents

1	Introduction	1
1.1	About CubeSat	1
1.2	About NCube	2
2	Mathematical background	6
2.1	Notation	6
2.2	Coordinate frames	6
2.3	Vector transformations	7
2.4	Rotating reference frames	13
3	Mathematical modelling	15
3.1	Dynamic attitude model for the satellite	15
3.2	Magnetic field	16
3.3	Moment of inertia	17
3.4	Gravitational torque	18
3.5	Gravitational stabilization	20
4	Moment of inertia calculations	24
4.1	Geometric shapes	24
4.2	Modelling and calculation	26
4.3	Results	28
5	Design	29
5.1	Boom/Antennas	30
5.2	Boxes	33
5.3	Complete nadir side	33
6	Testing	35
6.1	Rigidness/Deployment	36
6.2	Vacuum chamber	38
6.3	Cold tunnel	41
6.4	Parabolic flight	41

7	Vibrations	80
7.1	Analysis of resonance frequencies	80
7.1.1	Constrained modes	81
7.1.2	Unconstrained modes	83
8	Conclusion	87
A	Matlab code	88
B	Application for parabolic campaign	100
B.1	Title of the experiment and Team name	100
B.2	Experiment objectives	100
B.3	Experiment description	100
B.4	Technical description of the experiment set-up	101
B.5	Installation of the experiment in the aircraft	102
B.6	Electrical	103
B.7	Mechanical resistance of the experiment	104
B.8	In flight procedures and In flight personnel	105
B.9	Hazard analysis	106
B.10	Pressure vessel certification (if applicable)	107
B.11	Vent line connection and other requests	107
B.12	Outreach section	107
B.13	Figures/Pictures	107
	Bibliography	114

Chapter 1

Introduction

1.1 About CubeSat

The CubeSat project was initiated in 1999 as a collaboration between California Polytechnic State University and Stanford University's Space Systems Development Laboratory. The objective for the project is to provide a standard for the design of picosatellites in order to reduce cost and development time for the satellites. The idea is that this will lead to increased accessibility to space and more frequent launches. It is too early to pass judgment over the last statement due to the short time aspect, but it seems clear that their cost/time reductive objective has been accomplished.

To make the launch compatible with the reduced-cost-policy several satellites will be launched at once using a designated p-pod. This will put the launch of a single CubeSat in the 25000-35000 U.S. dollars range. The CubeSats (and p-pod) specifications and requirements are stated in full in the official CubeSat homepage (<http://cubesat.calpoly.edu/index.html>) and the most important is listed below:

- Mass: $< 1kg$
- Dimension: $10cm \times 10cm \times 10cm$
- Center of mass located within 2cm the geometrical center
- Designated space materials approved by NASA must be used
- The CubeSat must be designed NOT to jam when ejected from the p-pod
- All parts must be connected to the CubeSat during launch, ejection and operation in order to reduce space junk (the CubeSat will be space junk itself in approximately 3 months (or less)).
- The CubeSat must be turned off during launch

- There must be a time delay between release from the p-pod and deployables/communication (in the order of minutes for deployables and minutes-one hour for communication) to provide separation from the other satellites
- The frequency used for communication must be within the radio amateur frequency band.

The CubeSat must also complete several tests to be included in the launch. These tests include a vibration and shock absorption test of 125% of launch-loads (can be performed by the developer (tests of NCube will be performed at Andøya rocket range)) and test in the p-pod with the rest of the CubeSats which are to be launched (thermal-vacuum test and vibration-shock-test (100% of launch load)). These tests are performed by Cal Poly)

1.2 About NCube

The Norwegian student satellite (NCube) is a project involving students from NTNU, NLH, HiST and UiO co-operating with Andøya Rocket Range, NAROM and the Norwegian space centre. The project also has several industrial partners (Kongsberg, Telenor, FFI and Nammo Raufoss).

The aim of the project is to:

- Design, build, integrate, test and launch a small satellite
- Simulate interest in science among Norwegian students
- Simulate interest in space technology
- Increase co-operation between industry and educational institutions
- Increase co-operation between educational institutions
- Launch the first Norwegian satellite

No date has been set for the launch of NCube but it will be no earlier than summer 2004.

The parts of the satellite which will be discussed in this report are mainly the ADCS and the Antenna-Boom system.

Payload

The payload in NCube will be an AIS (Automatic Identification System) receiver/transmitter. The AIS is a maritime surveillance system and will help increase the safety of ships.

The system will be mandatory for ships above 300 bruttotons, and the ships will transmit their position, course, speed and information about the ship. The interval this information is transmitted is dependent on the speed (and the tonnage) of the ship.

In the NCube project AIS transmitters will be placed on reindeer (around their neck) to monitor their activity (no reindeer will be harmed during this experiment), and test the AIS receivers. The satellite will also pick up transmissions from ships equipped with the transmitter. The information will be relayed back to the ground segment. For more information about the AIS see Furebotten (2002).

ADCS

The ADCS (Attitude Determination and Control System) groups members are:

- Kjell Magne Fauske
- Fredrik Mietle Indergaard
- Kristian Svartveit

Its goal is to stabilize the satellite attitude within 20 b_0 about nadir in order to make efficient use of the payload and the small attitude dependent antenna. To achieve this goal the satellite must be detumbled and stabilized. The ADCS most important tasks are

- Detumble the satellite
- Deploy boom
- Estimate attitude, angular velocity and position
- Stabilize the satellite

When the satellite is released from the p-pod it will most likely have a significant and certainly unknown angular velocity. This makes accurate control of the satellite difficult, and deployment of the boom at this point is not an option. To lose the unwanted spin, the satellite has to be detumbled. The detumbling control law is presented below (Fauske 2002) and the torque is supplied by the magnetic coils

$$\mathbf{m}^b = -k\dot{\mathbf{B}}^b - \mathbf{m}_c \quad (1.1)$$

This control law is crude and based solely on the derivative of the measured local magnetic field. It is important to state that no estimation of the state vector is used in this law.

When the satellite has been sufficiently detumbled (the changes in the local magnetic field is sufficiently low) the boom can be deployed. The deployment of the boom

will change the distribution of the satellites moment of inertia to keep the satellite stabilized. The boom will be deployed by a telecommand from the ground. If the boom is to be released the wrong way the ADCS contains a mode called invert-boom-mode who can solve this issue (for stability considerations whether the boom points towards or from the earth does not matter, but for the communication and payload (and thus in all aspects the satellite) systems it is a major problem.

When the boom is deployed the stabilization control law below can be invoked.

$$\mathbf{m}^b = h\boldsymbol{\omega}_{ob}^b \times \mathbf{B}^b \quad (1.2)$$

This law is used for accurate pointing desired by the payload. This control law is based on the angular velocity of the satellite and the local magnetic field. The magnetic field is measured by the magnetometers (Svartveit 2003) and the angular velocity is estimated by a Kalman filter (the Kalman-filter uses measurements from the magnetometer and solar panels together with a magnetic field model to estimate attitude, angular velocity and position (Svartveit 2003)).

The stabilization control law can achieve sufficient pointing accuracy without the boom, but not for longer periods of time (due to power restrictions). When stabilization control is turned off the satellite would start to tumble again if it were not passively stabilized by the boom, so the boom is indeed critical for the operation of the satellite. For simulations of the booms influence on the attitude see Indergaard (2002).

Antenna-Gravity boom system

The Antenna-Gravity boom groups members are:

- Fredrik Mietle Indergaard
- Jan Otterstad

Its goal is to design and mechanically construct the nadir-side of the satellite. This is the side where the boom, antennas and batteries (internally) is located. The Antenna-Gravity boom systems most important tasks are to:

- Stabilize the satellite passively
- Telecommunication with the ground segment
- Receive AIS from Reindeer

The satellite is going to receive at 145 and 162 MHz and going to transmit at 435 MHz and 2279.5 MHz. The VHF and UHF frequencies will be received by monopole (omnidirectional) antennas. The Uplink RX, 145 MHz, is the frequency where the satellite receives commands from the ground segment and the UHF TX, 435 MHz, is the frequency with which the satellite transmits down to the ground segment. These to

antennas have to be operational as soon as the satellite is in orbit so communication can start.

The 162 MHz, AIS (Automatic Identification System) frequency, is the frequency where the satellite is going to receive data from ships and reindeers. This antenna does not have to be operational before proper communication with the ground segment is established.

Chapter 2

Mathematical background

2.1 Notation

In this text we will use the following notations:

Points/positions

$\mathbf{V}^{frame} = \begin{bmatrix} x_{frame} \\ y_{frame} \\ z_{frame} \end{bmatrix}$, hence $\mathbf{p}^e = \begin{bmatrix} x_e \\ y_e \\ z_e \end{bmatrix}$ is the position in the earth frame, $\mathbf{p}^b = \begin{bmatrix} x_b \\ y_b \\ z_b \end{bmatrix}$ is the position in the body frame.

Linear/angular velocities

$\mathbf{v}_{point}^{frame}$, hence \mathbf{v}_p^b is the linear velocity of point P decomposed in the b frame
 $\omega_{respect-to/frame}^{decomposed-in}$, hence ω_{eb}^o is the angular velocity of the b frame with respect to the e frame decomposed in the o frame.

Rotation matrices

\mathbf{R}_{from}^{to} , hence \mathbf{R}_b^o represent a rotation from the body to the orbit frame.

Rotations about one axis will be denoted $\mathbf{R}_{\lambda,\beta}$ where λ is the axis of rotation and β is an angle.

2.2 Coordinate frames

Inertial frame

An inertial frame is a frame in which Newton's laws of motion apply. This means that an inertial frame may have linear motion, but can not be accelerating. In an expanding

universe there are few true inertial frames since the galaxies are accelerating according to Hubbles law $v = H * d$, where H is a constant and d is the distance between the galaxies (Bergström et al 1999). Thus the only true inertial frame is the center of the universe, assuming there is only one universe. If more than one universe exists, well that's beyond the scope of this text.

For many engineering and discussion purposes, it's convenient to define an inertial frame that at any given time is coincident with the earth's center of mass. The x-axis point towards the vernal equinox, the z-axis parallel to the earth's spin-axis, and the y-axis completes the right-handed orthogonal coordinate system. In the following sections, this is defined to be an inertial coordinate frame.

Earth-centered earth-fixed frame

The Earth-centered earth-fixed (ECEF) coordinate system has its origin fixed to the center of the earth, its x-axis through the intersection of the prime meridian and the equator, its z-axis parallel to the earth spin axis, and the y-axis completes the right-handed orthogonal coordinate system. The ECEF has a spin with frequency $\omega_{ie} \approx 7.22115 * 10^{-5} rad/s$ relative to the inertial system (about its z-axis) due to the daily rotation of the earth, and its yearly revolution about the sun.

Orbit frame

The orbit frame coordinate system has its origin in the satellites center of mass, its x-axis parallel to the satellites velocity vector, its z-axis directed towards the center of the earth, and the y-axis completes the right-handed orthogonal coordinate system. The orbit system spins with a frequency $\omega_{eo} = 1.083 * 10^{-3} rad/s$ (assuming circular orbit) relative to the ECEF system (about its y-axis) due to the periodic revolution about the earth.

Body frame

The body frame coordinate system has its origin in the satellites center of mass and its axes locked in the satellite. Hence x-axis forward, z-axis downwards, and y-axis completes the right-handed orthogonal system. Choosing the center of mass as its origin will simplify the kinematic equations, as we will see later. In attitude control, the main objective will be to actuate the body frame to coincide with the orbit frame, in other words; to point the bottom of the satellite towards the earth.

2.3 Vector transformations

When several coordinate frames is used, we must have a way to transform vectors and points between the different orthogonal coordinate systems. This section will present

point transformations, vector transformations, Euler angle transformations and Euler Parameters (Quaternions).

In the context of attitude determination the most interesting system is the body-system in respect to the orbit-system, that is to determine the satellites orientation in respect to the earth.

Points

Given two right-handed orthogonal coordinate systems, ϕ_1 and ϕ_2 , a point P, relative to their origins, is represented by two sets of coordinates $(x_1, y_1, z_1)_{\phi_1}$ and $(x_2, y_2, z_2)_{\phi_2}$. The coordinates can be interpreted as the projection of the vectors \mathbf{V}_1 and \mathbf{V}_2 , from the coordinate systems origin to the point P, onto the coordinate systems axes:

$$\mathbf{V}_1 = x_1\mathbf{I}_1 + y_1\mathbf{J}_1 + z_1\mathbf{K}_1 \quad (2.1)$$

$$x_1 = (P - O_1) \cdot \mathbf{I}_1 \quad (2.2)$$

$$y_1 = (P - O_1) \cdot \mathbf{J}_1 \quad (2.3)$$

$$z_1 = (P - O_1) \cdot \mathbf{K}_1 \quad (2.4)$$

$$\mathbf{V}_2 = x_2\mathbf{I}_2 + y_2\mathbf{J}_2 + z_2\mathbf{K}_2 \quad (2.5)$$

$$x_2 = (P - O_2) \cdot \mathbf{I}_2 \quad (2.6)$$

$$y_2 = (P - O_2) \cdot \mathbf{J}_2 \quad (2.7)$$

$$z_2 = (P - O_2) \cdot \mathbf{K}_2 \quad (2.8)$$

where $\mathbf{I}_1, \mathbf{J}_1,$ and \mathbf{K}_1 are unit vectors along the ϕ_1 axes, $\mathbf{I}_2, \mathbf{J}_2,$ and \mathbf{K}_2 are unit vectors along the ϕ_2 axes, and \mathbf{O}_{12} is the vector from the origin of ϕ_1 to the origin of ϕ_2 .

The transformation of point coordinates from ϕ_1 to ϕ_2 will require two operations; translation and rotation. In ϕ_1 , P will be the vector sum of \mathbf{O}_{12} and \mathbf{V}_2 relative to ϕ_1 ; $\mathbf{V}_1 = \mathbf{O}_{12} + \mathbf{V}_2$.

$$\begin{bmatrix} x_P \\ y_P \\ z_P \end{bmatrix} = \begin{bmatrix} x_O \\ y_O \\ z_O \end{bmatrix} + [\mathbf{V}_2]_{\phi_1} \quad (2.9)$$

The problem is to calculate $[\mathbf{V}_2]_{\phi_1}$ when $[\mathbf{V}_2]_{\phi_2}$ and the relative orientation of the two coordinate systems are known. The way to accomplish this is to project the $[\mathbf{V}_2]_{\phi_2}$ vector onto the ϕ_1 axis:

$$[\mathbf{V}_2]_{\phi_1} = \begin{bmatrix} \mathbf{I}_1^T \\ \mathbf{J}_1^T \\ \mathbf{K}_1^T \end{bmatrix} (\mathbf{I}_2 x_2 + \mathbf{J}_2 y_2 + \mathbf{K}_2 z_2) = \begin{bmatrix} \mathbf{I}_1 \cdot \mathbf{I}_2 \\ \mathbf{J}_1 \cdot \mathbf{I}_2 \\ \mathbf{K}_1 \cdot \mathbf{I}_2 \end{bmatrix} x_2 + \begin{bmatrix} \mathbf{I}_1 \cdot \mathbf{J}_2 \\ \mathbf{J}_1 \cdot \mathbf{J}_2 \\ \mathbf{K}_1 \cdot \mathbf{J}_2 \end{bmatrix} y_2 + \begin{bmatrix} \mathbf{I}_1 \cdot \mathbf{K}_2 \\ \mathbf{J}_1 \cdot \mathbf{K}_2 \\ \mathbf{K}_1 \cdot \mathbf{K}_2 \end{bmatrix} z_2$$

We define

$$\mathbf{R} = \begin{bmatrix} \mathbf{I}_2 \cdot \mathbf{I}_1 & \mathbf{J}_2 \cdot \mathbf{I}_1 & \mathbf{K}_2 \cdot \mathbf{I}_1 \\ \mathbf{I}_2 \cdot \mathbf{J}_1 & \mathbf{J}_2 \cdot \mathbf{J}_1 & \mathbf{K}_2 \cdot \mathbf{J}_1 \\ \mathbf{I}_2 \cdot \mathbf{K}_1 & \mathbf{J}_2 \cdot \mathbf{K}_1 & \mathbf{K}_2 \cdot \mathbf{K}_1 \end{bmatrix} = \begin{bmatrix} \cos(\alpha_1) & \cos(\beta_1) & \cos(\gamma_1) \\ \cos(\alpha_2) & \cos(\beta_2) & \cos(\gamma_2) \\ \cos(\alpha_3) & \cos(\beta_3) & \cos(\gamma_3) \end{bmatrix} \quad (2.10)$$

Where $\alpha_n, \beta_n, \gamma_n, n = 1..3$ is the angles between the coordinate axis of ϕ_1 and ϕ_2 .
Hence

$$\begin{bmatrix} x_P \\ y_P \\ z_P \end{bmatrix}_{\phi_1} = \begin{bmatrix} x_O \\ y_O \\ z_O \end{bmatrix}_{\phi_1} + \mathbf{R}[\mathbf{V}_2]_{\phi_2} \quad (2.11)$$

and the reverse transformation is

$$\begin{bmatrix} x_2 \\ y_2 \\ z_2 \end{bmatrix}_{\phi_2} = \mathbf{R}^T \left(\begin{bmatrix} x_P \\ y_P \\ z_P \end{bmatrix}_{\phi_1} - \begin{bmatrix} x_O \\ y_O \\ z_O \end{bmatrix}_{\phi_1} \right) \quad (2.12)$$

Vectors

Consider a vector \mathbf{v} defined by the line segment from the points P_1 to P_2 . Relative to the coordinate system ϕ_1 we have

$$\begin{aligned} \mathbf{v}_{\phi_1} &= \begin{bmatrix} x_2 - x_1 \\ y_2 - y_1 \\ z_2 - z_1 \end{bmatrix}_{\phi_1} = \begin{bmatrix} x_2 \\ y_2 \\ z_2 \end{bmatrix}_{\phi_1} - \begin{bmatrix} x_1 \\ y_1 \\ z_1 \end{bmatrix}_{\phi_1} \\ &= \left(\begin{bmatrix} x_O \\ y_O \\ z_O \end{bmatrix}_{\phi_1} + \mathbf{R} \begin{bmatrix} x_2 \\ y_2 \\ z_2 \end{bmatrix}_{\phi_2} \right) - \left(\begin{bmatrix} x_O \\ y_O \\ z_O \end{bmatrix}_{\phi_1} + \mathbf{R} \begin{bmatrix} x_1 \\ y_1 \\ z_1 \end{bmatrix}_{\phi_2} \right) \\ &= \mathbf{R} \left(\begin{bmatrix} x_2 \\ y_2 \\ z_2 \end{bmatrix}_{\phi_2} - \begin{bmatrix} x_1 \\ y_1 \\ z_1 \end{bmatrix}_{\phi_2} \right) = \mathbf{R}\mathbf{v}_{\phi_2} \end{aligned} \quad (2.13)$$

Euler angels

Although Eq.(2.10) has nine angles, there are only three degrees of freedom, because of the three orthogonality constraints and the three normality constraints;

$$\mathbf{x}^T \mathbf{y} = 0 \quad (2.14)$$

$$\mathbf{y}^T \mathbf{z} = 0 \quad (2.15)$$

$$\mathbf{z}^T \mathbf{x} = 0 \quad (2.16)$$

$$\mathbf{x}^T \mathbf{x} = 1 \quad (2.17)$$

$$\mathbf{y}^T \mathbf{y} = 1 \quad (2.18)$$

$$\mathbf{z}^T \mathbf{z} = 1 \quad (2.19)$$

A more efficient parameterization is the Euler angles. The motivation for the Euler angle is to transform points and vectors between the orbit coordinate system and the body coordinate system. The two coordinate systems have the same origin so the transformations can be calculated if we have a rotation-matrix, \mathbf{R}_b^o , between the two coordinate systems. The rotation-matrix is defined by three plane rotations First, the orbit plane is rotated by ψ radians about the z-axis to algin the new x' -axis to the projection of the body system x-axis into the orbit plane. Second, the new orbit system is rotated by θ radians about the y' axis to algin the new x'' axis to the body systems x-axis. Third, the new orbit plane is rotated be ϕ radians about the x'' -axis to align the y'' and the z'' -axis the the body planes y and z -axis. Thus the \mathbf{R}_b^o is defined by the three rotations; roll, pitch, and yaw (ϕ, θ, ψ), the Euler angles.

$$\mathbf{R}_b^o = \mathbf{R}_{z,\psi} \mathbf{R}_{y,\theta} \mathbf{R}_{x,\phi} \quad (2.20)$$

$$\mathbf{R}_o^b = \mathbf{R}_{x,\phi}^T \mathbf{R}_{y,\theta}^T \mathbf{R}_{z,\psi}^T \quad (2.21)$$

$$\mathbf{R}_{x,\phi} = \begin{bmatrix} 1 & 0 & 0 \\ 0 & \cos(\phi) & -\sin(\phi) \\ 0 & \sin(\phi) & \cos(\phi) \end{bmatrix} \quad (2.22)$$

$$\mathbf{R}_{y,\theta} = \begin{bmatrix} \cos(\theta) & 0 & \sin(\theta) \\ 0 & 1 & 0 \\ -\sin(\theta) & 0 & \cos(\theta) \end{bmatrix} \quad (2.23)$$

$$\mathbf{R}_{z,\psi} = \begin{bmatrix} \cos(\psi) & -\sin(\psi) & 0 \\ \sin(\psi) & \cos(\psi) & 0 \\ 0 & 0 & 1 \end{bmatrix} \quad (2.24)$$

We will write $\sin(\psi)$ as $s(\psi)$ and $\cos(\psi)$ as $c(\psi)$ in order to save space

$$\begin{aligned} \mathbf{R}_b^o &= \begin{bmatrix} c(\psi)c(\theta) & -s(\psi)c(\phi) + c(\psi)s(\theta)s(\phi) & s(\psi)s(\phi) + c(\psi)s(\theta)c(\phi) \\ s(\psi)c(\theta) & c(\psi)c(\phi) + s(\psi)s(\theta)s(\phi) & -c(\psi)s(\phi) + s(\psi)s(\theta)c(\phi) \\ -s(\theta) & c(\theta)s(\phi) & c(\theta)c(\phi) \end{bmatrix} \\ &= \begin{bmatrix} R_{11} & R_{12} & R_{13} \\ R_{21} & R_{22} & R_{23} \\ R_{31} & R_{23} & R_{33} \end{bmatrix} \end{aligned} \quad (2.25)$$

Then, according to Eq.(2.13), $\mathbf{v}^o = \mathbf{R}_b^o \mathbf{v}^b$ and $\mathbf{v}^b = (\mathbf{R}_b^o)^T \mathbf{v}^o = \mathbf{R}_o^b \mathbf{v}^o$.

For small rotations the rotation matrix can be linearized. It is easy to see that when ϕ , θ and ψ are small,

$$\mathbf{R}_b^o \approx \begin{bmatrix} 1 & -\delta\psi & \delta\theta \\ \delta\psi & 1 & -\delta\phi \\ -\delta\theta & \delta\phi & 1 \end{bmatrix} = \mathbf{I} + \mathbf{S}(\delta\Theta) \quad (2.26)$$

To sum things up, the rotation matrix has three equivalent geometrical meanings (Sciavicco et al 1999):

- It describes the orientation between two coordinate frames
- It represents a coordinate transformation between the coordinates of a point expressed in two frames with the same origin
- It is a operator that rotates a vector in a coordinate frame

There is, however a problem with the Euler-angles representation. It is easy to see from 2.29 that singularity points exists for pitch angles $\theta = \pm(\frac{\pi}{2})$. The representation will break down if these angles occur since θ don't exist. This is not a problem when the representation is used on marine vessels but it is a problem when we are working with a satellite because these angles are likely to occur (during de-tumbling the satellite has an uncontrolled spin).

There are several ways to avoid this problem. We could construct a different representation (by defining the sequence of the simple rotations differently) with different singularity angles and toggle between these representations when they approach their singularity points, or we can use a singularity-free representation (quaternions).

Quaternions

To avoid the singularity of the Euler angles we will use a representation of unit quaternions, \mathbf{q} . This is a four-parameter complex number with one real part η and three imaginary parts $\boldsymbol{\varepsilon} = [\varepsilon_1 \ \varepsilon_2 \ \varepsilon_3]^T$. The unit quaternion has the constraint $\mathbf{q}^T \mathbf{q} = \varepsilon_1^2 + \varepsilon_2^2 + \varepsilon_3^2 + \eta^2 = 1$ and has hence three degrees of freedom, like the Euler angles representation. The Euler quaternions can be expressed in the form:

$$\mathbf{q} = \begin{bmatrix} \eta \\ \varepsilon_1 \\ \varepsilon_2 \\ \varepsilon_3 \end{bmatrix} = \begin{bmatrix} \cos(\frac{\beta}{2}) \\ \boldsymbol{\lambda} \sin(\frac{\beta}{2}) \end{bmatrix} \quad (2.27)$$

where β is the rotation angle and $\boldsymbol{\lambda}$ is a unit vector. The rotation matrix from orbit to body, \mathbf{R}_o^b is according to (Fossen 2002) .

$$\mathbf{R}_o^b = \begin{bmatrix} 1 - 2(\varepsilon_2^2 + \varepsilon_3^2) & 2(\varepsilon_1\varepsilon_2 - \varepsilon_3\eta) & 2(\varepsilon_1\varepsilon_3 + \varepsilon_2\eta) \\ 2(\varepsilon_1\varepsilon_2 + \varepsilon_3\eta) & 1 - 2(\varepsilon_1^2 + \varepsilon_3^2) & 2(\varepsilon_2\varepsilon_3 - \varepsilon_1\eta) \\ 2(\varepsilon_1\varepsilon_3 - \varepsilon_2\eta) & 2(\varepsilon_2\varepsilon_3 + \varepsilon_1\eta) & 1 - 2(\varepsilon_1^2 + \varepsilon_2^2) \end{bmatrix} \quad (2.28)$$

Quaternions from Euler angles

An algorithms to compute Euler parameters from Euler angles (Shepperd 1978) is presented below.

1. When the Euler angles are given the transformation matrix based on these angles is written:

$$\mathbf{R}_b^o = \begin{bmatrix} R_{11} & R_{12} & R_{13} \\ R_{21} & R_{22} & R_{23} \\ R_{31} & R_{23} & R_{33} \end{bmatrix}$$

2. The trace of \mathbf{R}_b^o is computed according to:

$$R_{44} = tr(\mathbf{R}_b^o) = R_{11} + R_{22} + R_{33}$$

3. Let $1 \leq i \leq 4$ be the index corresponding to:

$$R_{ii} = \max(R_{11}, R_{22}, R_{33}, R_{44})$$

4. Compute p_i corresponding to index i of Step 3 according to:

$$p_i = \left| \sqrt{1 + 2R_{ii} - R_{44}} \right|$$

where the sign ascribed to p_1 can be chosen either plus or minus

5. Compute the other three p-values from:

$$\begin{aligned} p_4 p_1 &= R_{32} - R_{23} \\ p_4 p_2 &= R_{13} - R_{31} \\ p_4 p_3 &= R_{21} - R_{12} \\ p_2 p_3 &= R_{32} + R_{23} \\ p_3 p_1 &= R_{13} + R_{31} \\ p_1 p_2 &= R_{21} + R_{12} \end{aligned}$$

by simply dividing the three equations containing the component p_i with the known value of p_i (from step 4) on both sides

6. Compute the Euler parameters for $j=1\dots3$, $\mathbf{q} = [\eta, \varepsilon_1, \varepsilon_2, \varepsilon_3]^T$ according to:

$$\varepsilon_j = \frac{p_j}{2}$$

$$\eta = \frac{p_4}{2}$$

Euler angles from Quaternions

To determine the Euler angles from Euler parameters eq (2.25) is used. The inverse problem is solved (finding ϕ, θ, ψ from R_{ii}).

$$\phi = \arctan 2(R_{32}, R_{33}) \quad (2.29)$$

$$\theta = -\arcsin(R_{31}) = -\arctan\left(\frac{R_{31}}{\sqrt{1 - R_{31}^2}}\right) \quad (2.30)$$

$$\psi = \arctan 2(R_{21}, R_{11}) \quad (2.31)$$

Where $\arctan 2(x, y)$ is the four quadrant $\arctan(x, y)$ of the real parts of x and y . When implemented in computers tis algorithm should include a singularity test for R_{31} .

2.4 Rotating reference frames

When the reference systems are in relative angular motion to each other it is necessary to calculate the derivative of the rotation matrices. This is easily seen by

$$\mathbf{p}^b = \mathbf{p}_a^b + \mathbf{R}_a^b \mathbf{p}^a \quad (2.32)$$

where \mathbf{p}_a^b is the vector from the a-frame origin to the b-frame origin and \mathbf{p}^a denotes the vector from the a-frame origin to the point. The rate of change then is:

$$\frac{d\mathbf{p}^b}{dt} = \frac{d\mathbf{p}_a^b}{dt} + \left(\frac{d\mathbf{R}_a^b}{dt}\right) \mathbf{p}^a + \mathbf{R}_a^b \frac{d\mathbf{p}^a}{dt} \quad (2.33)$$

The derivative between the coordinate systems is defined by

$$\begin{aligned} \dot{\mathbf{R}}_a^b(t) &= \lim_{\delta t \rightarrow 0} \frac{\mathbf{R}_a^b(t + \delta t) - \mathbf{R}_a^b(t)}{\delta t} = \frac{\mathbf{R}_a^b(\mathbf{I} + \mathbf{S}(\delta\Theta)) - \mathbf{R}_a^b(t)}{\delta t} \\ &= \mathbf{R}_a^b(t) \mathbf{S}(\delta\Theta) = \mathbf{R}_a^b \mathbf{S}(\boldsymbol{\omega}_{ba}^a) \end{aligned} \quad (2.34)$$

Then from 2.32 and ??

$$\frac{d\mathbf{p}^b}{dt} = \frac{d\mathbf{p}_a^b}{dt} + \mathbf{R}_a^b \mathbf{S}(\boldsymbol{\omega}_{ba}^a) \mathbf{p}^a + \mathbf{R}_a^b \mathbf{v}^a = \frac{d\mathbf{p}_a^b}{dt} + \mathbf{R}_a^b (\mathbf{S}(\boldsymbol{\omega}_{ba}^a) \mathbf{p}^a + \mathbf{v}^a) \quad (2.35)$$

and

$$\begin{aligned}
\frac{d^2 \mathbf{P}^b}{dt^2} &= \frac{d^2 \mathbf{P}_a^b}{dt^2} + \left(\frac{d\mathbf{R}_a^b}{dt} \right) (\mathbf{S}(\boldsymbol{\omega}_{ba}^a) \mathbf{P}^a + \mathbf{v}^a) + \\
&\quad \mathbf{R}_a^b \left(\mathbf{S}(\boldsymbol{\omega}_{ba}^a) \mathbf{v}^a + \mathbf{S}(\dot{\boldsymbol{\omega}}_{ba}^a) \mathbf{P}^a + \frac{d^2 \mathbf{P}^a}{dt^2} \right) \\
&= \frac{d^2 \mathbf{P}_a^b}{dt^2} + \mathbf{R}_a^b \left((2\mathbf{S}(\boldsymbol{\omega}_{ba}^a) \mathbf{v}^a) + (\mathbf{S}(\boldsymbol{\omega}_{ba}^a) (\mathbf{S}(\boldsymbol{\omega}_{ba}^a) \mathbf{P}^a + \mathbf{S}(\dot{\boldsymbol{\omega}}_{ba}^a) \mathbf{P}^a + \mathbf{a}^a) \right) \quad (2.36)
\end{aligned}$$

Chapter 3

Mathematical modelling

3.1 Dynamic attitude model for the satellite

In the dynamic attitude model for the satellite we will ignore the torques created by the following disturbances

- Air-resistance
- Solar wind
- Variations in the gravity field due to the earths unsymmetrical mass distribution
- Magnetic torque created in the satellite from other sources than the magnetic coils
- Thermal flexibility in the boom
- Collations with small particles and space-junk

Then, according to (Soglo 1994) the equation for the satellite rotational motion, assuming that the satellite is a rigid body, can be written as

$$\mathbf{I}\dot{\boldsymbol{\omega}}_{ib}^b + \boldsymbol{\omega}_{ib}^b \times (\mathbf{I}\boldsymbol{\omega}_{ib}^b) = \boldsymbol{\tau}^b \quad (3.1)$$

where, according to our notation, $\boldsymbol{\omega}_{ib}^b$ is the angular velocity of the body-system relative to the inertial system decomposed in the body system, \mathbf{I} is the moment of inertia, and $\boldsymbol{\tau}^b$ is the total torque acting on the satellite (when we ignore the conditions above). The only torques influencing the satellite then is gravitational torque and magnetic torque from the coils, thus

$$\boldsymbol{\tau}^b = \mathbf{g}_c^b + \boldsymbol{\tau}_m^b \quad (3.2)$$

Then, according to (Soglo 1994) we get the dynamic equations, including the quaternions

$$\dot{\boldsymbol{\omega}}_{ib}^b = \mathbf{I}^{-1}[-\boldsymbol{\omega}_{ib}^b \times \mathbf{I}\boldsymbol{\omega}_{ib}^b + \mathbf{g}_c^b + \boldsymbol{\tau}_m^b] \quad (3.3)$$

$$\dot{\eta} = -\frac{1}{2}\boldsymbol{\epsilon}^T \boldsymbol{\omega}_{ib}^b \quad (3.4)$$

$$\dot{\boldsymbol{\epsilon}} = \frac{1}{2}[\eta \mathbf{1} + \mathbf{S}(\boldsymbol{\epsilon})]\boldsymbol{\omega}_{ib}^b \quad (3.5)$$

3.2 Magnetic field

The Earth's geomagnetic field is produced by fluid motions in the metallic outer core and the Earth's rotation. The geomagnetic field can be visualized by imagining a simple dipole-field but a dipole-model is not accurate and should only be used for its simplicity (which works fine when the purpose is to construct an image in the mind) to save instructions in a micro-controller. The dipole-fields axis is inclined 12° to the Earth's rotation axis and paleomagnetic investigations have shown that the field reverses it's direction in a random way with an average period of about 10^4 to 10^5 years (Zeilik 1998). We will use the geomagnetic field has several important uses. First, and most important, it acts as a shield, protecting the earth from solar wind. It is therefore, among many factors, responsible for the appearance of the earth's life-forms (Goldsmith 2000). Second, it helps us control our satellite. The strength of the field can be measured by a magnetometer and used in the satellites controllers, and by using magnetic coils to apply a torque to the satellite, the geomagnetic field is also used to active control the satellites attitude (active because the torque depends on the current in the coils).

The geomagnetic field model used in our simulations is the IGRF (International Geomagnetic Reference Field) model created by the IAGA (International Association of Geomagnetism and Aeronomy). The IGRF is a series of mathematical models describing the Earth's main field and its secular variation. Each model comprises a set of spherical harmonic coefficients, in a truncated series expansion of a geomagnetic potential function of internal origin.

$$V = a \sum_{n=1}^N \sum_{m=0}^n \left(\frac{a}{r}\right)^{n+1} (g_n^m \cos(m\phi) + h_n^m \sin(m\phi)) P_n^m(\cos(\theta)) \quad (3.6)$$

where a is the mean radius of the Earth (6371.2 km) and r , ϕ and θ are the geocentric spherical coordinates. When converting from geodetic to geocentric system, the use of the IAU ellipsoid (International Astronomical Union, 1966) is recommended (equatorial radius of 6378.16km and flattening 1/298.25). The $P_n^m(\cos(\theta))$ are Schmidt quasi-normalized associated Legendre functions of degree n and order m . The maximum spherical harmonic degree of the expansion is N

The model produce a set of coefficients to represent the main field at a particular epoch. This model is revised every fifth year, and we will use the 1995 model (IGRF1995) in our simulations.

3.3 Moment of inertia

The moment of inertia of a body with density $\mu(\mathbf{r})$ with respect to any given axis is defined by the volume integral

$$\mathbf{I} = \int_V \mu(\mathbf{r}) r^2 dV \quad (3.7)$$

where r is the perpendicular distance from the axis of rotation. For a discrete mass distribution where r is the distance to a point and δ_{jk} is the Kronecker delta;

$$I_{jk} = \int_V \mu(\mathbf{r})(r^2 \delta_{jk} - x_j x_k) dV \quad (3.8)$$

This can be written in matrix form in terms of Cartesian axes as

$$\mathbf{I} = \int_V \mu(x, y, z) \begin{bmatrix} y^2 + z^2 & -xy & -xz \\ -xy & x^2 + z^2 & -yz \\ -xz & -yz & x^2 + y^2 \end{bmatrix} dx dy dz \quad (3.9)$$

When the principal axis coincide with the body axis

$$\mathbf{I} = \int_v \mu(x, y, z) \begin{bmatrix} y^2 + z^2 & 0 & 0 \\ 0 & x^2 + z^2 & 0 \\ 0 & 0 & x^2 + y^2 \end{bmatrix} dx dy dz \quad (3.10)$$

Parallel axis theorem

Let the vector \mathbf{r}_i describe the position of point mass in a rigid body consisting of a number of such masses. Then we can write

$$\mathbf{r}_i = \mathbf{R} + \mathbf{r}'_i \quad (3.11)$$

where \mathbf{R} is the center of mass. Then the moment of inertia, I_a about an axis $\hat{\mathbf{n}}$ is given by

$$I_a = \hat{\mathbf{n}} \cdot \mathbf{I} \cdot \hat{\mathbf{n}} = m_i [r_i^2 - (\mathbf{r}_i \cdot \hat{\mathbf{n}})^2] \quad (3.12)$$

$$= m_i (\mathbf{r}_i \times \hat{\mathbf{n}}) \cdot (\mathbf{r}_i \times \hat{\mathbf{n}}) = m_i [\mathbf{r}'_i + \mathbf{R}] \times \hat{\mathbf{n}}]^2 \quad (3.13)$$

$$= M(\mathbf{R} \times \hat{\mathbf{n}})^2 + m_i (\mathbf{r}'_i \times \hat{\mathbf{n}})^2 + 2m_i (\mathbf{R} \times \hat{\mathbf{n}}) \cdot (\mathbf{r}'_i \times \hat{\mathbf{n}}) \quad (3.14)$$

$$= M(\mathbf{R} \times \hat{\mathbf{n}})^2 + m_i (\mathbf{r}'_i \times \hat{\mathbf{n}})^2 - 2m_i (\mathbf{R} \times \hat{\mathbf{n}}) \cdot (\hat{\mathbf{n}} \times m_i \mathbf{r}'_i) \quad (3.15)$$

$$= M(\mathbf{R} \times \hat{\mathbf{n}})^2 + m_i (\mathbf{r}'_i \times \hat{\mathbf{n}})^2 - 2m_i (\mathbf{R} \times \hat{\mathbf{n}}) \cdot (\hat{\mathbf{n}} \times \mathbf{R}) \quad (3.16)$$

$$= M(\mathbf{R} \times \hat{\mathbf{n}})^2 + m_i (\mathbf{r}'_i \times \hat{\mathbf{n}})^2 \quad (3.17)$$

Then, letting $I_b = m_i(\mathbf{r}'_i \times \hat{\mathbf{n}})^2$ be the moment of inertia about the \mathbf{r}'_i -axis, I_a can be expressed as

$$I_a = I_b + M(\mathbf{R} \times \hat{\mathbf{n}})^2 = I_b + M(\mathbf{R} \times \hat{\mathbf{n}}) \cdot (\mathbf{R} \times \hat{\mathbf{n}}) = I_b + MR^2 \quad (3.18)$$

In other words, The moment of inertia of an object can be calculated by first calculating the moment of inertia about the objects centre of mass and then add MR^2 where R is the distance between the parallel axis of rotation. This theorem will be used extensively in the calculation of NCubes moment of inertia in section 5.2

3.4 Gravitational torque

A satellite in orbit is influenced by earths gravity. In fact the satellite is, at least in theory, influenced by the gravitational field of every stellar object in the universe. Due to the nature of the gravitational force (inverse square) most of the these objects contributes close to nothing and it is convenient to omit them from further analysis. The only objects which contributes enough to be of interest is the sun and the moon, but since there is no closed form solutions to the three body problem at the present time (Goldstein 2002) it is convenient to leave them out as well.

Other convenient simplifications is:

- The earth has a symmetrical mass distribution
- The spacecraft is small compared to the distance form the earths centre of mass
- The spacecraft consists of a single body

From (Hughes 1986) we have:

$$\mathbf{F} = -MG \int_b \frac{\mathbf{R}}{R^3} dm \quad (3.19)$$

and

$$\mathbf{g}_c = -MG \int_b \frac{\mathbf{r} \times \mathbf{R}}{R^3} dm \quad (3.20)$$

Where M is the mass of the earth, G is the universal gravitational constant, $R = R_c + r$, where R_c is the distance from the centre of the earth to the centre of the spacecraft and r is the distance from the centre of the spacecraft to dm . The gravitational torque is in the orbit frame

Using a binomial expansion $\left(\frac{r}{R_c} \ll 1\right)$ we get

$$R^{-3} = R_c^{-3} \left(1 - \frac{3(\mathbf{r} \cdot \mathbf{R}_c)}{R_c^2} \right) + \text{hot} \quad (3.21)$$

Thus

$$\mathbf{F} = -MG \int_b (\mathbf{R}_c + \mathbf{r}) (R_c^{-3} \left(1 - \frac{3(\mathbf{r} \cdot \mathbf{R}_c)}{R_c^2} \right)) dm = -\frac{GMm}{R_c^3} \mathbf{R}_c \quad (3.22)$$

since $\int_b \mathbf{r} dm = 0$

For the gravitational torque we get

$$\begin{aligned} \mathbf{g}_c &= -MG \int_b \frac{\mathbf{r} \times (\mathbf{r} + \mathbf{R}_c)}{R^3} dm = \\ &= MGR_c \times \int_b \frac{\mathbf{r}}{R^3} dm - MG \int_b \frac{\mathbf{r} \times \mathbf{r}}{R^3} dm \\ &= MGR_c \times \int_b \frac{\mathbf{r}}{R^3} dm \end{aligned} \quad (3.23)$$

Since $\mathbf{r} \times \mathbf{r} = \mathbf{0}$

Using 3.21 the gravitational torque then is:

$$\begin{aligned} \mathbf{g}_c &= MGR_c \times \int_b \mathbf{r} \left(R_c^{-3} \left(1 - \frac{3(\mathbf{r} \cdot \mathbf{R}_c)}{R_c^2} \right) \right) dm \\ &= MGR_c \times \int_b \frac{\mathbf{r}}{R_c^3} dm - \frac{3\mathbf{r}\mathbf{r}}{R_c^5} dm \cdot \mathbf{R}_c \\ &= -\frac{3MG}{R_c^5} \mathbf{R}_c \times \int_b \mathbf{r}\mathbf{r} dm \cdot \mathbf{R}_c \end{aligned} \quad (3.24)$$

again using $\int_b \mathbf{r} dm = 0$

Writing the gravitational torque in terms of the moment of inertia tensor, $\mathbf{I}_o = \int_b (r^2 \mathbf{1} - \mathbf{r}\mathbf{r}) dm$, $\mu = MG$, and $\hat{\mathbf{r}} = -\frac{\mathbf{R}_c}{R}$ we get

$$\mathbf{g}_c = 3 \frac{\mu}{R_c^3} \hat{\mathbf{r}} \times \mathbf{I}_o \cdot \hat{\mathbf{r}} \quad (3.25)$$

which in body coordinates is written as

$$\mathbf{g}_c = 3 \frac{\mu}{R_c^3} \mathbf{c}_3^\times \mathbf{I} \mathbf{c}_3 \quad (3.26)$$

In scalar:

$$g_1 = 3 \frac{\mu}{R_c^3} [(I_{33} - I_{22})c_{23}c_{33} + I_{23}(c_{23}^2 - c_{33}^2) + I_{31}c_{13}c_{23} - I_{12}c_{33}c_{13}] \quad (3.27)$$

$$g_2 = 3 \frac{\mu}{R_c^3} [(I_{11} - I_{33})c_{33}c_{13} + I_{31}(c_{33}^2 - c_{13}^2) + I_{12}c_{23}c_{33} - I_{23}c_{13}c_{23}] \quad (3.28)$$

$$g_3 = 3 \frac{\mu}{R_c^3} [(I_{22} - I_{11})c_{13}c_{23} + I_{12}(c_{13}^2 - c_{23}^2) + I_{23}c_{33}c_{13} - I_{31}c_{23}c_{33}] \quad (3.29)$$

When the principal axis coincides with the body axis the moment of inertia tensor

$$I = \begin{bmatrix} I_{11} & 0 & 0 \\ 0 & I_{22} & 0 \\ 0 & 0 & I_{33} \end{bmatrix} = \begin{bmatrix} I_x & 0 & 0 \\ 0 & I_y & 0 \\ 0 & 0 & I_z \end{bmatrix} \quad (3.30)$$

and the scalar expressions simplifies to

$$\begin{aligned} g_1 &= 3 \frac{\mu}{R_c^3} (I_{33} - I_{22})c_{23}c_{33} \\ g_2 &= 3 \frac{\mu}{R_c^3} (I_{11} - I_{33})c_{33}c_{13} \\ g_3 &= 3 \frac{\mu}{R_c^3} (I_{22} - I_{11})c_{13}c_{23} \end{aligned} \quad (3.31)$$

The moment of inertia matrix for the NCUBE satellite will be calculated in chapter 4 and appendix A.

3.5 Gravitational stabilization

The motivation for using a gravity boom on the NCube satellite is to take advantage of the gravitational torque to achieve passive control of the satellites (which will relive the active control system, the magnetic coils, in order to save power). When a gravitational boom is used, the satellite moment of inertia is manipulated to suit our goals. To know in what way we shall manipulate the MoI we have to analyze the influence on the satellites attitude (and orbit).

It is easy to see from (2.25) that the directional cosines in (3.31) becomes:

$$c_{13} = -\sin(\theta) \quad (3.32)$$

$$c_{23} = \cos(\theta) \sin(\phi) \quad (3.33)$$

$$c_{33} = \cos(\theta) \cos(\phi) \quad (3.34)$$

Then eq (3.31) gives:

$$\begin{aligned}
g_1 &= 3\frac{\mu}{R_c^3}(I_{33} - I_{22})\sin(\theta)\cos(\theta)\cos^2(\phi) \\
g_2 &= 3\frac{\mu}{R_c^3}(I_{33} - I_{11})\cos(\theta)\sin(\phi)\cos(\phi) \\
g_3 &= 3\frac{\mu}{R_c^3}(I_{11} - I_{22})\sin(\theta)\sin(\phi)\cos(\phi)
\end{aligned} \tag{3.35}$$

From these equations we can see that the gravity torque is independent on yaw. To see how moment of inertia influences the Euler angles we linearize (3.35) which gives for small angles:

$$g_1 = 3\frac{\mu}{R_c^3}(I_{33} - I_{22})\theta \tag{3.36}$$

$$g_2 = 3\frac{\mu}{R_c^3}(I_{33} - I_{11})\phi \tag{3.37}$$

$$g_3 = 0 \tag{3.38}$$

This clearly states that if the roll angle deviates from zero and $I_{11} > I_{33}$ the gravitational torque will act as a stabilizing torque about the roll-axis. The same holds for the pitch angle if $I_{22} > I_{33}$. This analysis is static and will only hold for a satellite standing still. When the satellite orbits the earth clearly the z-axis of the orbit-coordinate will change direction so that the Euler angles will change, and the gravitational torque may/may not influence enough to achieve sufficient accuracy. For more in depth answers a dynamic analysis is necessary.

Stability of Equilibria

Using eq (3.1) where the term for magnetic torque and removing the term due to the magnetic coils gives:

$$\mathbf{I}\dot{\boldsymbol{\omega}}_{ib}^b + \boldsymbol{\omega}_{ib}^b \times (\mathbf{I}\boldsymbol{\omega}_{ib}^b) = \mathbf{g}_c^b \tag{3.39}$$

On component form, using (3.31) and $\boldsymbol{\omega}_c = \left(\frac{\mu}{R_c^3}\right)^{1/2}$ this becomes

$$\begin{aligned}
I_1\dot{\omega}_{ib1}^b &= (I_2 - I_3)(\omega_{ib2}^b\omega_{ib3}^b - 3\boldsymbol{\omega}_c^2 c_{23}c_{33}) \\
I_2\dot{\omega}_{ib2}^b &= (I_3 - I_1)(\omega_{ib3}^b\omega_{ib1}^b - 3\boldsymbol{\omega}_c^2 c_{33}c_{13}) \\
I_3\dot{\omega}_{ib3}^b &= (I_1 - I_2)(\omega_{ib1}^b\omega_{ib2}^b - 3\boldsymbol{\omega}_c^2 c_{13}c_{23})
\end{aligned} \tag{3.40}$$

Obviously:

$$\boldsymbol{\omega}_{ib}^b = \boldsymbol{\omega}_{io}^b + \boldsymbol{\omega}_{ob}^b = \mathbf{R}_o^b \boldsymbol{\omega}_{io}^o + \boldsymbol{\omega}_{ob}^b \quad (3.41)$$

and

$$\dot{\mathbf{R}}_b^o = \mathbf{R}_b^o \mathbf{S}(\boldsymbol{\omega}_{bo}^o) \quad (3.42)$$

Since $\boldsymbol{\omega}_{io}^o = [0 \quad -\omega_c \quad 0]$ we can write (3.41) and (3.42) as:

$$\boldsymbol{\omega}_{ib}^b = \boldsymbol{\omega}_{ob}^b - \omega_c \mathbf{c}_2 \quad (3.43)$$

$$\dot{\mathbf{c}}_1 = -\boldsymbol{\omega}_{ib}^b \times \mathbf{c}_1 + \omega_c \mathbf{c}_3$$

$$\dot{\mathbf{c}}_2 = -\boldsymbol{\omega}_{ib}^b \times \mathbf{c}_2$$

$$\dot{\mathbf{c}}_3 = -\boldsymbol{\omega}_{ib}^b \times \mathbf{c}_3 - \omega_c \mathbf{c}_1 \quad (3.44)$$

The desired solution (for earth pointing satellites) is the gravitational torques influence on the Euler angles: $\boldsymbol{\omega}_{ob}^b$, that is how the satellite rotates in respect to the orbit coordinates. In order to solve this problem, we have to integrate ((3.40) and at least two equations of (3.44). Unfortunately there are no closed form solution of this differential equation set, so approximate solutions have to be found. Linearization around a working point (in Euler angles) gives:

$$\boldsymbol{\omega}_{ob}^b = \dot{\boldsymbol{\alpha}} \quad (3.45)$$

$$\mathbf{R}_o^b = \mathbf{I} + \mathbf{S}(\boldsymbol{\alpha}) \quad (3.46)$$

Inserting this linearization in (3.40), (3.44) and (3.43) gives, according to Hughes (1986)

$$\begin{aligned} I_1 \ddot{\theta} - (I_3 + I_1 - I_2) \omega_c \dot{\psi} + (I_2 - I_3) \omega_c^2 \theta &= 3\omega_c^2 (I_3 - I_2) \theta \\ I_2 \ddot{\phi} &= 3\omega_c^2 (I_3 - I_1) \phi \\ I_3 \ddot{\psi} + (I_3 + I_1 - I_2) \omega_c \dot{\theta} + (I_2 - I_1) \omega_c^2 \psi &= 0 \end{aligned} \quad (3.47)$$

We see from these equations that pitch is decoupled from roll and yaw. We can also recognize the right side as the contribution from the gravitational torque. The left hand side is the dynamical behavior of the Euler angles.

It is easy to see that $I_1 > I_3$ is a sufficient condition for stability in pitch. For roll/yaw stabilization we decouple the pitch from (3.47) and write the equation as:

$$\mathbf{M} \ddot{\boldsymbol{\alpha}} + \mathbf{D} \dot{\boldsymbol{\alpha}} + \mathbf{G} \boldsymbol{\alpha} = \mathbf{0} \quad (3.48)$$

where

$$\alpha = \begin{bmatrix} \theta \\ \psi \end{bmatrix} \quad (3.49)$$

$$\mathbf{M} = \text{diag}(I_1, I_3) \quad (3.50)$$

$$\mathbf{D} = (I_3 + I_1 - I_2)\omega_c \begin{bmatrix} 0 & -1 \\ 1 & 0 \end{bmatrix} \quad (3.51)$$

$$\mathbf{G} = \omega_c^2 \begin{bmatrix} 4(I_2 - I_3) & 0 \\ 0 & (I_2 - I_1) \end{bmatrix} \quad (3.52)$$

This implies that $\mathbf{G} > 0$, that positive definite, is a sufficient conditions for roll/yaw stability. It is easy to a that \mathbf{G} is positive definite for $I_2 > I_3$ and $I_2 > I_3$. Combining these conditions for roll/yaw stability with the condition for pitch stability, we get: $I_2 > I_1 > I_3$. This means that we can make control the satellite passively (I know it's a contradiction) by manipulate the moment of inertia to satisfy the condition above. This result is based on a linearization of equations (3.43) and (3.44). It can, however, be extended to the non-linear case by applying Lyapunov-theory (see Hughes (1986)).

Chapter 4

Moment of inertia calculations

When the origin of the body coordinate system coincides with the center of mass, the moment of inertia matrix becomes:

$$\mathbf{I} = \begin{bmatrix} I_x & 0 & 0 \\ 0 & I_y & 0 \\ 0 & 0 & I_z \end{bmatrix} = \begin{bmatrix} \int_b y^2 dm + \int_b z^2 dm & 0 & 0 \\ 0 & \int_b x^2 dm + \int_b z^2 dm & 0 \\ 0 & 0 & \int_b x^2 dm + \int_b y^2 dm \end{bmatrix} \quad (4.1)$$

To calculate the moment of inertia matrix of the satellite, we will divide the satellite into several parts. This parts will be cylinders, hoops, rods, cubes, and rectangles. To make the calculations more readable we will first review the calculation of moment of inertia for these shapes.

4.1 Geometric shapes

Cylinder

Moment of inertia about z-axis is calculated in cylindrical coordinates:

$$I_z = \int_b r^2 dm = \int_0^R r^2 (2\pi r \mu h) dr = 2\pi \mu h \int_0^R r^3 dr = \frac{1}{2} \pi \mu h R^4 = \frac{1}{2} MR^2 \quad (4.2)$$

Since the cylinder is symmetrical about its z-axis; $\int_b x^2 dm = \int_b y^2 dm$, and since $I_z = \int_b x^2 dm + \int_b y^2 dm$

$$\int_b x^2 dm = \int_b y^2 dm = \frac{1}{4} MR^2 \quad (4.3)$$

calculating $\int_b z^2 dm$ yields;

$$\begin{aligned}\int_b z^2 dm &= \int_{-\frac{1}{2}h}^{\frac{1}{2}h} z^2 dm = \int_{-\frac{1}{2}h}^{\frac{1}{2}h} z^2 \pi r^2 \mu dz = \frac{1}{3} \pi r^2 \mu \left[\left(\frac{1}{2}h\right)^3 - \left(-\frac{1}{2}h\right)^3 \right] = \\ \frac{1}{12} \pi r^2 \mu h^3 &= \frac{1}{12} M h^2\end{aligned}\quad (4.4)$$

This gives:

$$\begin{aligned}I_x &= \frac{1}{12} M h^2 + \frac{1}{4} M R^2 \\ I_y &= \frac{1}{12} M h^2 + \frac{1}{4} M R^2 \\ I_z &= \frac{1}{2} M R^2\end{aligned}\quad (4.5)$$

Hoop

For a hoop we use R_2 and R_1 as limits for the integrals (4.2) and (4.4). This gives

$$I_x = I_y = \frac{1}{12} \pi h \mu (R_2^2 - R_1^2) (h^2 + 3R_1^2 + R_2^2) \quad (4.6)$$

$$I_z = \frac{1}{2} \pi h \mu (R_2^4 - R_1^4) \quad (4.7)$$

Using $M = \pi h \mu (R_2^2 - R_1^2)$ and $(R_2^4 - R_1^4) = (R_2^2 + R_1^2)(R_2^2 - R_1^2)$ we get

$$\begin{aligned}I_x &= I_y = \frac{1}{12} M (h^2 + 3R_2^2 + 3R_1^2) \\ I_z &= \frac{1}{2} M (R_2^2 + R_1^2)\end{aligned}\quad (4.8)$$

Rods and Cubes

Most of the components of the satellite will be modelled as rods and cubes, or a combination of several rods. The moment of inertia of a rod, about the axis perpendicular to centre of mass is:

$$\int_b z^2 dm = \int_{-\frac{1}{2}h}^{\frac{1}{2}h} z^2 dm = \frac{1}{3} \mu A \left[\left(\frac{1}{2}h\right)^3 - \left(-\frac{1}{2}h\right)^3 \right] = \frac{1}{12} M h^2 \quad (4.9)$$

which gives

$$I_x = I_y = \frac{1}{12}Mh^2 \quad (4.10)$$

$$I_z = 0 \quad (4.11)$$

For a cube, by symmetry

$$\int_b x^2 dm = \int_b y^2 dm = \int_b z^2 = \frac{1}{12}Mh^2 \quad (4.12)$$

and clearly

$$I_x = I_y = I_z = \frac{1}{6}Mh^2 \quad (4.13)$$

4.2 Modelling and calculation

The moment of inertia for the nadir-side of the satellite is calculated. This is the side consisting of the gravitational boom, the antennas (with boxes and deployment mechanisms), the batteries and of course the satellite surface. Starting with the satellite before deployment.

Boom

The tip end is a lead cylinder. Using (4.5) and the parallel axis theorem we get:

$$\begin{aligned} I_{xlead} &= \frac{1}{12}M_b h^2 + \frac{1}{4}M_b R^2 + M_b r_x^2 \\ I_{ylead} &= \frac{1}{2}M_b R^2 + M_b r_y^2 \\ I_{zlead} &= \frac{1}{12}M_b h^2 + \frac{1}{4}M_b R^2 + M_b r_z^2 \end{aligned} \quad (4.14)$$

The coiled measuring tape is modelled as a hoop. Using (4.8) and the parallel axis theorem we get:

$$\begin{aligned} I_{xcoil} &= \frac{1}{12}M_{mt}(h^2 + 3R_2^2 + 3R_1^2) + M_{mt}r_x^2 \\ I_{ycoil} &= \frac{1}{2}M_{mt}(R_2^2 + R_1^2) + M_{mt}r_y^2 \\ I_{zcoil} &= \frac{1}{12}M_{mt}(h^2 + 3R_2^2 + 3R_1^2) + M_{mt}r_z^2 \end{aligned} \quad (4.15)$$

The box is modelled as homogeneous and rectangular. Using (??) and the parallel axis theorem we get:

$$\begin{aligned}
 I_{xbox} &= \frac{1}{12}M_{box}l_y^2 + \frac{1}{12}M_{box}l_z^2 + M_{box}r_x^2 \\
 I_{ybox} &= \frac{1}{12}M_{box}l_x^2 + \frac{1}{12}M_{box}l_z^2 + M_{box}r_y^2 \\
 I_{zbox} &= \frac{1}{12}M_{box}l_x^2 + \frac{1}{12}M_{box}l_y^2 + M_{box}r_z^2
 \end{aligned} \tag{4.16}$$

Antennas

The antennas are modelled as hoops. Using (4.8) and the parallel axis theorem we get:

$$I_{xan} = \frac{1}{12}M_{an}(h^2 + 3R_2^2 + 3R_1^2) + M_{an}r_x^2 \tag{4.17}$$

$$I_{yan} = \frac{1}{12}M_{an}(h^2 + 3R_2^2 + 3R_1^2) + M_{an}r_y^2 \tag{4.18}$$

$$I_{zan} = \frac{1}{2}M_{an}(R_2^2 + R_1^2) + M_{an}r_z^2 \tag{4.19}$$

The antenna boxes are modelled in a similar way as the boombox (see appendix A).

Coils

The coils are divided and modelled as rods. Their moment of inertia will be (for the two parts parallel to the x-axis)

$$\begin{aligned}
 I_{xcoilx} &= \frac{1}{6}m_c d^2 + \frac{1}{6}m_c h^2 + 2m_c r_x^2 \\
 I_{ycoilx} &= \frac{1}{6}m_c w^2 + \frac{1}{6}m_c h^2 + 2m_c r_y^2 \\
 I_{zcoilx} &= \frac{1}{6}m_c w^2 + \frac{1}{6}m_c d^2 + 2m_c r_z^2
 \end{aligned} \tag{4.20}$$

For the rods parallel with the y-axis the moment of inertia is

$$\begin{aligned}
 I_{xcoily} &= \frac{1}{6}m_c h^2 + \frac{1}{6}m_c w^2 + 2m_c r_x^2 \\
 I_{ycoily} &= \frac{1}{6}m_c h^2 + \frac{1}{6}m_c d^2 + 2m_c r_y^2 \\
 I_{zcoily} &= \frac{1}{6}m_c w^2 + \frac{1}{6}m_c d^2 + 2m_c r_z^2
 \end{aligned} \tag{4.21}$$

Adding (4.20) and (4.21) and using $m_c = \frac{1}{4}M_{coil}$ we get

$$\begin{aligned}
I_{xcoil} &= \frac{1}{12}M_{coil}h^2 + \frac{1}{24}M_{coil}w^2 + \frac{1}{24}M_{coil}d^2 + M_{coil}r_x^2 \\
I_{ycoil} &= \frac{1}{12}M_{coil}h^2 + \frac{1}{24}M_{coil}w^2 + \frac{1}{24}M_{coil}d^2 + M_{coil}r_y^2 \\
I_{zcoil} &= \frac{1}{12}M_{coil}w^2 + \frac{1}{12}M_{coil}d^2 + M_{coil}r_z^2
\end{aligned} \tag{4.22}$$

It is easy to see that this reduces to at cube (4.13) when $h = w = d$ and $r_x = r_y = r_z$.

Surface and internal structures

The satellite surface are divided into rectangular parts and calculated. This is just a repetition of the calculations above (4.16) and are therefore left out here. This also applies the battery and the circuit boards.

When boom and antennas are deployed their moment of inertia will change. The boom will then be modelled as a rod with a cylinder at the end and (see matlab code in appendix A) the antennas as rotated rods. Their moment of inertia will be

$$I_{xant} = \frac{1}{12}M_{ant}l_z^2 \sin(\phi) + \frac{1}{12}M_{ant}l_y^2 \cos(\phi) + M_{ant}r_x^2 \tag{4.23}$$

$$I_{yant} = \frac{1}{12}M_{ant}l_x^2 + \frac{1}{12}M_{ant}l_z^2 \sin(\phi) + M_{ant}r_y^2 \tag{4.24}$$

$$I_{zant} = \frac{1}{12}M_{ant}l_x^2 + \frac{1}{12}M_{ant}l_y^2 \cos(\phi) + M_{ant}r_y^2 \tag{4.25}$$

for each antenna. For the complete calculation of moment of inertia of the satellite see the matlab code in the appendix A..

4.3 Results

When the Matlab program is put to work the results becomes

:

	Undeployed boom	Deployed boom
I_x	0.000721	0.1043
I_y	0.00039	0.1020
I_z	0.000656	0.0031

This result is just an indication of the real result, since most of the measurements used are not final. But it is easy to see that the condition for pitch stability is satisfied. The condition for roll/yaw stability however, is not satisfied, but only minor adjustments are required to satisfy this condition. If, for example the antennas were to point in the x-direction, roll/yaw stability would be obtained. The circuit cards will also help achieve roll/yaw stability

Chapter 5

Design

The nadir side of the satellite consist of most of the mechanical (moving) parts of the satellite. This will be the heaviest side and the most challenging from a structural point of view. In addition to the gravity boom this side will also include two monopole antennas, a patch antenna, deployment devices for the boom and monopole antennas, two batteries, RJ-connector, mechanical structure and of course attachment equipment (screws, bolts and nuts). Before the designphase is started several factors must be taken into account. The most important of these are listed below:

- The side should ideally be constricted to as little space as possible and must be adapted to the other subsystems (most importantly the coils and circuit cards. This is also valid the other way around, the other subsystems must adapt to the nadir side).
- The total mass budget of the satellite (less than one kg) must be overheld.
- The center of mass must be located within 2 cm of the geometrical center.
- The material used must be designated space components.
- The material used should be easily available.

Some decisions about which solutions/components to be used on the nadir side of the satellite were made late 2002-early 2003 (in the final design review documents/project reports for the different subsystems). The most critical of these will be summarized below:

- The batteries to be used are two Danionics Li-ion polymer DLP485368 (Cederblad et al 2003).
- The antennas (other than the boom) to be used are 17 cm and 40 cm long (Otterstad 2002).

- For the gravity boom coiled measuring tape is to be used instead of the spring-rod approach discussed in (Indergaard 2002). The gravity booms length is to be 1.5 meter long. This length is chosen as a trade off between an appropriate length for antenna frequencies and ADCS. See (Otterstad 2002) and (Indergaard 2002). This length may be adjusted slightly according to the results of impedance matching-simulations for optimal antenna performance. The tip-ends mass should be around 40 gram. This mass may also change depending on the mass budget of the other subsystems.
- The nadir-side of the satellite will be constructed in cooperation between Indergaard-Otterstad, the mechanical workshop of the department of telecommunication and the University in Oslo.

5.1 Boom/Antennas

The main structural task for the antennas and gravity boom is to be easy to implement, robust, adjustable (in case of changes regarding length, volume, mass, placement), and of course to deploy correctly. Two different ways of constructing a gravity boom were discussed (Indergaard 2002). The two alternatives were:

- a design based upon coiled measuring tape deployed when the restrainer was removed (the tape will then behave as a string)
- a design based upon a telescope (car antenna or similar) where springs are used to deploy the telescope. See Indergaard (2002).

It quickly became clear that the first design had several advantages over the second. When the boom should be used as an antenna, it need to be insulated. This requires the boom to be stored in a box and even though the telescope boom has less volume than the measuring-tape boom, the housing for the telescope boom (and spring) would require a larger surface and the telescope is not as compact as the measuring-tape alternative, which is contained to 5 cm above the nadir-side. Another advantage of alternative 1 is that the boom and the monopole antennas will be constructed the same way, and this will simplify design and manufacturing of the housing and deployment mechanisms.

The gravity boom

The boom is constructed the following way: One end of the 1.5 metre long measuring tape is attached to a metal cylinder (with a screw). The measuring tape will act as the boom rod, and the metal cylinder as the tip-mass when deployed. To store the boom before deployment the loose end of the measuring tape is attached to the containment box and the tape is then coiled around the cylinder. When the tape is coiled all the

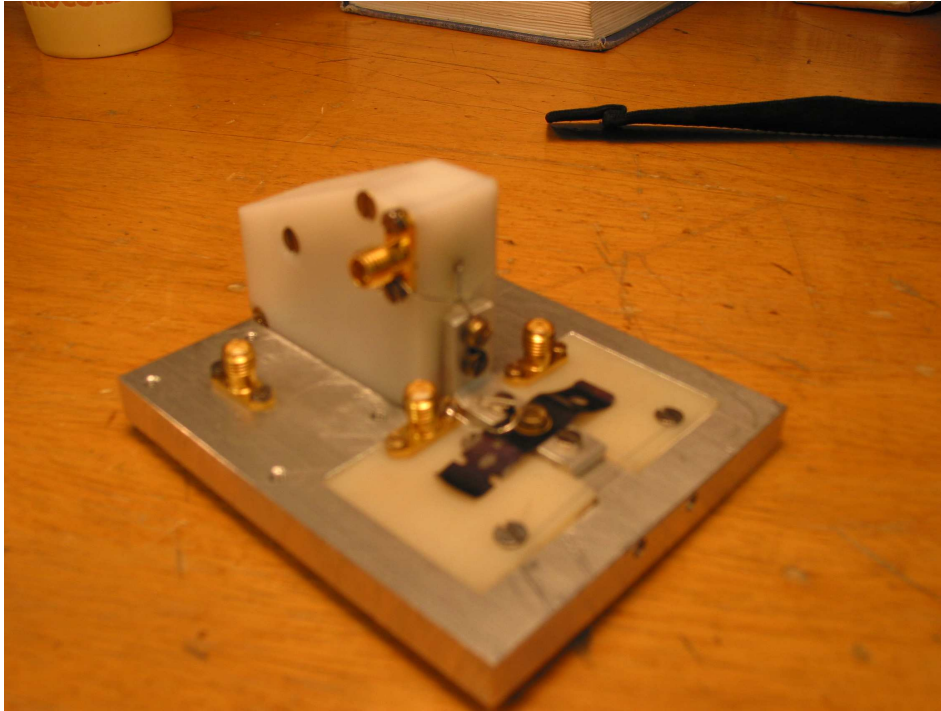


Figure 5.1: The inside of the nadir-side. The metal "springs" deploy the antennas. Mounted on a prototype model (thick aluminium plate)

way up it is constrained to the box with fishing line which is tightened around the box. The fishing line is knotted to one side of the box and screwed to another, to make it possible to tighten the line sufficiently. Two Nichrome wires are coiled around the fishing line and connected to the batteries. When the satellite is safely launched from the p-pod into orbit and been stabilized it is time to deploy the boom to achieve passive stabilization. This is done by applying voltage (3.6 V) to the Nichrome wires which will make them melt the fishing line (two wires are used for redundancy) and thus release the now-free-to-act-out-his/hers-nature measuring tape aka gravity boom. Boom released.

The materials used to construct this not so high technology stabilization device is regular off-the-shelf measuring tape; thickness 1 mm, width 13 mm. It was finally decided to use lead for the cylinder. To save space it was clear that a high-density material was to be used, and the best candidates for the job were Lead ($\mu = 11340 \text{ kg/m}^3$) and Tungsten ($\mu = 19250 \text{ kg/m}^3$). Even though Tungsten has a density ≈ 1.7 times that of Lead, the latter was chosen. Since the cylinders height has to be chosen equal to the measuring tapes width, the diameter of the cylinder (and thus the height of the box) is what must be taken into account when choosing the material. For a 40 gram cylinder with height 13 mm, these diameters become: $d_{tung} = \sqrt{\frac{4m}{h\pi\mu_{tung}}}m =$

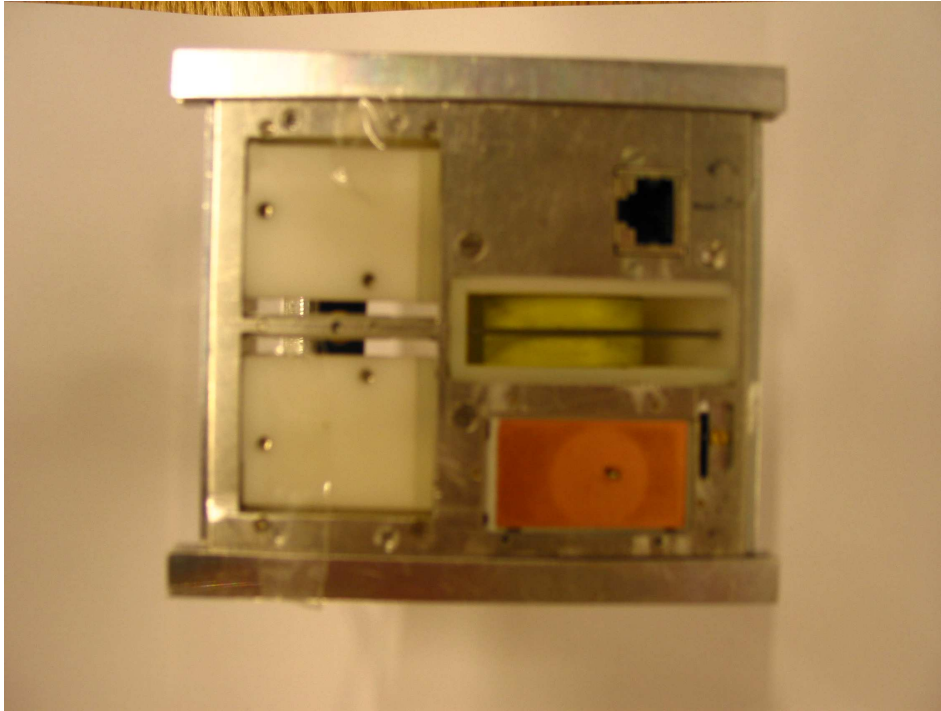


Figure 5.2: The outside of the nadir-side. The boom is coiled up and restrained inside its box

$$\sqrt{\frac{4*0.04}{0.013*3.14*19250}}m = 1.43 \text{ cm}. \quad d_{lead} = \sqrt{\frac{4m}{h\pi\mu_{lead}}}m = \sqrt{\frac{4*0.04}{0.013*3.14*11340}}m = 1.86 \text{ cm}.$$

As we can see the difference in diameter (and accordingly height of the boxes) is less than half a cm. This difference is so small that it has little significance, and represents no major drawback for lead. Since the mechanical workshop had no previous experience with Tungsten and the availability was low compared to lead. Lead it was.

The Antennas

The monopole antennas will also be constructed by measuring tape. This is a tape of slightly smaller dimension; thickness 1 mm, width 8 mm. The two antennas will be placed on the opposite side of the boom, pointing in different directions of each other. When deployed they will point with an angle of 45 degrees in respect to the nadir side and the boom, thus their deployment mechanism will have to be different. This is solved by placing "springs" on the backside (fig 5.1 and 5.3) of the boxes which will push them into the right angle when deployed. They are also mechanical restrained so that they are locked into the right position. The monopole antennas will be 17 cm and 40 cm long.

The patch antenna is a microstrip antenna. That is a rectangular metal plate printed onto a dielectric substrate with ground plane on one side. This kind of antenna needs

no deployment and will be placed directly on the nadir side. The patch antenna will have a dimension of 4 cm * 2cm * 1 mm. The final dimension will also in this case depend on the impedance matching.

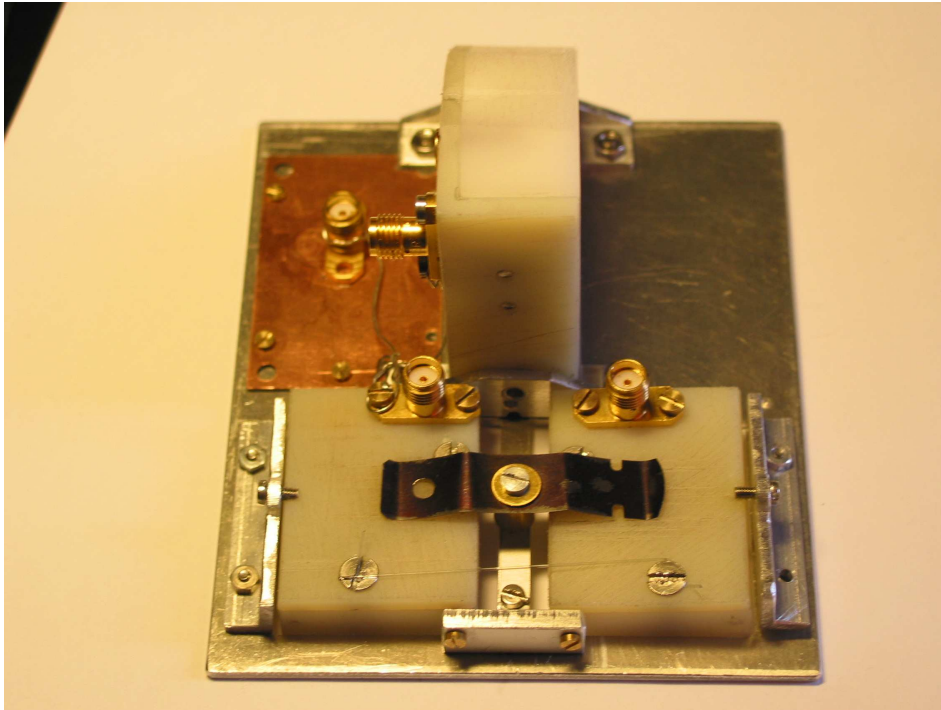


Figure 5.3: Another picture of the nadir-side. New prototype (thin aluminium)

5.2 Boxes

The boxes used for containment and insulation for the antennas/boom were created by the same approach used by Montana University for their MEROPE (Montana EaRth-Orbiting Pico-Explorer) CubeSat (see fig 5.4). The boxes are made from plastic and the essential part of their construction is the curvature inside the box. This curvature will affect the deployment of the boom and because of the room taken up by the curvature the box has to be higher than the diameter of the tip-mass. It took several prototypes to get the dimensions of the boxes right as up to this moment in time they are 5 cm* 5cm *2 cm. See figure (5.1-5.3) for the boxes and how they are attached to the satellite.

5.3 Complete nadir side

The complete nadir siden with batteries, boxes, antenna, RJ-45 and mechanical structure is seen on figure (satbak). The placenent of the batteries are essential to get the

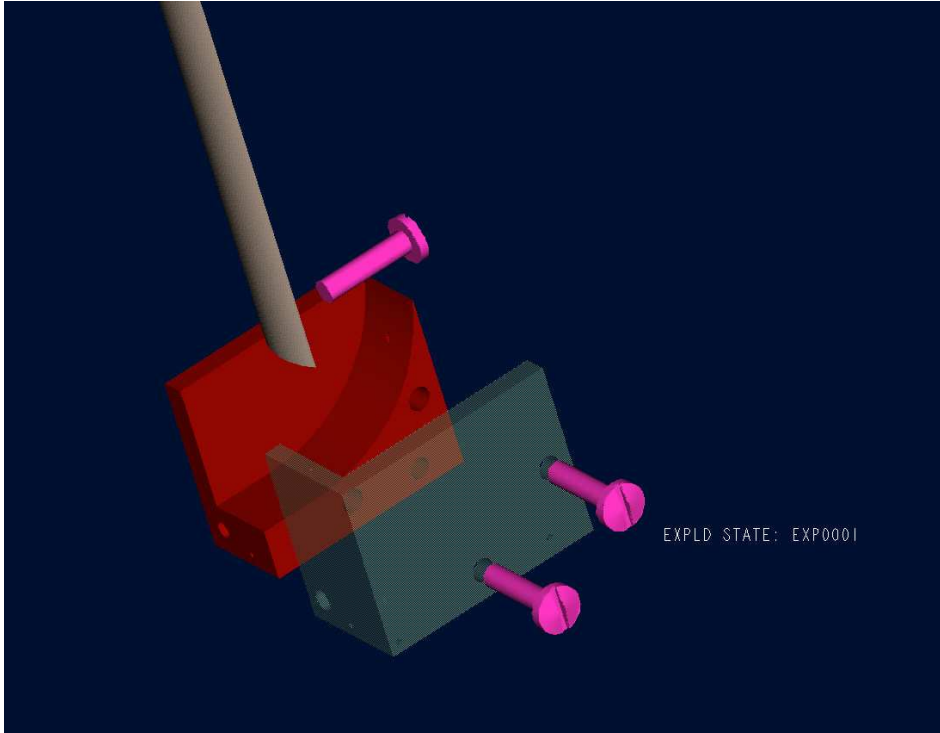


Figure 5.4: How the box is designed.

height of gravity within the specifications given by Stanford (2 cm of the geometrical center). To calculate height of gravity we use:

$$H = \frac{\sum_i m_i h_i}{\sum_i m_i} \quad (5.1)$$

For the satellite most of the parts is symmetrical xy-plane so the only components which needs to be taken into consideration are; batteries, gravityboom/box, antennas/boxes, coil in xy-plane, satellite sides (outer structure) penetrated by the z-axis. This gives

$$H = \frac{m_{batt}h_{batt} + m_{boom}h_{boom} + m_{ant}h_{ant} + m_{coil}h_{coil} + m_{upper}h_{upper} + m_{lower}h_{lower}}{m_{batt} + m_{boom} + m_{ant} + m_{coil} + m_{upper} + m_{lower}} \quad (5.2)$$

Using data from table xx we get

$$H = \left(\frac{66 * 7.5 + 91 * 2.5 + 33 * 0.5 + 17 * 8 + 25 * 9 + 46 * 1}{66 + 91 + 33 + 17 + 25 + 46} \right) = 3.9cm$$

which is almost a cm within the limit set by Stanford.

Chapter 6

Testing

Space, the final frontier. When a satellite is modelled mathematically the main aspects of space environment of concern is gravity, or rather, the lack of it. When the satellite and in specific the boom is constructed, other aspects of space environment must be taken into the equation. or one might say, the consideration, as well. Gravity is still of importance, to determine how rigid the boom has to be (not to break or bend to much from the moment constructed by the satellite (magnetic coils) in order to apply force to the mass-end). Other aspects to consider is how vacuum and varying temperature will influence the materials used to construct the boom and its deployment mechanisms. Vacuum will have several consequences; the materials used will be exposed for out-gassing, that is the materials will lose mass from the resulting difference in pressure. This can influence the structure of the deployment mechanisms and in worst case result in jamming the boom in the box. Vacuum also effects the melting of the fishing line. In vacuum very few molecules are present (true vacuum is just a theoretical curiosity). This leads to that the nichrome wire just will dispose of energy (cool down) by radiation, not by convection. That is, energy dissipation by;

$$\frac{\partial Q}{\partial t} = \varepsilon \sigma A (T^4 - T_s^4) \quad (6.1)$$

(where, ε is the emissivity of the satellite, $\sigma = 5.67 * 10^{-8} W m^{-2} K^{-4}$ is the Stefan-Boltzmann constant, A is the radiation surface, T is the temperature of the satellite and T_s is the temperature of the surroundings) rather than by;

$$\frac{\partial Q}{\partial t} = hA(T - T_s) \quad (6.2)$$

(where h is the heat transfer coefficient. Dependent on the conductivity of the material and the boundary layer. Typical in the order or 0.1. In vacuum $h = 0$). It is easy to see that convection is much more efficient when temperatures are low (radiation does not become efficient before temperatures arising from nuclear reactions in stars). This affects the satellite as a whole (problems with overheating), not just the boom and antenna release mechanisms.

The final issue is the varying temperatures. In space they will vary between -40 and 80 degrees Celsius depending on whether the satellite is behind the earth or in front of it, with respect to the sun. This will cause the structure of the materials to change, and may have serious consequences for the gravity boom. If the boom or tip-mass expands (or the plastic "shrinks") before boom-release the mechanism may jam. When the satellite are behind the earth the cold temperature may alter the booms rigidity after deployment. This may result in a too rigid and crisp boom (breaks when the control algorithms are used). When the satellite faces the sun, the temperature gets high and this may result in a boom who lack rigidity (the boom bends and the tip-end don't follow the rotation of the satellite. This will also cause an oscillation in the satellite-boom system).

All these aspect needs to be taken into consideration when the boom-antenna system is being designed, and the system will undergo testing to discover flaws in the design and construction.

6.1 Rigidity/Deployment

The slowness of it all

Testing by thought. Imagine a cube floating in space. It is the NCube. Radio contact has been established, the detumbling control law has been initiated, and the magnetic coils has de spun the satellite and directed its nadir side towards earth. The boom is ready to be deployed. Deploy boom! Then what happens? It is difficult to predict the exact progress in terms of acceleration and angular velocity vectors of the tip-mass and measuring tape because of the nature of the coiled measuring tape (difficult to obtain the spring "constant" because it is dependent of the way the tape is coiled). It is also difficult of calculate the impact of deployment on the cube because of the same reason. But one thing is evident. Given enough time and no spin the boom will assume its outreached position. Why? Let's say that the measuring tapes task is to bring the tip-mass into a steady position 1.5 meters from the Cube. To accomplish this task the measuring tape has to do mechanical work on the tip-mass, move it from point a to b. As long as the measuring tape is coiled, bent or twisted it will have some potential energy left in it and use it to accomplish its task. Since the Cube is in a zero-g environment (disturbances can be modelled as white noise) there will be no resistance and the tape will eventually accomplish it's task. Even if occiliations occur, the boom will eventually become rigid as the energy dissipated through radiation because of the heat created when the steel bends.

The abers of this deployment scenario are present. If the following nice idealized scenario are to take place the following things must be avoided during deployment.

- Knots on the measuring tape
- Severe bending of the measuring tape

Experimental deployments in harsh environment (one g) has shown that any of these situations are very unlikely (not occurred during testing). But the unlikelyness of things does not mean to exclude them from consideration. If one of this structural deformations occurs during deployment the boom will not point in the desired position and destabilize the satellite. Another thing which must be taken into consideration is the rotation of the satellite during deployment. The measuring tapes ability to withstand windup and bending during rotation, the tapes rigidity along x, y, z, will be tested in one of the next sections.

Boom in a box!

To imagine a zero-g vacuum environment is not a problem. To create one is a whole different ballgame. Threads can be used to simulate a zero-g environment if the motions are small and one-directional (this will be used later to test the rigidity of the boom when the cube rotates). For deployment testing this is not sufficient because the tip-mass and measuring tape has to be able to move in all directions during deployment. A crude way to simulate this is to restrain the coiled tape with your hand and simply throw the satellite up in the air. The boom will then be released in a free-fall, and although the air resistance will corrupt the tests it will at least give an indication of the deployment. The satellites designated landing area should be soft to avoid deformation of the lead tip-mass.

To make the simulation more repeatable and reliable a mechanical device should be throwing the satellite in the air. A box with a spring at the base will work fine. The coiled measuring tape is then withheld by the walls of the box and the spring is used to throw the satellite upwards. To throw the satellite 4 meters upward a spring with potential energy $U = mgh = 39.24 J$ should be used. This will keep the satellite in free fall for $t = \sqrt{\frac{8h}{g}} = 1.8 \text{ sec}$.

Strings attached

To simulate zero-g environment and test the rigidity of the boom when the satellite is rotated about one axis strings are attached to the cube, tip-mass and several places along the boom. This will give an approximation to zero-g. This test did not give any numeric results, since the satellite (and boom) were not equipped with gyros and accelerometers. The results was only be visual and consists of observing the tip-ends displacement for the vertical-line in case of roll and pitch rotations of the cube, and rotating of the tip-end in case of yaw rotation. Displacements were observed during roll, pitch and yaw rotations..

6.2 Vacuum chamber

To test how the deployment mechanisms (melting the fishing line) work in space environment such a environment must be simulated. An optimal testing environment would be a cold vacuum chamber (the temperature will change from hot to cold depending on where the satellite is in its orbit (in the sun or behind the earth) but we are interested in the worst case time for deployment so we just have to test for the cold situation) but since NTNU does not have such a facility we had to separate into two separate environments (vacuum and cold) and be less bombastic about the conclusions drawn. The vacuum test are presented below and the cold test are presented in section 5.3.



Figure 6.1: Our pcv "deployment" device. 6 fishing lines across the pipe.

For the vacuum test we used the Vacuum lab located in Chemistry block 2, room 413, who belong to the section for inorganic chemistry The experiment was to measure the time and current used to melt the fishing line using different voltage (with constant number of windings and winding area). The vacuum chamber consists of two chamber. The main chamber, where the experiment takes place, and the intermediate chamber, where the equipment first are placed. The main chamber is a constant low pressure environment with electrical outlets and working -gloves (see figure 6.3) to make it possible operate equipment in vacuum environment. The intermediate chamber is used to create a vacuum in the experiments components and their surroundings. When the

pressure in the two chambers are sufficient low the seal between the chambers can be broken and the equipment can be moved to the main chamber and experiments can be conducted. The process of depressurizing the equipment range from 2-24 hours depending on the number of components and what kind of component used. To operate with the gloves in the vacuum chamber is at best a clumsy affair (to tie a knot on fishing line is difficult enough under normal circumstances. To coil nichrome wire is an even harder task) so it is of importance to have some kind of prearranged fishing line and nichrome wire set up to save time. We constructed a device of a divided pvc-cylinder with 6 screws on each side (see figure 6.1 and 6.2). The screws are used to tighten the fishing line. Nichrome wire was then coiled around the line and we could conduct 6 "deployments" with and just depressurize one time. For the experiment we used;

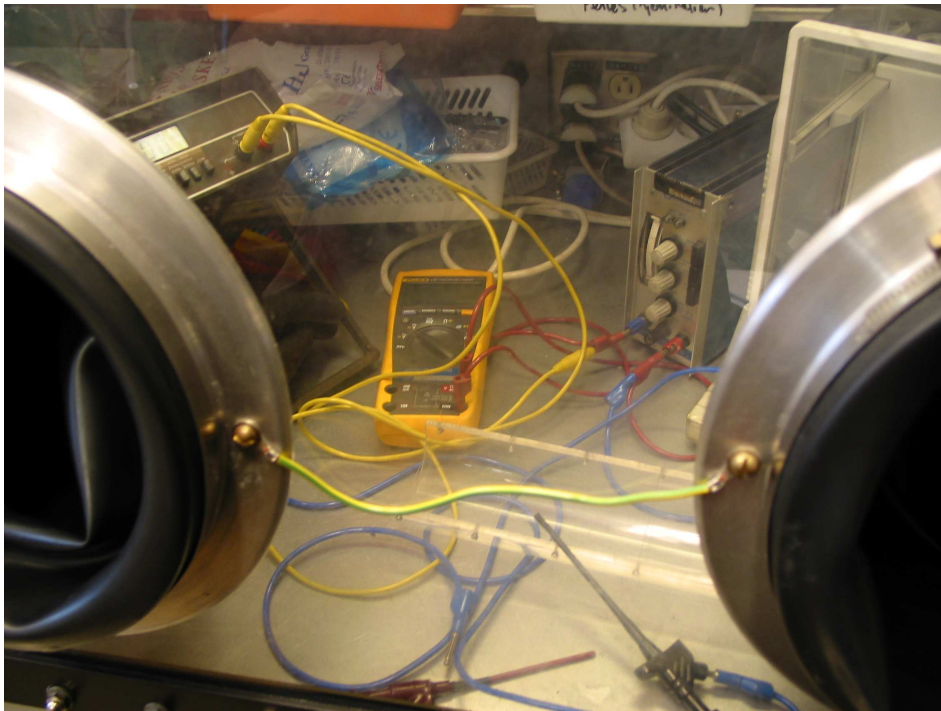


Figure 6.2: Inside the vacuum chamber.

- 1 Voltage generator
- 1 Multimeter
- 1 Prearranged line-wire set up
- electrical wires and clamps

The Multimeter was placed in series with the circuit and the voltage generator in parallel. The experiment was conducted twice and results are presented in the table

below. The results are well within the critical limit for deployment time of the boom and antennas.



Figure 6.3: Me conducting the experiment. Hard work

Voltage	Current	Time (seconds)
2	0.4	2.3
2.5	0.5	2.4
3	0.6	1.6
3.6	0.7	<1
3.6	0.7	<1
4	0.8	<1
2	0.4	1.8
2.5	0.5	2.2
3	0.6	1.7
3.6	0.7	<1
3.6	0.7	<1
4	0.8	<1

6.3 Cold tunnel

Deployment mechanism test

As part two of the space environment simulation test for the deployment mechanisms a cold tunnel was used. The tunnel belongs to the section for industrial process engineering and is located in the basement of the Kielhouse. The tunnel is 1.5 meter wide, 2.5 meter high, 6 meter long and can go as low as -40 degrees Celsius. When we conducted our experiment we could not go lower than -35, because of a failure with one of the pumps.

The experiment is nearly the same as the one in the vacuum chamber. Due to the cold we had to make an insulated briefcase for the voltage generator to keep it from malfunctioning. The current was not measured, and the voltage was fixed to 3.6 Volts (the voltage which will be used in the satellite). The reason for the fixed voltage is to keep the suitcase closed. The same arrangement of fishing line and nichrome wire as in the vacuum chamber was used. Results were similar to the results in vacuum, but with a slight delay.

Deployment impact test

Concerns that the structure of the box containing the boom would collapse when the boom is deployed in a cold environment were uttered on one Ncube meeting. This was also tested in the cold tunnel. This test is not very realistic since the boom is deployed under one-g, but if the box can withstand this deployment there will certainly be no collapse in zero-g. It should also be noted that the box used in this experiment was already breached due to extensive screwing (too many holes were drilled too tight on the prototype).

In the experiment an early prototype (box, boom and tip-end) were used. The prototype were stored in the tunnel over night to ensure that the material were frozen all the way through. The boom were deployed by applying voltage to the nichrome wire and thus melting the fishing line. The experiment were repeated several times and the result were always the same. The box' structure did not collapse even though there were already some damage and one-g was applied. It should also be noted that the prototype used was constructed of a structurally weaker material than the final product.

6.4 Parabolic flight

About parabolic flight

The problem with the previous test have been that it has been difficult to obtain a controlled zero-g environment. Parabolic flight overcomes this problem, although the timescale to perform the experiment are limited.

In parabolic flight weightlessness is obtained by putting an aircraft into a sub-orbital trajectory . The aircraft begins its flight with level flight, altitude 5333 meters. Then it begins its ascent to altitude of 8000 meters. During this ascent the aircraft pitches up to approximately 45 degrees and subjects the passengers to a 1.8g pull lasting about 20 seconds. When the aircraft reaches the altitude of 6666 meters the engines are powered down (not turned off). The aircraft will then follow a parabolic trajectory and the passengers inside expire about 20 seconds of zero-g (in perfect conditions that is. Most likely the aircrafts motion due to turbulence will perpetuate and make it a micro-g environment with disturbances in the order of +/- 0.05g). When the attitude of 6666 meters again are reached, the aircraft will start its pull out manoeuvre, again subjecting the passengers to 1.8g for 20 seconds and level the craft at 5333 meters. The aircraft is then ready for another aerobatic manoeuvre.

ESA student parabolic flight campaign

ESA (European Space Agency) yearly invites students from its countries to take part in a parabolic flight. The 2003 campaign was the 6th student parabolic flight campaign to take place. The location of the campaign was at the Bordeaux-Mérignac airport in France and it took place from 16-25 July 2003. The purpose of the campaigns are to stimulate space research among students all over Europe and it is part of ESAs outreach program. 120 students are selected (30 teams of four) for each campaign. The parabolic flight is preformed by Novespace and the aircraft used is a Airbus 300 (with the interior modified to fit experimental uses). Two flight per experiment was performed, where each flight contained 30 parabolas. The parabolic flight and accommodation (at an university in Bordeaux) were both paid by ESA.

NCube parabolic flight team

The conditions for participation in the student parabolic flight are the following

- A student group of four members must be established
- The students must be located in a ESA member country
- A zero-g experiment must be made
- The experiment must be endorsed by a university professor
- The group members must pass the medical examination
- The experiment must pass the safety evaluation

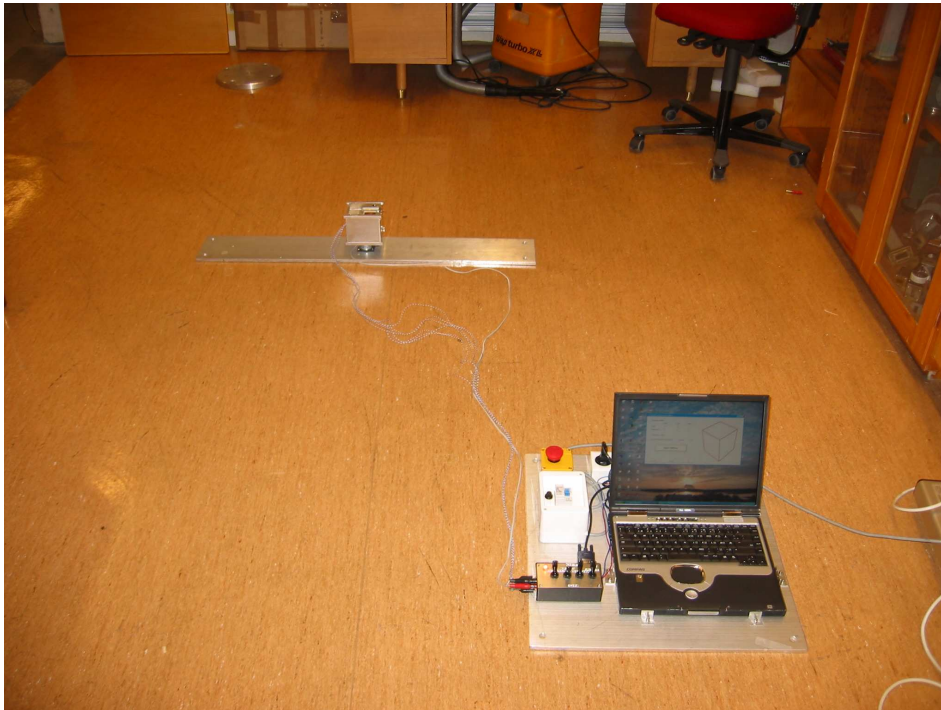


Figure 6.4: Testing the controlpanel and the electromagnet in Trondheim.

A four member team from the Ncube project was established, consisting of Fredrik Mietle Indergaard (leader), Jan Otterstad, Kristian Svartveit and Eystein Sæther. After several application phases we were accepted (by Esa) together with 29 other experiment from all over Europe. An experimental form were created (see Appendix B) and after a meeting with Frederic Gai from Novespace concerning the safety aspect of the experiment were changed and cleared by Novespace.

Every experimenter also had to undergo medical examination (JAR FLC3 class 2) and a impedance tympanometry test (a pressure test of the ears) to get medical clearance to participate in the parabolic flight. Funding for the NCube parabolic flight project were received from Norwegian Spacecentre and the Department of Engineering Cybernetics at NTNU to cover the costs of medical examinations and traveling expenses.

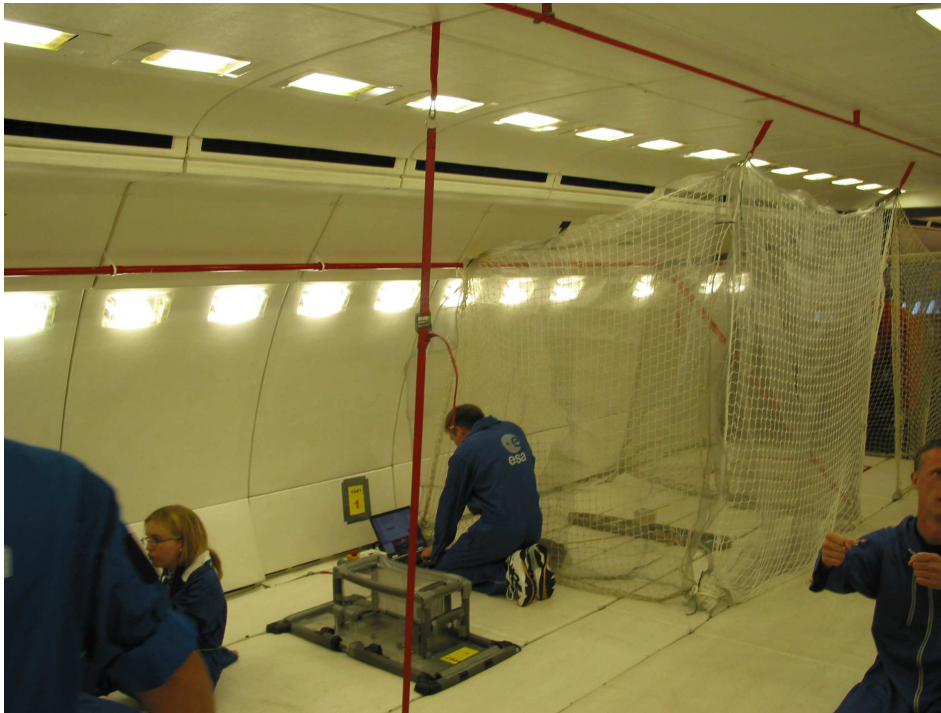


Figure 6.5: The experiment set-up aboard the plane. Eystein in control.

Experiment Objectives

The main objective of the experiment is to test the deployment system repeatedly under a controlled micro-g environment, and observe the effects of a deployment on the satellite. The experiment will be documented visually by a camera. The satellite will also be equipped with 3-axis accelerometer and gyros whose raw data will be stored in a laptop.



Figure 6.6: The gyro used.

The second objective of the experiment is to derive a relationship of the length (or inner/outer radius) of the boom and the impact of the satellite. The potential energy of the boom will be transferred to the satellites kinetic energy upon deployment, and can be measured by the gyros and accelerometers, so it can be expressed:

$$E_{kb} = \frac{1}{2} \mathbf{v}^T m \mathbf{v} \quad (6.3)$$

so that a relationship similar to that of a spring can be derived. To help achieve the objective booms of different length will be used.

Experimental set-up

The experimental space aboard the aircraft (and the 10 electrical outlets) must be sheared between the 15 groups experiments, so it must be made as small as possible. Another concern is the safety. Ideally we would have a totally free-floating experiment but due to safety measures the satellites movement had to be restrained with ropes, an electromagnet and security nets (see figure 6.5.). All of the equipment were required to be strapped down to the aircraft floor (connected to rails) to enhance safety. The experiment were therefore divided into two subsystems; the satellite sub-system and the control sub-system, each system fastened to an aluminium base plate which were

attached to the rails with screws. During level flight and at the 1.8g phase of the ascent the electromagnet restrains satellite movements.



Figure 6.7: Experimental set-up.

When the zero-g phase is entered the magnet is turned off to grant the satellite "free movement" (it is still restrained by the ropes and the nest for safety reasons, but it were our opinion that the satellite would not pitch or roll enough to reach the nets, or achieve enough upwards speed to stretch the ropes to their full length. This were later proven wrong.). When the satellite is released, antenna and boom deployment can commence. The satellites movement is then recorded visually by a camera, and measured by the accelerometers and gyros inside the satellite (the raw data will be transmitted by a serial cable to the laptop). 20 prearranged boomboxes (containing booms of different length) will be stored aboard the plane to make the experiment repeatable. When the aircraft pulls out of the parabolas 1.8g phase and enters level flight the deployed boombox is changed with a undeployed one (the boomboxes are connected to the satellite with metal clips to provide an easy and quick way the change them), the electromagnet is turned on, the satellite is once again restrained before entering the next parabola and the experiment can be repeated. See appendix B for a more detailed experiment set-up description.

Problems encountered

According to Murphy's law, things do not always go according to plan. Experiments are no exception. In preparation to, and during the parabolic flight, we encountered several problems, none of them critical, but some less fortunate.

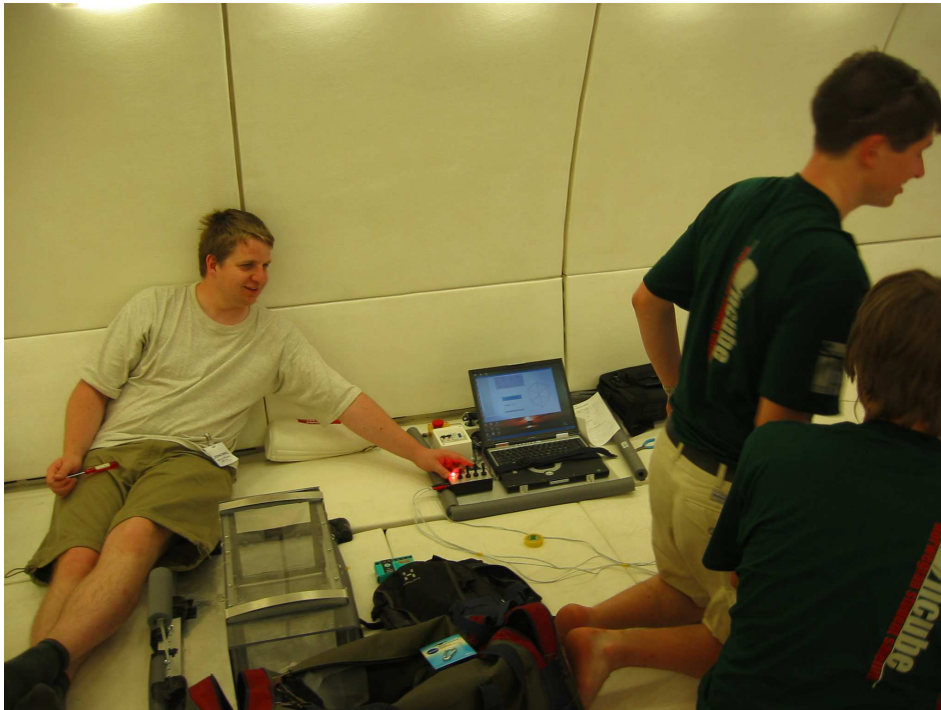


Figure 6.8: Last minute preparations.

To control the current in the nichrome wire the current were put through a small network of resistors. This applied both for the deployment mechanisms for the boom and the antennas. During one of the last test trails inside the aeroplane the day before take-off the resistors sustained to much effect during a longer period of time. This resulted in a bad odor and destroyed resistors. There were not enough time for the group to replace the resistors before flight and as a consequence of this the antenna system could not be deployed during flight. The antennas were therefore not restrained at all during flight.

The second problem occurred during the first flight. The electromagnet was too strong. When it was tested in a 1-g environment the force seemed to be zero (after about a 1 second latency). This soon proved to be wrong. During the first parabola the satellite stuck to the magnet even though power where turned off. During 0-g a force so small that seemed to be zero in 1-g could retain the satellite. This is of course no surprise since it was the only force present (when the weak and strong forces are not taken into the equation), but it were still a stressful moment. This problem was solved in a ad hoc manner by taping a rubberband across the magnet, and thus making the magnetic force smaller.

The most serious problem occurred during the second flight. After 5 parabolas the deployment mechanism stopped working. This problem most likely occurred because of a bad contact inside the satellite. During the 5 next parabolas we tried to find the

source of error, but to no effect. Tools are not allowed inside the aeroplane during flight, and 1.8/0-g are not the easiest environment for an untrained person to work in, so opening the satellite for debugging was not an option. Therefore the experiment was abandoned after 10 parabolas on the second flight.

The last problem we encountered was noise on the measurements from the accelerometer. The noise looked like glitches in the signal. Most of the noise were easily filtered out because of its absurd nature. The most frequent noise were in the order of 100 times the original signal. The filters used are included in appendix (A).

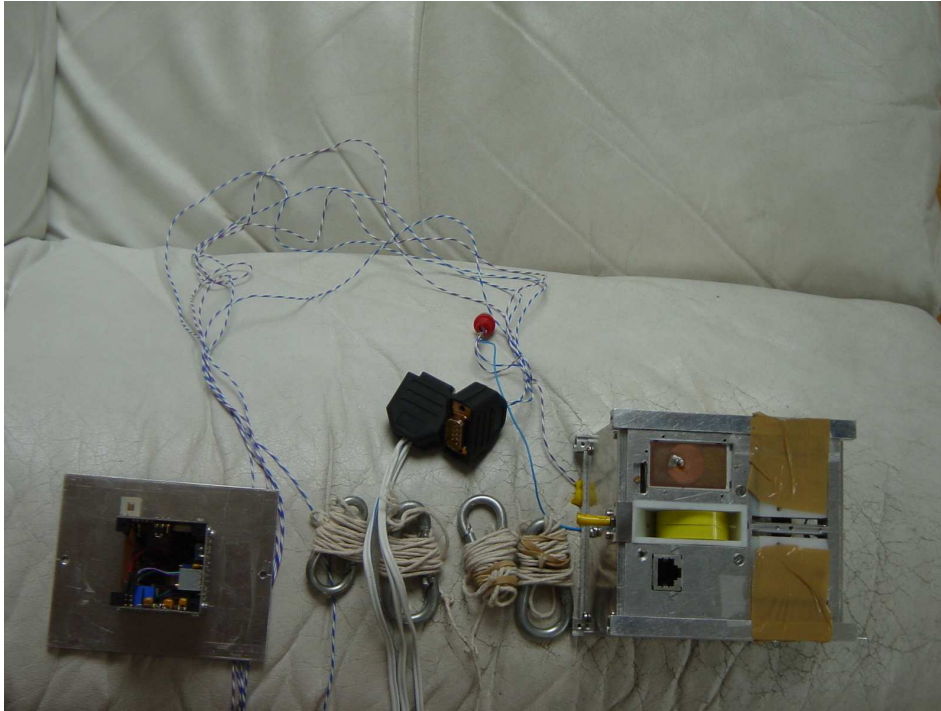


Figure 6.9: Satellite deconstructed and ready for debugging.

Flight 1

The persons controlling the experiment on this flight were Eystein Sæther and Jan Otterstad. The events are documented in the table below

Parabola nr.	Boom nr.	Boom length	Comment
0	1	70 cm	Electromagnet restraining the satellite
1	2	90 cm	Successful deployment
2	3	110 cm	Successful deployment
3	4	130 cm	Successful deployment
4	5	150 cm	Bad contact, no deployment
5	6	70 cm	Late release
6	7	90 cm	Late release
7	8	110 cm	Late release
8	-	-	-
9	9	130 cm	Successful deployment
10	10	150 cm	Successful deployment
11	11	70 cm	Bad contact
12	12	70 cm	Restrained by ropes
13	13	90 cm	Successful deployment
14	14	90 cm	Successful deployment
15	15	110 cm	No contact
16	16	110 cm	Restrained by ropes
17	17	130 cm	Late release
18	18	130 cm	Successful deployment
19	19	150 cm	Bad contact
20	20	150 cm	Restrained by ropes

Flight 2

The persons controlling the experiment on this flight were Kristian Svartveit and Fredrik Miete Indergaard. The events are documented in the table below.

Parabola nr.	Boom nr	Boom length	Comment
0	1	70 cm	Bad contact
1	2	90 cm	Bad timing
2	3	110 cm	Bad timing
3	4	130 cm	Bad timing
4	5	150 cm	Bad contact
5	6	70 cm	Bad contact
6	7	90 cm	Bad contact
7	8	110 cm	Bad contact
8	9	130 cm	Bad contact
9	10	150 cm	Bad contact
10	-	-	Experiment abandoned
11	-	-	-
12	-	-	-
13	-	-	-
14	-	-	-
15	-	-	-
16	-	-	-
17	-	-	-
18	-	-	-
19	-	-	-

Results/Comments

The results of the measurements made by the gyroscope. The data presented are acceleration, velocity and Kinetic energy. The coordinate system in which they are presented is body (satellite) in respect to the plane. All of the satellites were restrained by the ropes or the nets, and that decreased the amount of free floating time they got. To make it easier to understand the results, a table of each booms' (satellite) free floating time is presented below.

Boom nr	Free floating period (sec)
2	5-6
3	10-13
4	10-17
9	6-8
10	26-30
13	28-30
14	32-35
18	20-24

It is not easy to get anything conclusive out of these results. This is mainly because the satellite did not get enough free-floating time, because they were constrained by the nets and ropes (this makes it impossible to derive any connection between the length of

the boom and kinetic energy for example. The graphs clearly states this). The sudden movements applied to the satellite when restrained/catapulted by the ropes also seems to influence the performance of the gyro/accelerometer. This produces some strange results on the velocity plots, where the satellite, according to the accelerometers, have a speed relative to the aircraft, even though it is stuck to the floor at 1.8g. The only thing the results can be used to is to analyze the satellites movement during free floating, which is not all that interesting, since we have it recorded on tape.

When the satellite experiences free-floating, small acceleration can be seen (it is moving because it is not in a perfect zero-g), until the boom is deployed. The boom deployment causes increase in acceleration and most of the times causes the satellite to hit the net or the ropes. When it does this, the data just represents a bouncing satellite in zero-g.

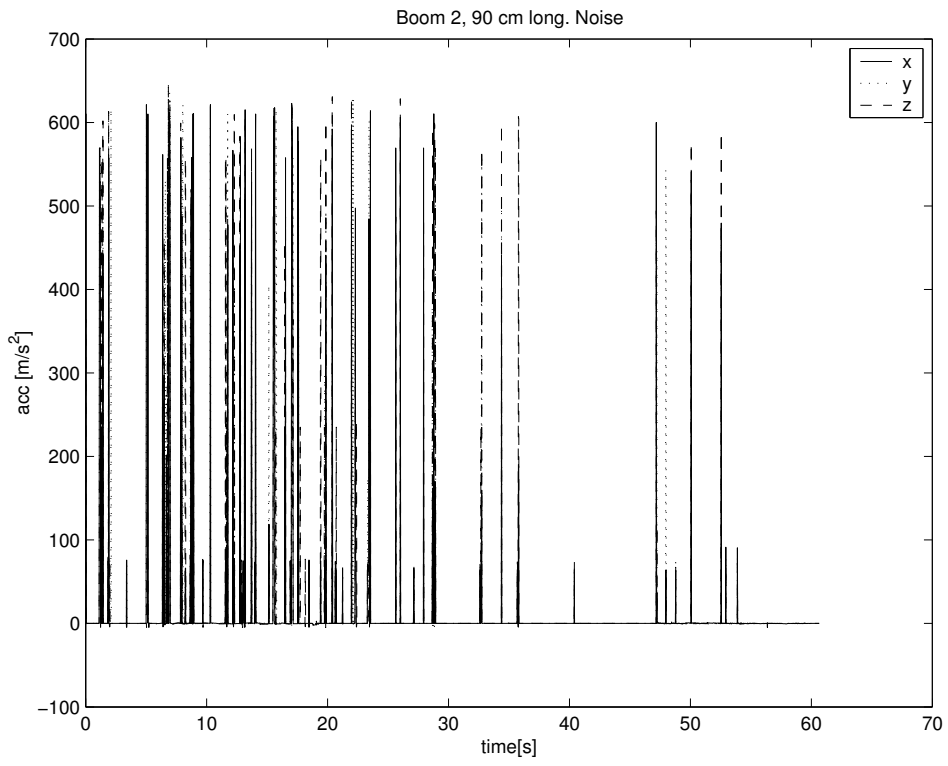


Figure 6.10: Unfiltered measurements for bom2.

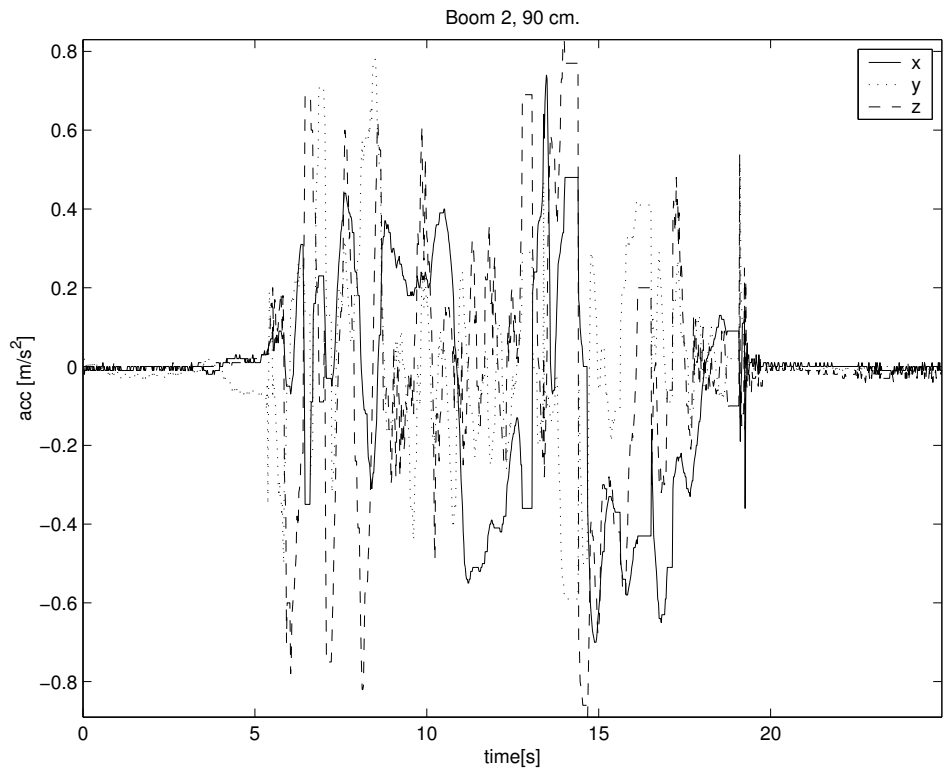


Figure 6.11: Filtered measurements for bom2.

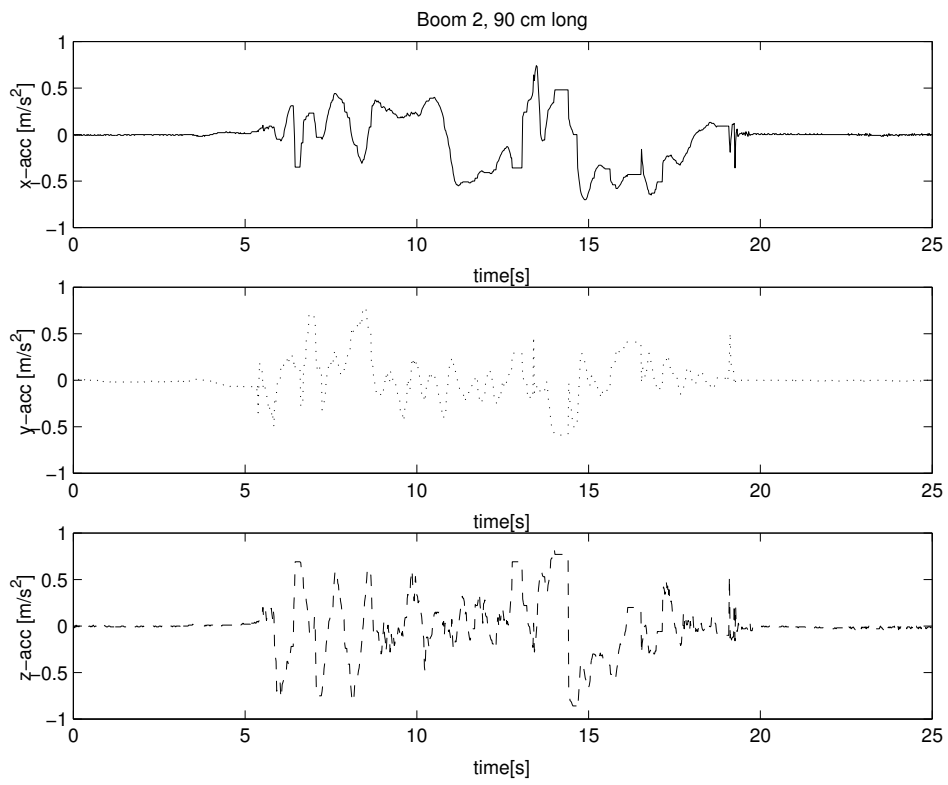


Figure 6.12: x, y, and z-acceleration for bom2.

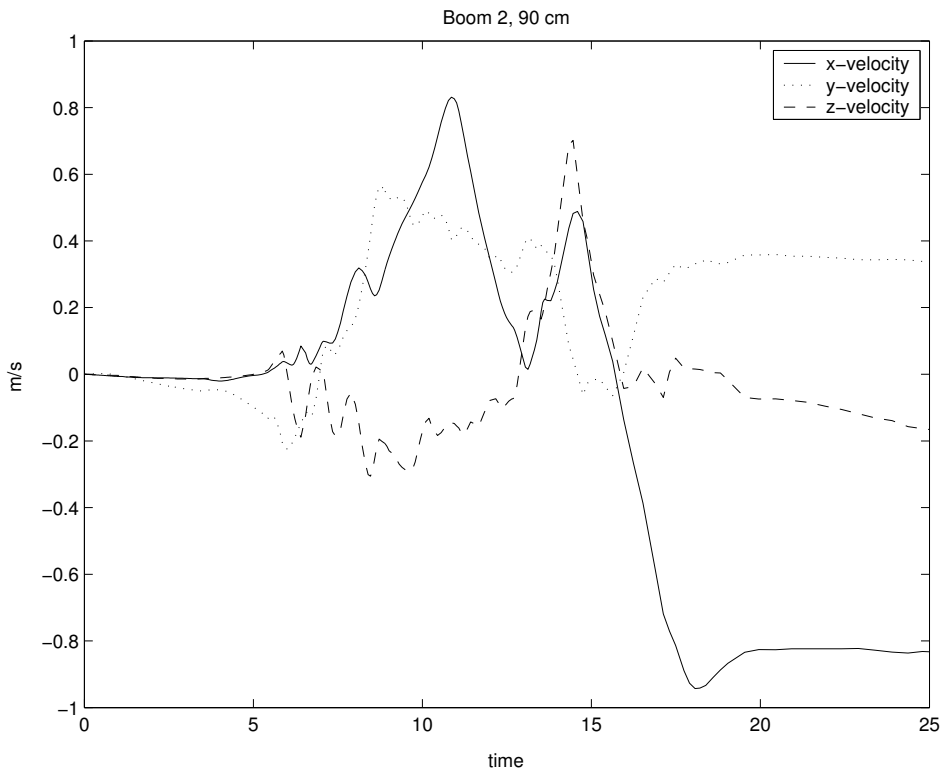


Figure 6.13: x, y, and z-velocity for bom2.

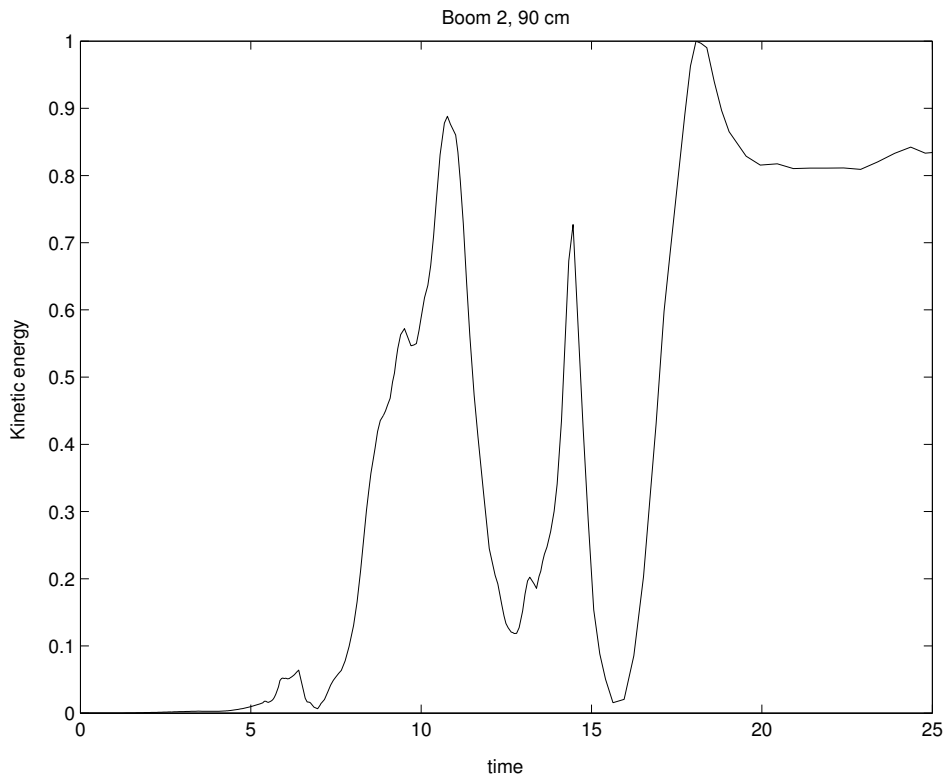


Figure 6.14: Kinetic energy for bom2.

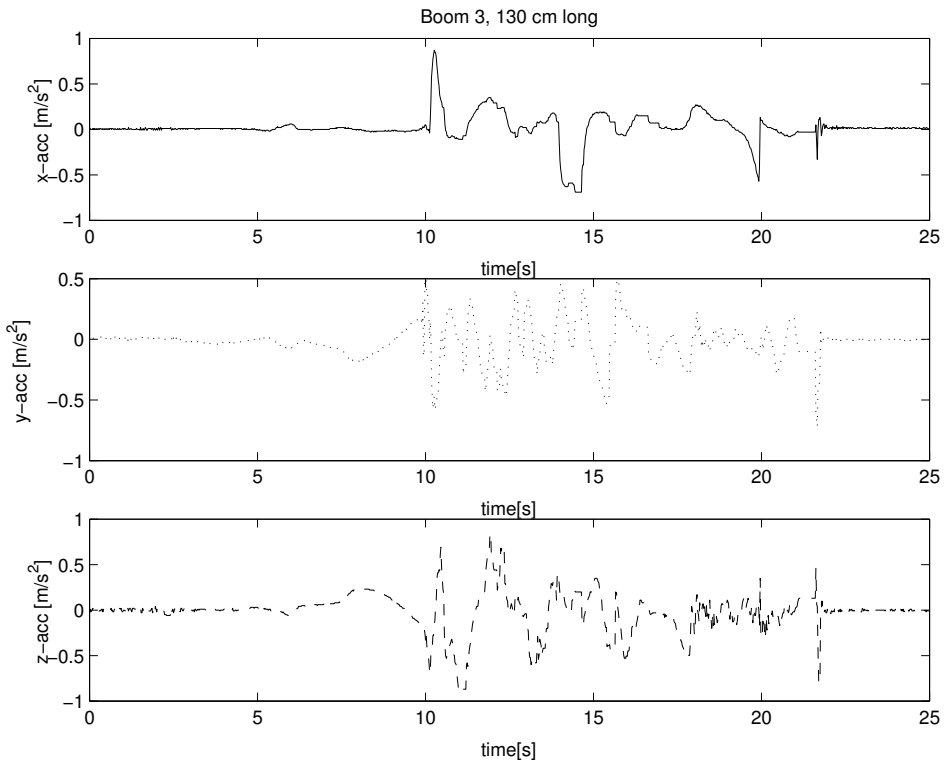


Figure 6.15: x, y, and z-acceleration for bom3.

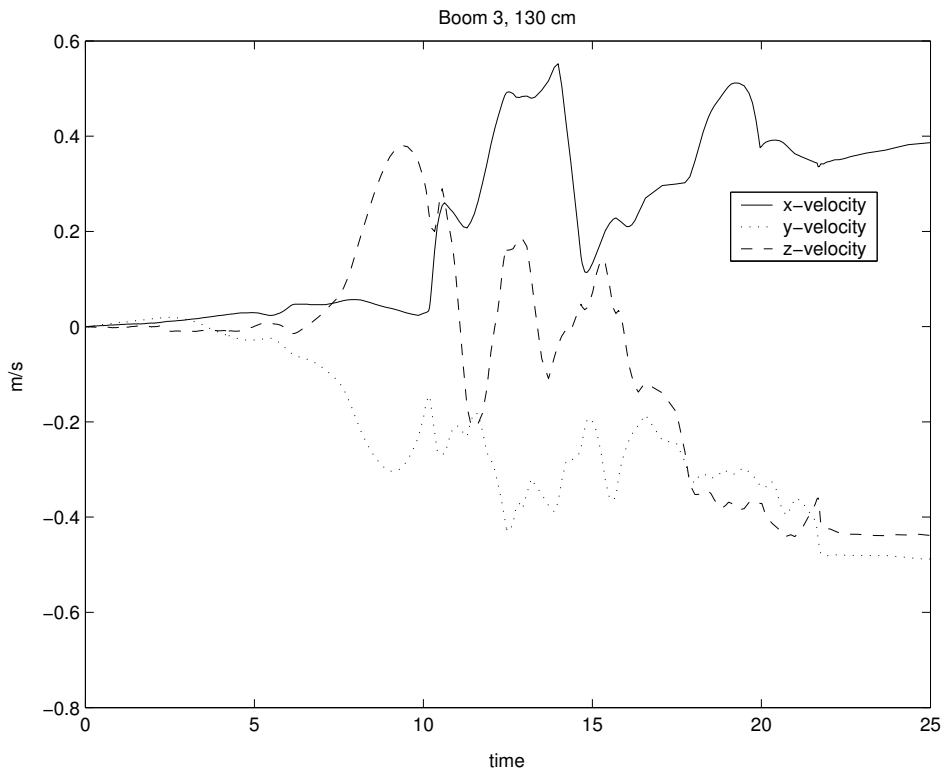


Figure 6.16: x, y, and z-velocity for bom3.

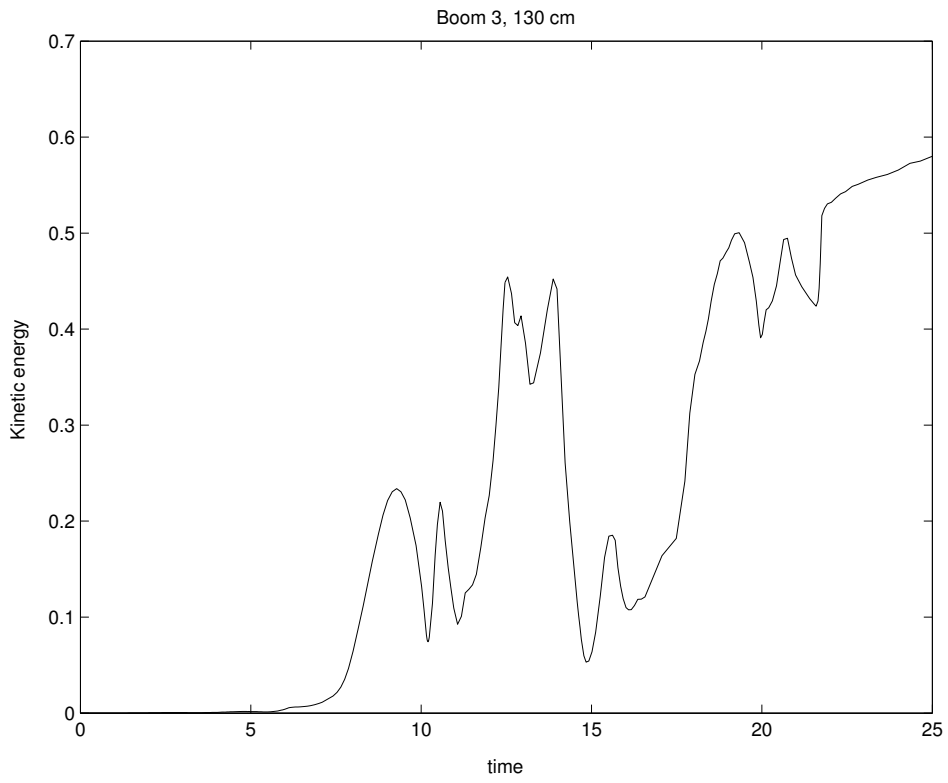


Figure 6.17: Kinetic energy for bom3.

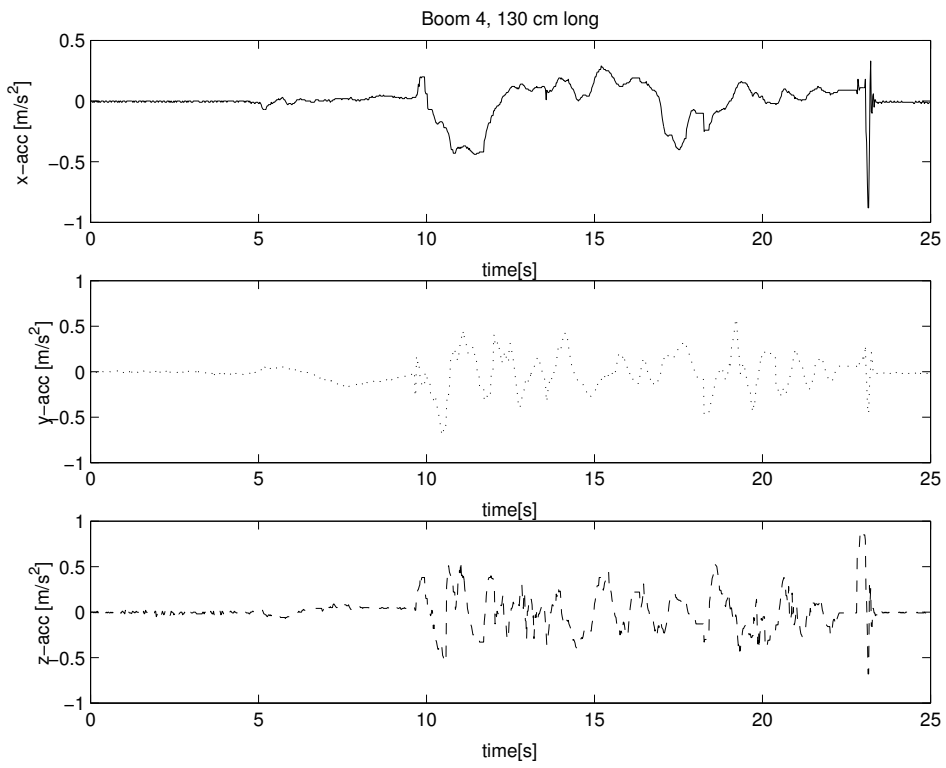


Figure 6.18: x, y, and z-acceleration for bom4.

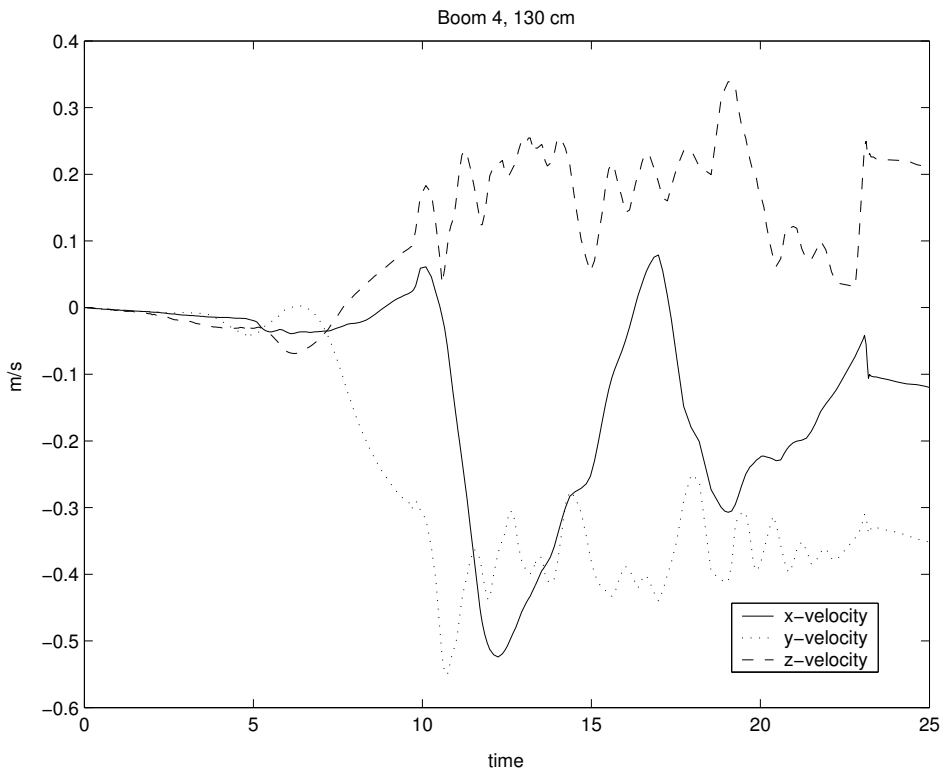


Figure 6.19: x, y, and z-velocity for bom4.

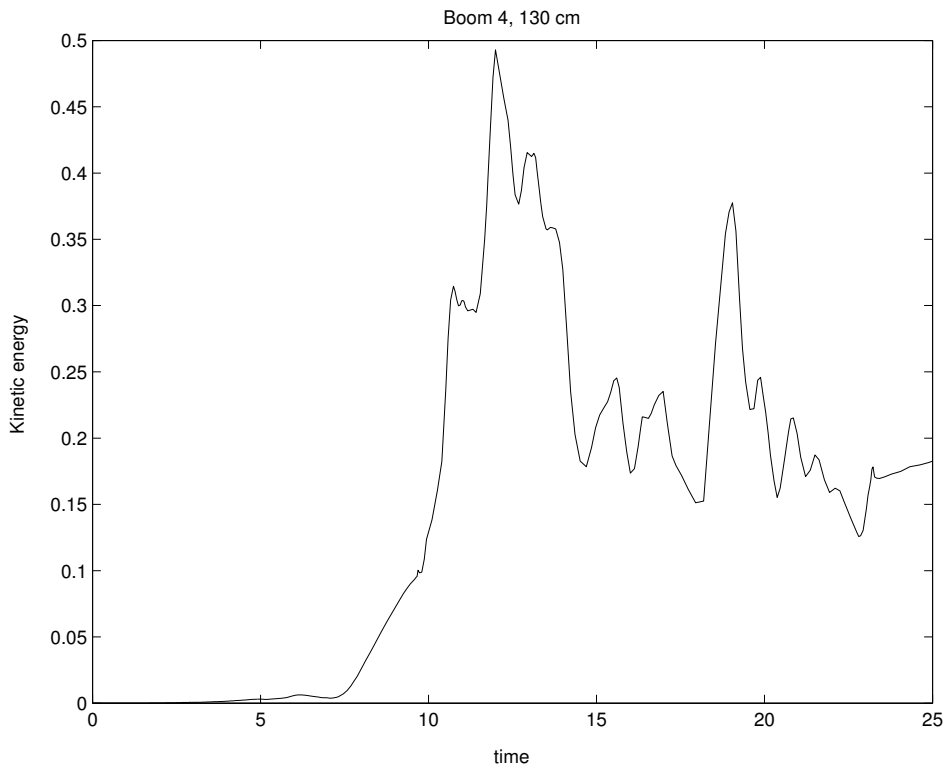


Figure 6.20: Kinetic energy for bom4.

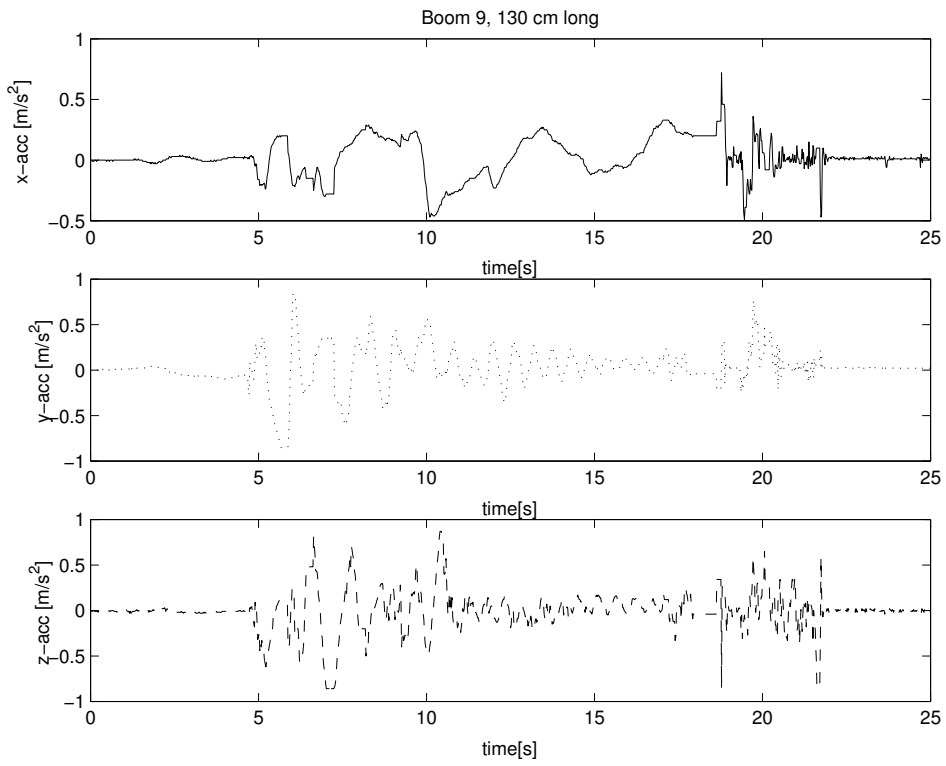


Figure 6.21: x, y, and z-acceleration for bom9.

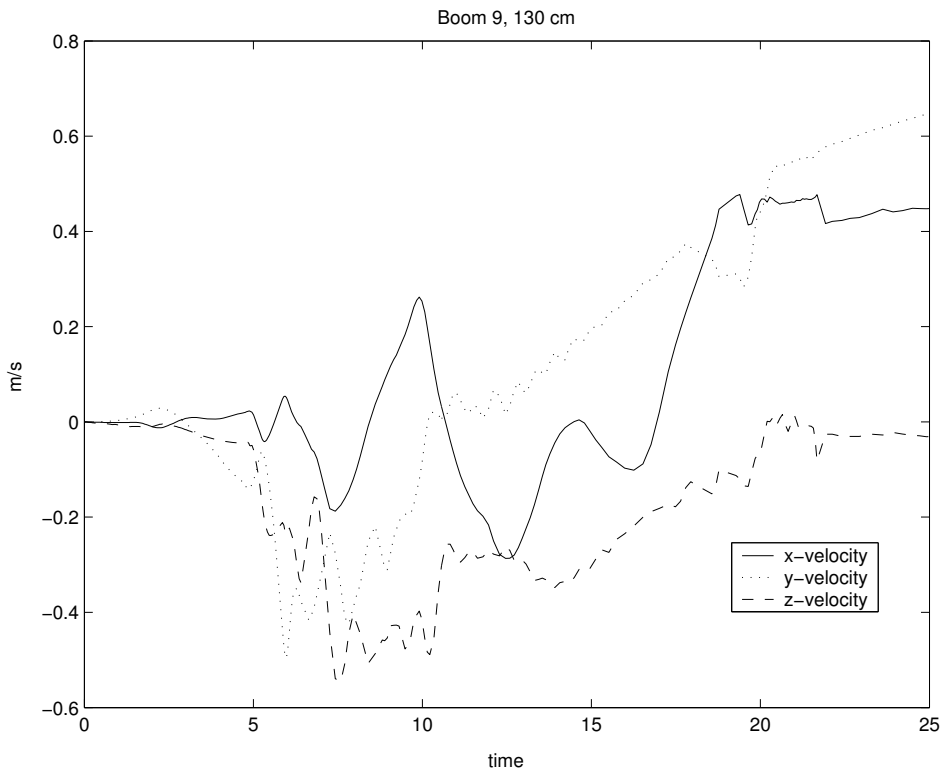


Figure 6.22: x, y, and z-velocity for bom9.

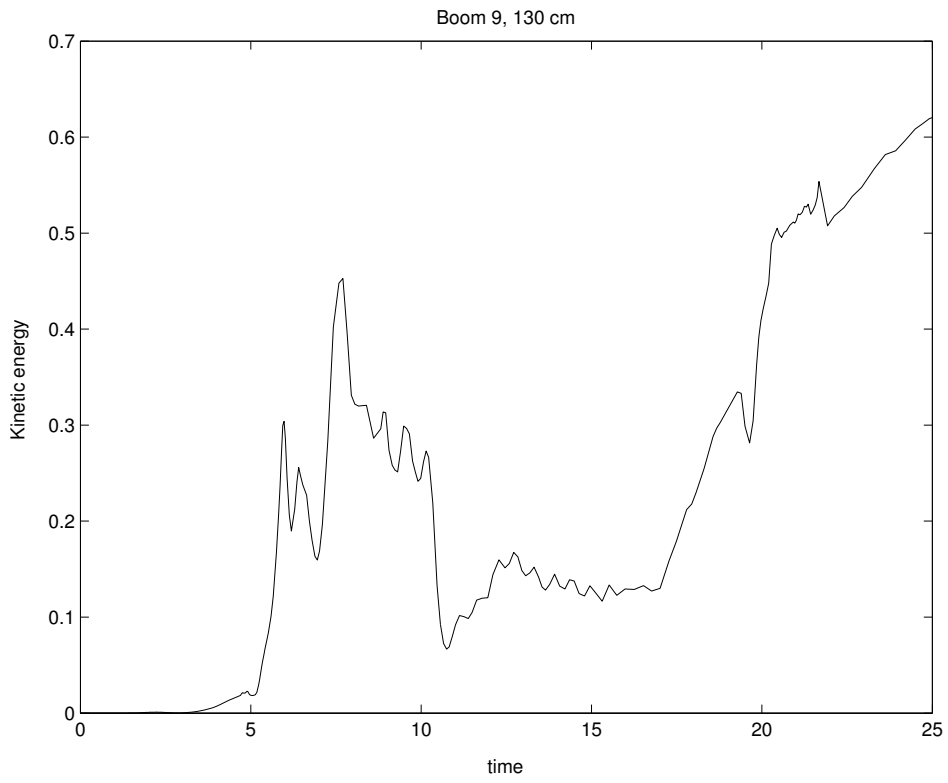


Figure 6.23: Kinetic energy for for bom9.

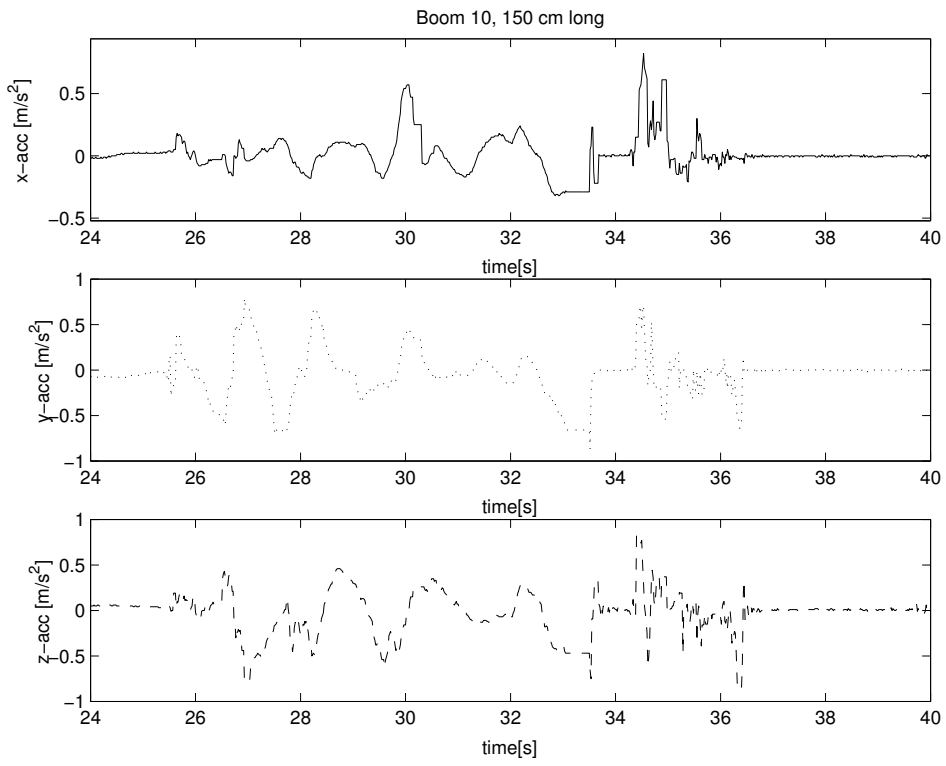


Figure 6.24: x, y, and z-acceleration for bom10.

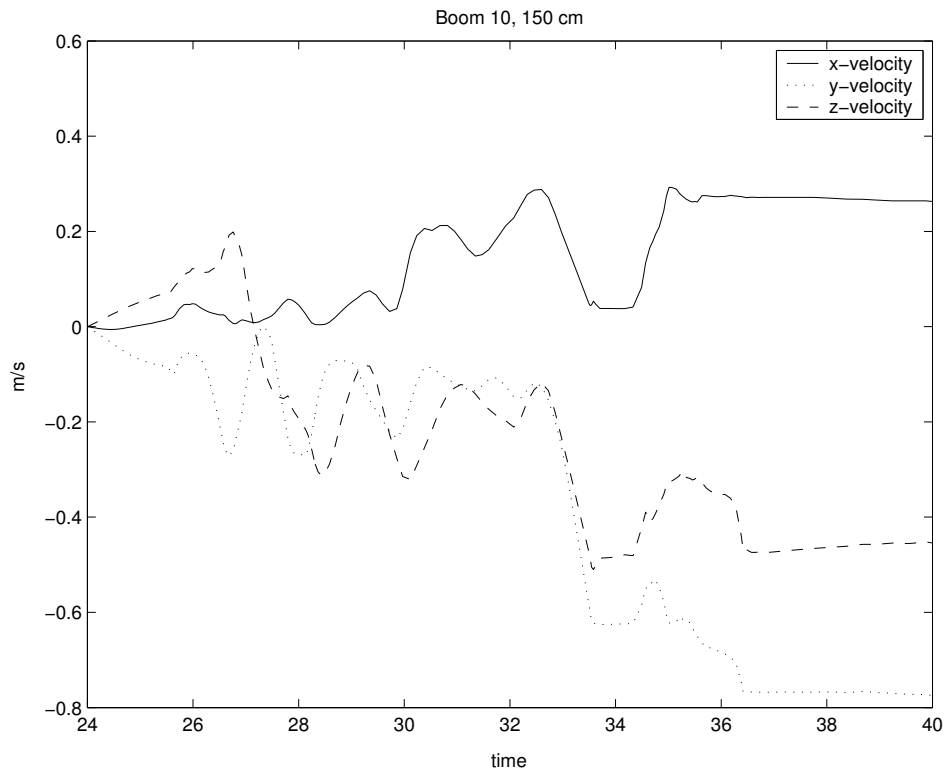


Figure 6.25: x, y, and z-velocity for bom10.

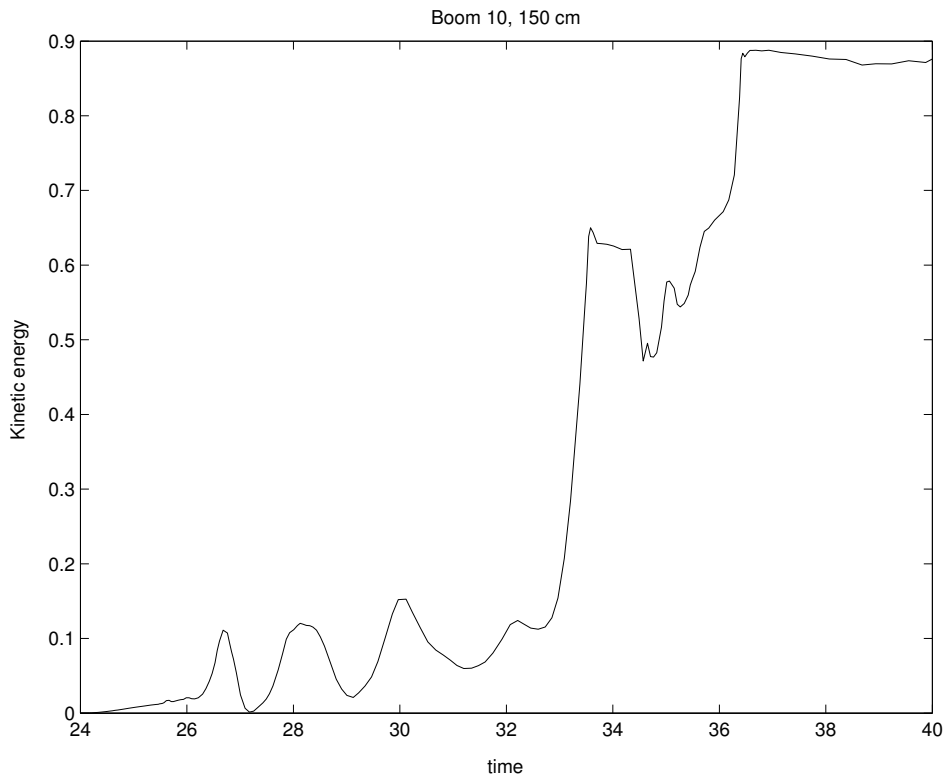


Figure 6.26: Kinetic energy for bom10.

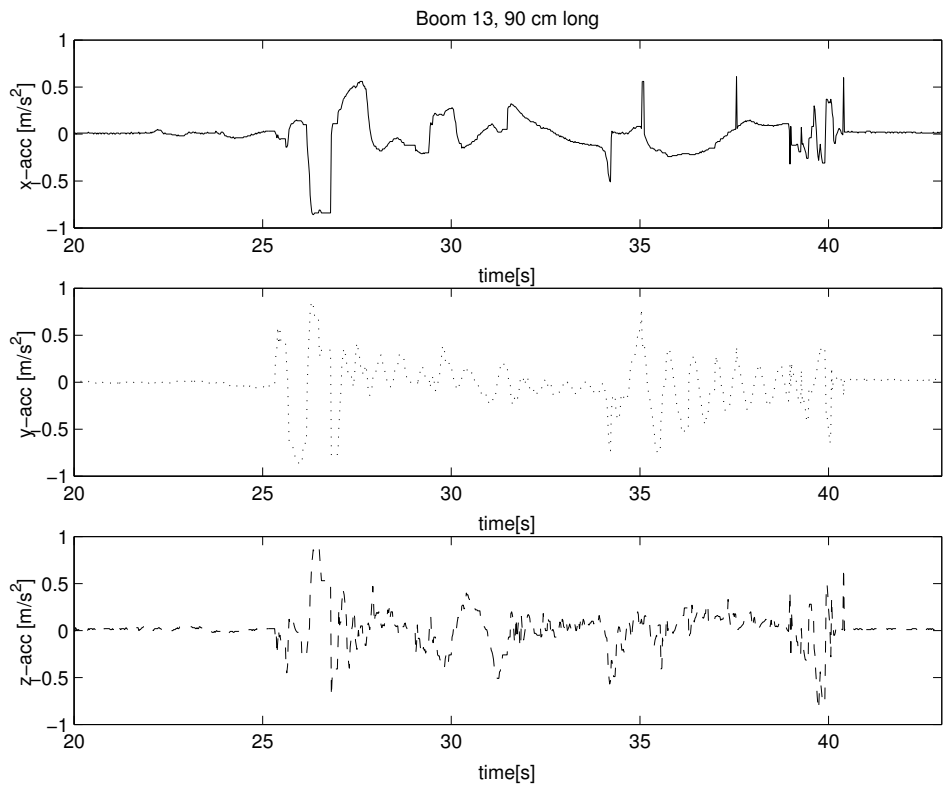


Figure 6.27: x, y, and z-acceleration for bom13.

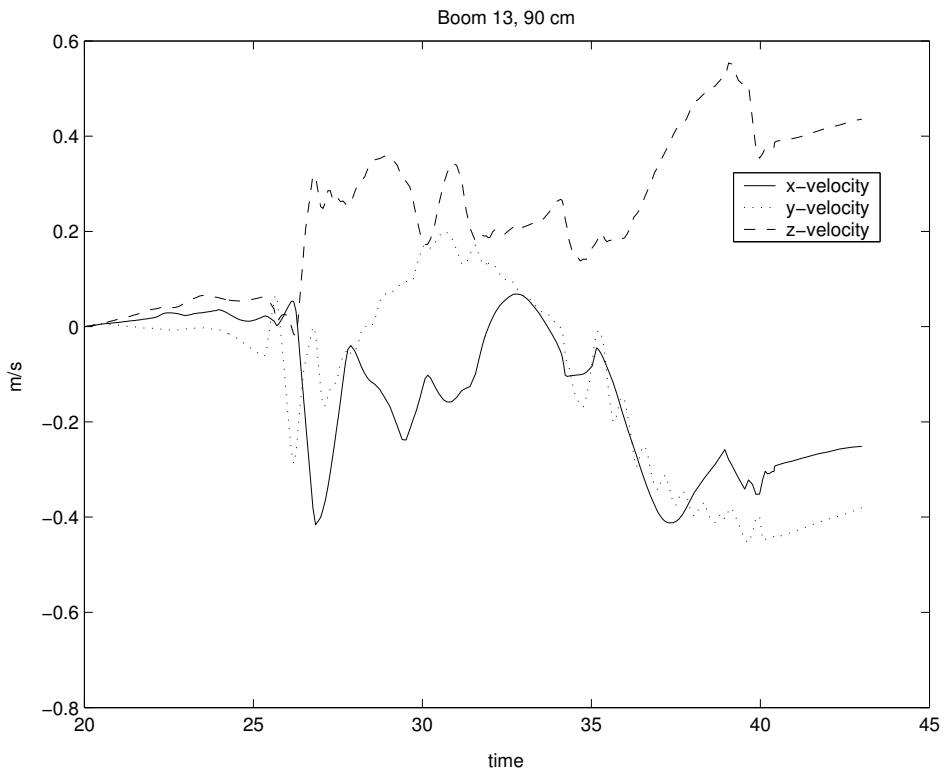


Figure 6.28: x, y, and z-velocity for bom13.

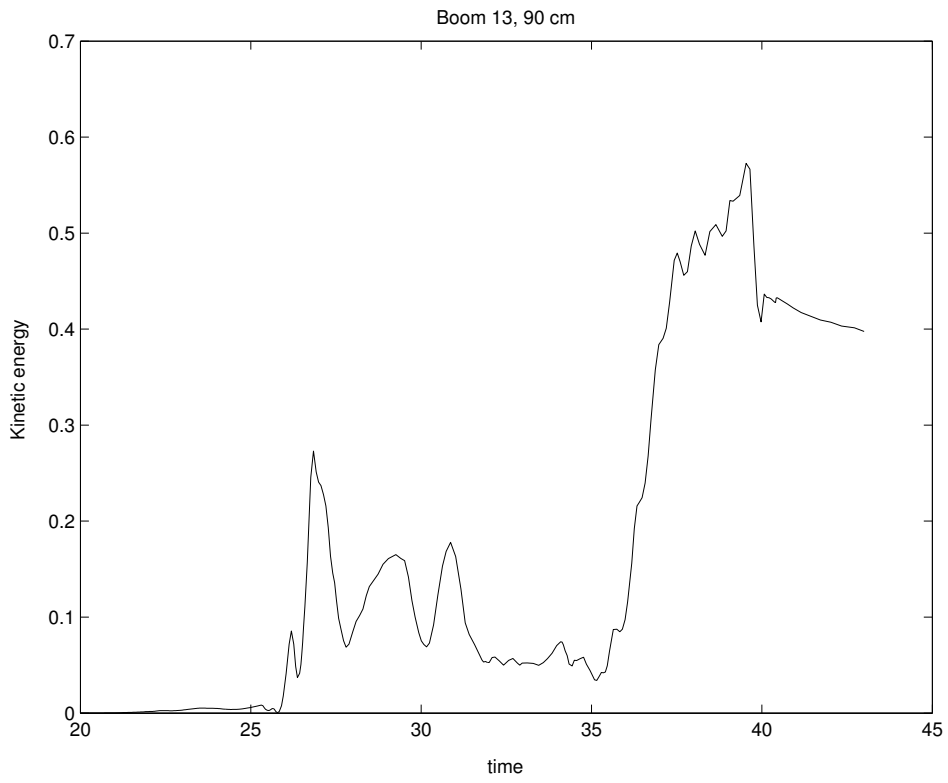


Figure 6.29: Kinetic energy for bom13.

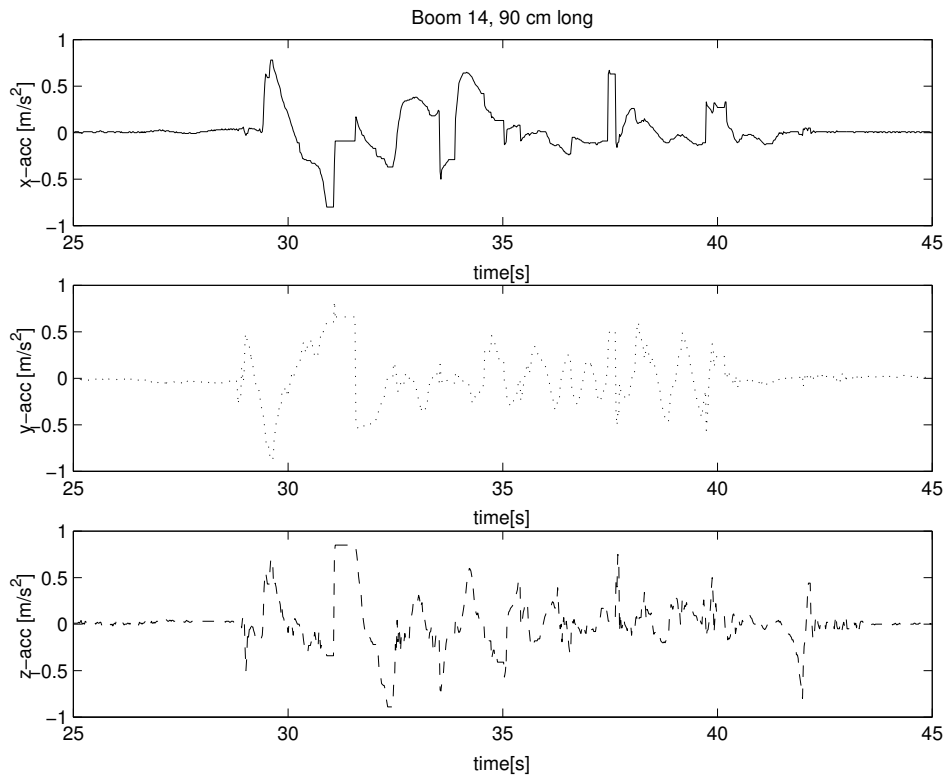


Figure 6.30: x, y, and z-acceleration for bom13.

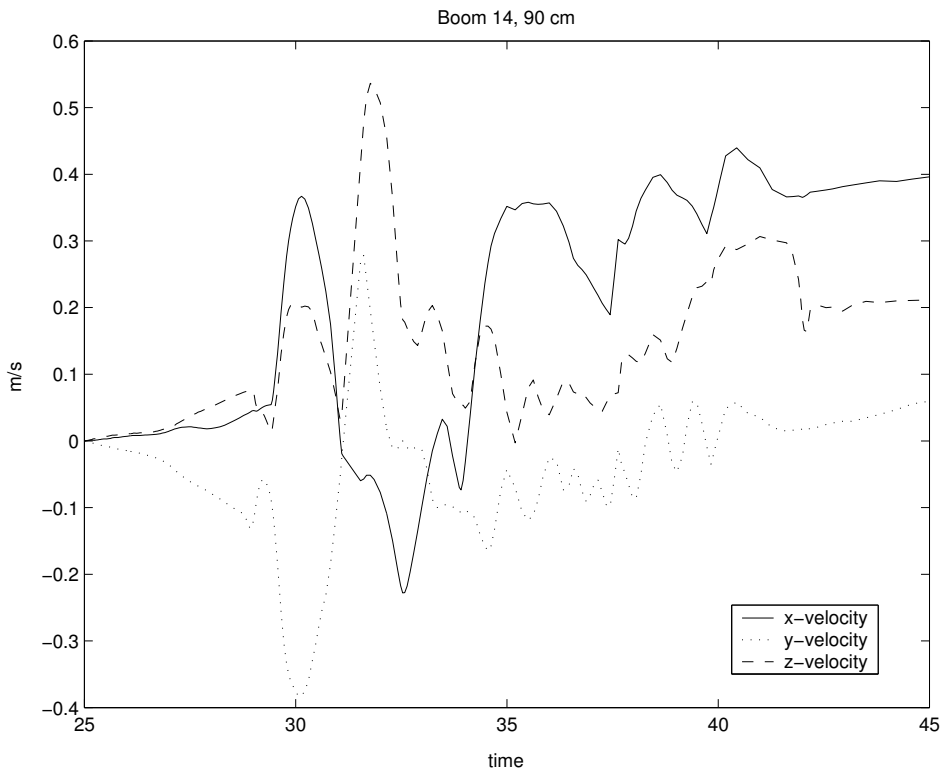


Figure 6.31: x, y, and z-velocity for bom14.

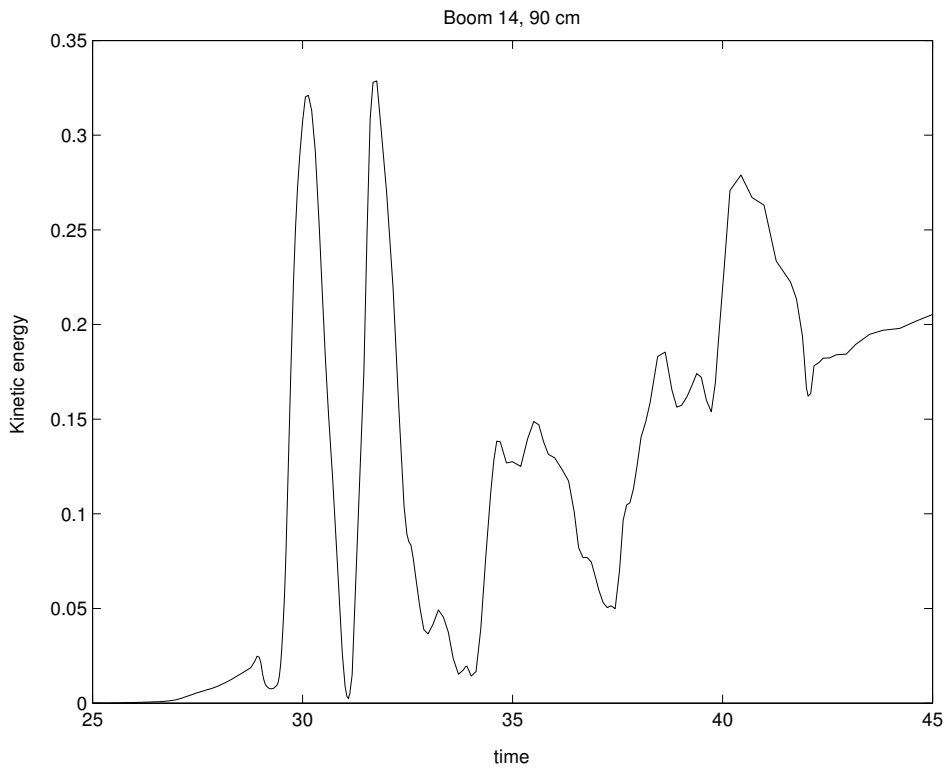


Figure 6.32: Kinetic energy for bom14.

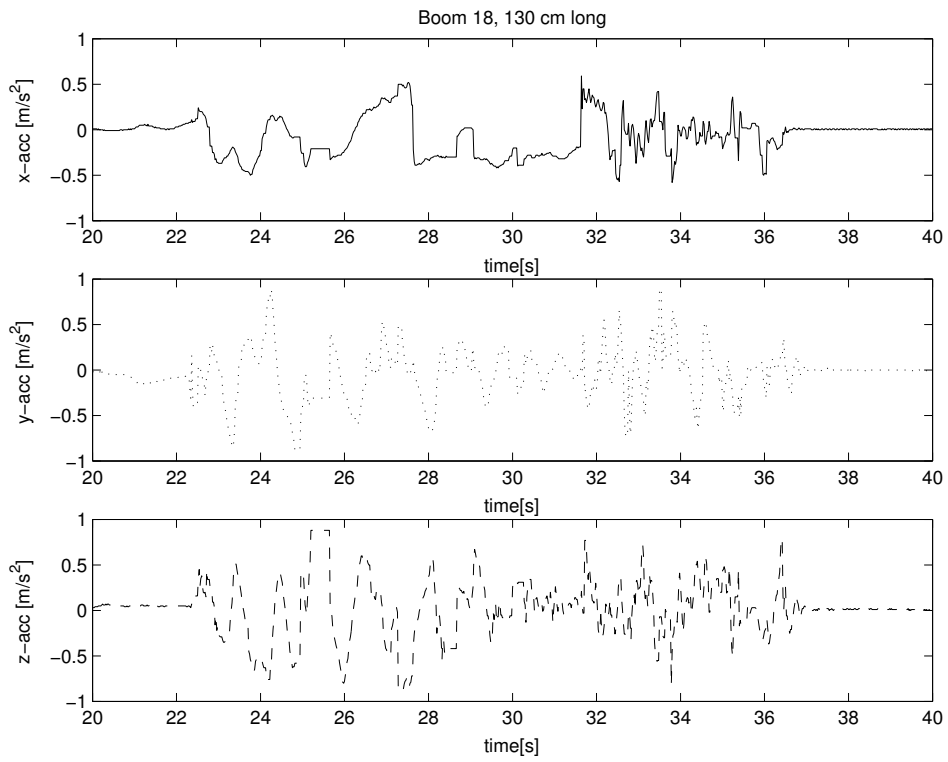


Figure 6.33: x, y, and z-acceleration for bom18.

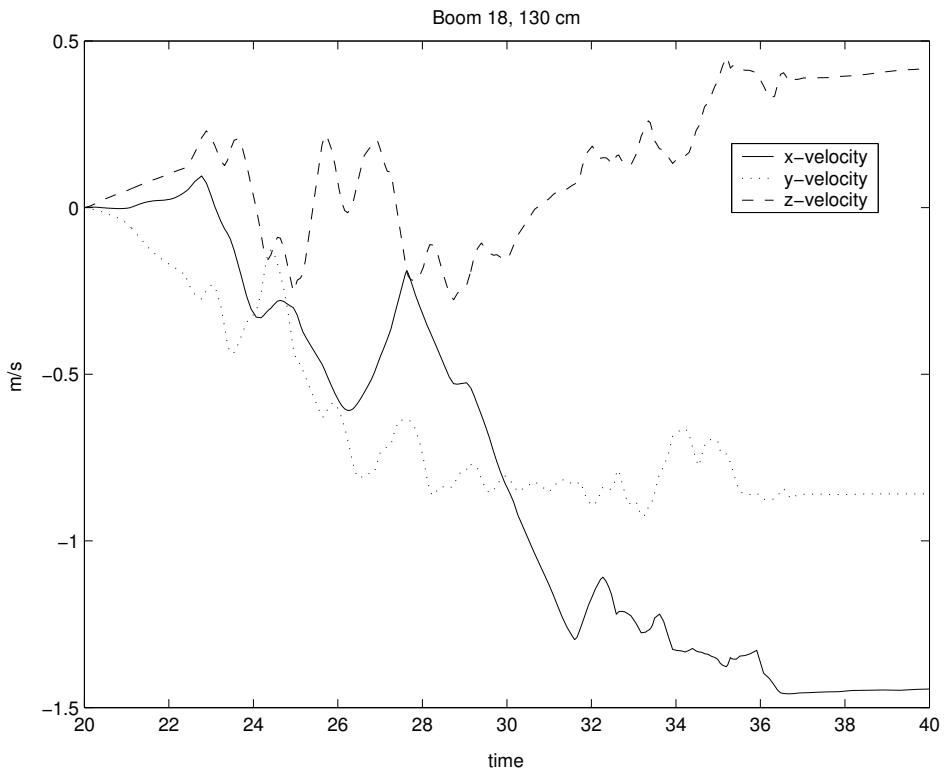


Figure 6.34: x, y, and z-velocity for bom18.

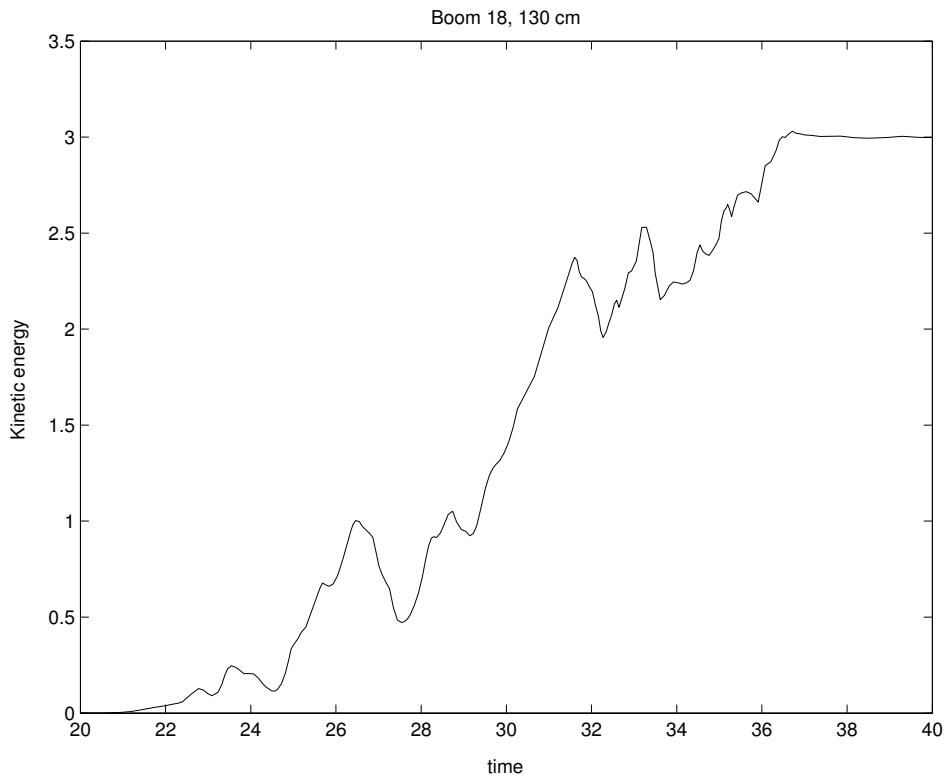


Figure 6.35: Kinetic energy for bom18.

Chapter 7

Vibrations

7.1 Analysis of resonance frequencies

It is important to identify the resonance frequencies of the satellite and boom in order to construct the control system properly (or modify the booms length and mass to fit the control system). If the resonance frequencies are not taken into consideration, magnetic torques from the active actuators may excite elastic oscillations and cause large control deviations. In this chapter we will analyze and identify the satellites resonance frequencies to avoid this problem.

The boom is modelled as a homogeneous Euler-Beroulli beam of length l . The elastic deformation is denoted $w(x, t)$ where x is the boom-coordinate and the mass, m_b is fixed at the end of the boom $x = l$. The equation describing the lateral vibrations is:

$$c^2 \frac{\delta^4 w}{\delta x^4} + \frac{\delta^2 w}{\delta t^2} = 0 \quad (7.1)$$

where $c^2 = \frac{EI}{\rho}$, E =elastic modulus, I = area moment of inertia where the tip-mass is attached to the boom= $\int_0^x \int_{-y/2}^{y/2} y^2 dy dx = \frac{\text{thickness} \cdot \text{width}^3}{12}$ and ρ =density of the boom (kg/m).

Using 7.1 with separation of variables $w(t) = \phi(x)q(t)$ gives

$$c^2 \phi^{(4)}(x)q(t) + \ddot{q}(t)\phi(x) = 0 \quad (7.2)$$

$$\frac{\phi^{(4)}(x)}{\phi(x)} = -\frac{\ddot{q}(t)}{c^2 q(t)} = \beta^4 \quad (7.3)$$

this gives the two differential equations

$$\ddot{q}(t) + \omega^2 q(t) = 0 \quad (7.4)$$

$$\phi^{(4)}(x) - \beta^4 \phi(x) = 0 \quad (7.5)$$

where

$$\beta^4 = \frac{\omega^2}{c^2} \quad (7.6)$$

We see that the differential equation for $q(t)$ 7.4 is a simple harmonic oscillator and the differential equation for $\phi(x)$ is of fourth order. The solution is:

$$\phi(x) = C_1 \cos(\beta x) + C_2 \sin(\beta x) + C_3 \cosh(\beta x) + C_4 \sinh(\beta x) \quad (7.7)$$

where $C_{i=1..4}$ are constraints found by the boundary conditions.

Derivative of 7.7 gives:

$$\phi'(x) = -\beta[C_1 \sin(\beta l) - C_2 \cos(\beta l) - C_3 \sinh(\beta l) - C_4 \cosh(\beta l)] \quad (7.8)$$

$$\phi''(x) = -\beta^2[C_1 \cos(\beta l) + C_2 \sin(\beta l) - C_3 \cosh(\beta l) - C_4 \sinh(\beta l)] \quad (7.9)$$

$$\phi'''(x) = \beta^3[C_1 \sin(\beta l) - C_2 \cos(\beta l) + C_3 \sinh(\beta l) + C_4 \cosh(\beta l)] \quad (7.10)$$

7.1.1 Constrained modes

First we will investigate the unrealistic but relative simple constrained modes. We are assuming that the satellite is non-moving, which implies that the boom is fixed on the satellite end (at $x = 0$). In this scenario we have four boundary conditions. The first two comes from the fact that the boom end connected to the satellite is fixed and non-moving

$$\phi(0) = 0 \quad (7.11)$$

$$\phi'(0) = 0 \quad (7.12)$$

At the boom end connected to the tip-mass ($x = l$) the boundary conditions arise from the fact that the bending moment at the tip end is zero:

$$\phi''(l) = 0 \quad (7.13)$$

and that the shearing force is proportional to the acceleration of mass:

$$EIq(t)\phi'''(l) = m_b \ddot{q}(t)\phi(l) \quad (7.14)$$

Using 7.11 and 7.12 we get that $C_3 = -C_1$ and $C_4 = -C_2$. This implies that:

$$\phi(x) = C_1(\cos(\beta x) - \cosh(\beta x)) + C_2(\sin(\beta x) - \sinh(\beta x)) \quad (7.15)$$

$$\phi'(x) = -\beta[C_1(\sin(\beta x) + \sinh(\beta x)) - C_2(\cos(\beta x) - \cosh(\beta x))] \quad (7.16)$$

$$\phi''(x) = -\beta^2[C_1(\cos(\beta x) + \cosh(\beta x)) + C_2(\sin(\beta x) + \sinh(\beta x))] \quad (7.17)$$

$$\phi'''(x) = \beta^3[C_1(\sin(\beta x) - \sinh(\beta x)) - C_2(\cos(\beta x) + \cosh(\beta x))] \quad (7.18)$$

Using 7.13 we get:

$$C_1(\cos(\beta l) + \cosh(\beta l)) + C_2(\sin(\beta l) + \sinh(\beta l)) = 0 \quad (7.19)$$

Using 7.4 with 7.14 we get

$$EIq(t)\phi'''(l) = -\omega^2 q(t)m_b\phi(l) \quad (7.20)$$

$$EIq(t)\phi'''(l) = -\beta^4 \frac{EI}{\rho} q(t)m_b\phi(l) \quad (7.21)$$

$$\phi'''(l) = -\beta^4 \frac{m_b}{\rho} \phi(l) \quad (7.22)$$

Using 7.18 and 7.15 with the last function, we get

$$\begin{aligned} & C_1[\sin(\beta l) - \sinh(\beta l) + \frac{m_b}{\rho}\beta(\cos(\beta l) - \cosh(\beta l))] \\ & + C_2[-\cos(\beta l) - \cosh(\beta l) + \frac{m_b}{\rho}(\sin(\beta l) - \sinh(\beta l))] \\ & = 0 \end{aligned} \quad (7.23)$$

7.19 and 7.23 can be written in matrix form

$$\mathbf{D}_{uc} \begin{bmatrix} C_1 \\ C_2 \end{bmatrix} = 0 \quad (7.24)$$

where

$$\mathbf{D}_{uc} = \begin{bmatrix} \cos(\beta l) + \cosh(\beta l) & \sin(\beta l) + \sinh(\beta l) \\ \sin(\beta l) - \sinh(\beta l) + \frac{m_b}{\rho}\beta(\cos(\beta l) - \cosh(\beta l)) & -\cos(\beta l) - \cosh(\beta l) + \frac{m_b}{\rho}(\sin(\beta l) - \sinh(\beta l)) \end{bmatrix} \quad (7.25)$$

A nontrivial solution for C_1 and C_2 exist when $\det \mathbf{D}_{us} = 0$. When we solve this we get:

$$1 + \cos(\beta l) \cosh(\beta l) + \frac{m_b}{\rho}\beta(\cos(\beta l) \sinh(\beta l) - \sin(\beta l) \cosh(\beta l)) \quad (7.26)$$

7.1.2 Unconstrained modes

The unconstrained modes are the modes of the actual physical system. The boundary conditions on the satellite side of the boom are made realistic by assuming that the boom is fixed to a mass m_s and a torque supplied by the magnetic coils (around the axis where the boom is attached to the satellite) I_s . The first boundary condition on the satellite side of the boom is that the bending moment is

$$EIq(t)\phi''(0) = -I_s\ddot{q}\phi'(0) \quad (7.27)$$

The second boundary condition is that the shearing force is proportional to the acceleration of the mass:

$$EIq(t)\phi'''(0) = m_s\ddot{q}\phi'(0) \quad (7.28)$$

The boundary conditions on the tip-mass-end of the boom are the same as in the constrained mode, namely

$$\phi''(l) = 0 \quad (7.29a)$$

$$EIq(t)\phi'''(l) = m_b\ddot{q}(t)\phi(l) \quad (7.30a)$$

Inserting 7.4 in 7.27 gives

$$\phi''(0) = \beta^4 \frac{I_s}{\rho} \phi'(0) \quad (7.31)$$

Inserting 7.8 and 7.9 into the last expression we get

$$C_3 = C_1 + a_1(C_2 + C_4) \quad (7.32)$$

where

$$a_1 = \frac{I_s}{\rho} \beta^3 \quad (7.33)$$

Continuing with the next boundary condition 7.28 and once again inserting 7.4 we get

$$\phi'''(0) = -\beta^4 \frac{m_s}{\rho} \phi(0) \quad (7.34)$$

Inserting 7.7 and 7.10 into the last expression we get

$$C_4 = C_2 + a_2(C_1 + C_3) \quad (7.35)$$

where

$$a_2 = -\frac{m_s}{\rho}\beta \quad (7.36)$$

Combining 7.32 and 7.35 we get

$$C_3 = b_2C_1 + b_3C_2 \quad (7.37)$$

$$C_4 = b_1C_1 + b_2C_2 \quad (7.38)$$

where

$$b_1 = \frac{2a_2}{1 - a_1a_2} \quad (7.39)$$

$$b_2 = \frac{1 + a_1a_2}{1 - a_1a_2} \quad (7.40)$$

$$b_3 = \frac{2a_1}{1 - a_1a_2} \quad (7.41)$$

Combining the boundary condition 7.29a and 7.9, and using 7.37 and 7.38 we get

$$\begin{aligned} & C_1[-\cos(\beta l) + b_2 \cosh(\beta l) + b_1 \sinh(\beta l)] \\ & + C_2[-\sin(\beta l) + b_3 \cosh(\beta l) + b_2 \sinh(\beta l)] \\ & = 0 \end{aligned} \quad (7.42)$$

Rewriting the last boundary condition (7.30a) we get

$$\phi'''(l) = -\beta^3 a_3 \phi(l) \quad (7.43)$$

where

$$a_3 = \frac{m_b}{\rho}\beta \quad (7.44)$$

Inserting 7.10, 7.7, 7.37, and 7.38 into this boundary condition we get

$$\begin{aligned} & C_1[\sin(\beta l) + b_1 \cosh(\beta l) + b_2 \sinh(\beta l) \\ & + a_3(\cos(\beta l) + b_1 \sinh(\beta l) + b_2 \cosh(\beta l))] \\ & + C_2[-\cos(\beta l) + b_2 \cosh(\beta l) + b_3 \sinh(\beta l) \\ & + a_3(\sin(\beta l) + b_2 \sinh(\beta l) + b_3 \cosh(\beta l))] \\ & = 0 \end{aligned} \quad (7.45)$$

As for the unconstrained mode, 7.42 and 7.45 can be written in matrix form:

$$\mathbf{D}_c \begin{bmatrix} C_1 \\ C_2 \end{bmatrix} = 0 \quad (7.46)$$

with obvious matrix-elements d_{ij} . Nontrivial solutions for C_1 and C_2 exist when $\det \mathbf{D}_c = 0$, which gives the quite unpleasant equation

$$\begin{aligned} & 1 + b_2^2 - b_1 b_3 + b_1(\sin(\beta l) \cosh(\beta l) - \cos(\beta l) \sinh(\beta l)) & (7.47) \\ & - 2b_2(\cos(\beta l) \cosh(\beta l)) \\ & - b_3(\cos(\beta l) \sinh(\beta l) + \sin(\beta l) \cosh(\beta l) + a_3[2b_1(\sin(\beta l) \sinh(\beta l)) \\ & + 2b_2(\sin(\beta l) \cosh(\beta l) \\ & - \cos(\beta l) \sinh(\beta l)) - 2b_3(\cos(\beta l) \cosh(\beta l)) \\ & = 0 \end{aligned}$$

Who can, with the introduction of some constants, be written as

$$\begin{aligned} & d_1 - d_2 \cos(\beta l) \cosh(\beta l) - d_3 \cos(\beta l) \sinh(\beta l) & (7.48) \\ & + d_4 \sin(\beta l) \cosh(\beta l) + d_5 \sin(\beta l) \sinh(\beta l) \\ & = 0 \end{aligned}$$

where the constants are defined as

$$d_1 = 1 - b_2^2 - b_1 b_3 \quad (7.49)$$

$$d_2 = 2b_2 + 2a_3 b_3 \quad (7.50)$$

$$d_3 = b_1 + b_3 + 2a_3 b_2 \quad (7.51)$$

$$d_4 = b_1 - b_3 + 2a_3 b_2 \quad (7.52)$$

$$d_5 = 2a_3 b_1 \quad (7.53)$$

7.48 is solved in matlab and the following frequencies are found.

For the curved side of the boom (pitch movement):

Mode	$\frac{\omega}{2\pi}$	$T = \frac{2\pi}{\omega}$
0	0	∞
1	0.012 Hz	83.33 s
2	18.71 Hz	0.053 s
3	305.55 Hz	0.0033 s
4	979.3 Hz	0.0010 s

For the thin side of the boom (roll movement):

Mode	$\frac{\omega}{2\pi}$	$T = \frac{2\pi}{\omega}$
0	0	∞
1	661 Hz	0.0015 s
2	778 Hz	0.0013 s
3	936 Hz	0.0011 s
4	1954 Hz	0.0005 s

Chapter 8

Conclusion

During the work with this report a gravity boom/antenna system for the NCube satellite has been designed, build, and tested in several environments. The deployment mechanisms are working in vacuum and under severe temperature conditions. The structural aspect of the system is also tested in the cold tunnel and found satisfactory. The rigidness of the boom has been tested in zero-g, and even though no connection between the length of the boom and impact on the satellite were discovered, some lessons were learned, namely that the boom is rigid enough, and that the satellite will achieve both spin and acceleration when the boom deploys, and that the magnetic coils will have to compensate for these unwanted effects. A more accurate moment of inertia modelling and calculation were also done, even though the answers did not deviate much from the rudimentary calculations done in Indergaard (2002) This was expected because of the significance the boom have in these kind of calculations.

Appendix A

Matlab code

```
% ncubemoi.m
% Calculates the Ncube satellites moment of inertia
% for boom and antennas deployed and undeployed.

% The satellite is divided into different sides (termed Z, N, A, B, C, D)
% and the moment if inertia is calculated for each parts with respect to
% the center of the satellite

% The N-side
% Undelopyed boom
% Tip mass

M_1=0.040;           % Tip mass
h_1=0.013;          % Height of cylinder
r_1=0.009;          % Radius of cylinder
r_x_1=0.029;        % Distance between parallel x-axis
r_y_1=0.015;        % Distance between parallel y-axis
r_z_1=0.015;        % Distance between parallel z-axis

I_x_1=(1/12)*M_1*(h_1^2) + (1/4)*M_1*(r_1^2) + M_1*(r_x_1^2);
I_y_1=(1/2)*M_1*(r_1^2) + M_1*(r_y_1^2);
I_z_1=(1/12)*M_1*(h_1^2) + (1/4)*M_1*(r_1^2) + M_1*(r_z_1^2);

% Coiled measuring tape

M_2=0.015;          % Mass of measuring tape
h_2=0.013;          % Height of measuring tape
r_22=0.017;         % Outer radius of measuring tape
r_21=0.01;          % Inner radius of measuring tape
r_x_2=0.029;        % Distance between parallel x-axis
```

r_y_2=0.015; % Distance between parallel y-axis
r_z_2=0.015; % Distance between parallel z-axis

I_x_2=(1/12)*M_2*(h_2)^2 + (1/4)*M_2*((r_22^2)+(r_21^2)) + M_2*(r_x_2^2);
I_y_2=(1/2)*M_2*((r_22^2)+(r_21^2)) + M_2*(r_y_2^2);
I_z_2=(1/12)*M_2*(h_2)^2 + (1/4)*M_2*((r_22^2)+(r_21^2)) + M_2*(r_y_2^2);

% Boom box

M_3=0.03; % Mass boom box
l_x_3=0.05; % Length of box in x-direction
l_y_3=0.02; % Length of box in y-direction
l_z_3=0.05; % Length of box in z-direction
r_x_3=0.025; % Distance between parallel x-axis
r_y_3=0.025; % Distance between parallel y-axis
r_z_3=0.025; % Distance between parallel z-axis

I_x_3=(1/12)*M_3*(l_y_3^2) + (1/12)*M_3*(l_z_3^2) + M_3*(r_x_3^2);
I_y_3=(1/12)*M_3*(l_x_3^2) + (1/12)*M_3*(l_z_3^2) + M_3*(r_y_3^2);
I_z_3=(1/12)*M_3*(l_x_3^2) + (1/12)*M_3*(l_y_3^2) + M_3*(r_z_3^2);

% Undeployed antennas

% Coiled antenna 1

M_4=0.001; % Mass of antenna 1
h_4=0.008; % Height of antenna 1
r_42=0.01; % Outer radius of antenna 1
r_41=0.005; % Inner radius of antenna 1
r_x_4=0.01; % Distance between parallel x-axis
r_y_4=0.03; % Distance between parallel y-axis
r_z_4=0.03; % Distance between parallel z-axis

I_x_4=(1/12)*M_4*(h_4)^2 + (1/4)*M_4*((r_42^2)+(r_41^2)) +
M_4*(r_x_4^2);
I_y_4=(1/12)*M_4*(h_4)^2 + (1/4)*M_4*((r_42^2)+(r_41^2)) +
M_4*(r_y_4^2);
I_z_4=(1/2)*M_4*((r_42^2)+(r_41^2)) + M_4*(r_z_4^2);

% Coiled antenna 2

M_5=0.003; % Mass of antenna 2
h_5=0.008; % Height of antenna 2
r_52=0.01; % Outer radius of antenna 2

```

r_51=0.005;           % Inner radius of antenna 2
r_x_5=0.01;          % Distance between parallel x-axis
r_y_5=0.03;          % Distance between parallel y-axis
r_z_5=0.03;          % Distance between parallel z-axis

I_x_5=(1/12)*M_5*(h_5)^2 + (1/4)*M_5*((r_52^2)+(r_51^2)) +
M_5*(r_x_5^2);
I_y_5=(1/12)*M_5*(h_5)^2 + (1/4)*M_5*((r_52^2)+(r_51^2)) +
M_5*(r_y_5^2);
I_z_5=(1/2)*M_5*((r_52^2)+(r_51^2)) + M_5*(r_z_5^2);

% The antenna boxes

M_6=0.03;            % Mass of both antenna boxes!!!!
l_x_6=0.03;          % Length of box in x-direction
l_y_6=0.03;          % Length of box in y-direction
l_z_6=0.01;          % Length of box in z-direction
r_x_6=0.01;          % Distance between parallel x-axis
r_y_6=0.03;          % Distance between parallel y-axis
r_z_6=0.03;          % Distance between parallel z-axis

I_x_6=(1/12)*M_6*(l_y_6^2) + (1/12)*M_6*(l_z_6^2) +
M_6*(r_x_6^2);
I_y_6=(1/12)*M_6*(l_x_6^2) + (1/12)*M_6*(l_z_6^2) +
M_6*(r_y_6^2);
I_z_6=(1/12)*M_6*(l_x_6^2) + (1/12)*M_6*(l_y_6^2) +
M_6*(r_z_6^2);

% Deployed boom
% Tip mass

M_7=0.04;            % Tip mass
h_7=0.013;           % Height of cylinder
r_7=0.009;           % Radius of cylinder
r_x_7=1.5;            % Distance between parallel x-axis
r_y_7=1.5;            % Distance between parallel y-axis
r_z_7=0.009;         % Distance between parallel z-axis

I_x_7=(1/12)*M_7*(h_7^2) + (1/4)*M_7*(r_7^2) +
M_7*(r_x_7^2);
I_y_7=(1/2)*M_7*(r_7^2) + M_7*(r_y_7^2);

```

$$I_{z_7} = (1/12) * M_7 * (h_7^2) + (1/4) * M_7 * (r_7^2) + M_7 * (r_{z_7}^2);$$

% Measuring tape

M_8=0.015; % Mass measuring tape
 l_x_8=0.001; % Length of tape in x-direction
 l_y_8=0.013; % Length of tape in y-direction
 l_z_8=1.5; % Length of tape in z-direction
 r_x_8=0.75; % Distance between parallel x-axis
 r_y_8=0.75; % Distance between parallel y-axis
 r_z_8=0; % Distance between parallel z-axis

$$I_{x_8} = (1/12) * M_8 * (l_{y_8}^2) + (1/12) * M_8 * (l_{z_8}^2) + M_8 * (r_{x_8}^2);$$

$$I_{y_8} = (1/12) * M_8 * (l_{x_8}^2) + (1/12) * M_8 * (l_{z_8}^2) + M_8 * (r_{y_8}^2);$$

$$I_{z_8} = (1/12) * M_8 * (l_{x_8}^2) + (1/12) * M_8 * (l_{y_8}^2) + M_8 * (r_{z_8}^2);$$

% Deployed antennas

% Antenna 1

M_9=0.01; % Mass Antenna 1
 l_x_9=0.008; % Length of Antenna 1 in x-direction
 l_y_9=0.17; % Length of Antenna 1 in y-direction
 l_z_9=0.001; % Length of Antenna 1 in z-direction
 r_x_9=0.13; % Distance between parallel x-axis
 r_y_9=0.03; % Distance between parallel y-axis
 r_z_9=0.16; % Distance between parallel z-axis
 phi=45; % Angle between nadir and antenna

$$I_{x_9} = (1/12) * M_9 * \cos(\phi) * (l_{y_9}^2) + (1/12) * M_9 * \sin(\phi) * (l_{z_9}^2) + M_9 * (r_{x_9}^2);$$

$$I_{y_9} = (1/12) * M_9 * (l_{x_9}^2) + (1/12) * M_9 * \sin(\phi) * (l_{z_9}^2) + M_9 * (r_{y_9}^2);$$

$$I_{z_9} = (1/12) * M_9 * (l_{x_9}^2) + (1/12) * M_9 * \cos(\phi) * (l_{y_9}^2) + M_9 * (r_{z_9}^2);$$

% Antenna 2

M_10=0.02; % Mass Antenna 2
 l_x_10=0.008; % Length of Antenna 2 in x-direction

```

l_y_10=0.55; % Length of Antenna 2 in y-direction
l_z_10=0.001; % Length of Antenna 2 in z-direction
r_x_10=0.32; % Distance between parallel x-axis
r_y_10=0.03; % Distance between parallel y-axis
r_z_10=0.32; % Distance between parallel z-axis

I_x_10=(1/12)*M_10*cos(phi)*(l_y_10^2) +
(1/12)*M_10*sin(phi)*(l_z_10^2) + M_10*(r_x_10^2);
I_y_10=(1/12)*M_10*(l_x_10^2) +
(1/12)*M_10*sin(phi)*(l_z_10^2) + M_10*(r_y_10^2);
I_z_10=(1/12)*M_10*(l_x_10^2) +
(1/12)*M_10*cos(phi)*(l_y_10^2) + M_10*(r_z_10^2);

% Antenna boxes

M_11=0.03; % Mass of both Antenna boxes!!!!
l_x_11=0.03; % Length of box in x-direction
l_y_11=0.03; % Length of box in y-direction
l_z_11=0.01; % Length of box in z-direction
r_x_11=0.01; % Distance between parallel x-axis
r_y_11=0.03; % Distance between parallel y-axis
r_z_11=0.03; % Distance between parallel z-axis

I_x_11=(1/12)*M_11*cos(phi)*(l_y_11^2) +
(1/12)*M_11*sin(phi)*(l_z_11^2) + M_11*(r_x_11^2);
I_y_11=(1/12)*M_11*(l_x_11^2) +
(1/12)*M_11*sin(phi)*(l_z_11^2) + M_11*(r_y_11^2);
I_z_11=(1/12)*M_11*(l_x_11^2) +
(1/12)*M_11*cos(phi)*(l_y_11^2) + M_11*(r_z_11^2);

% Batteries

M_12=0.08; % Mass of both batteries!!!!
l_x_12=0.03; % Length of battery in x-direction
l_y_12=0.003; % Length of battery in y-direction
l_z_12=0.04; % Length of battery in z-direction
r_x_12=0.02; % Distance between parallel x-axis
r_y_12=0.02; % Distance between parallel y-axis
r_z_12=0; % Distance between parallel z-axis

I_x_12=(1/12)*M_12*(l_y_12^2) +
(1/12)*M_12*(l_z_12^2) + M_12*(r_x_12^2);

```

$$I_{y_12}=(1/12)*M_{12}*(l_{x_12}^2) + (1/12)*M_{12}*(l_{z_12}^2) + M_{12}*(r_{y_12}^2);$$

$$I_{z_12}=(1/12)*M_{12}*(l_{x_12}^2) + (1/12)*M_{12}*(l_{y_12}^2) + M_{12}*(r_{z_12}^2);$$

% Coils
% Coil in N-Z-plane

M_13=0.025;	% Mass of one coil
h=0.005;	% height of coil
w=0.08;	% width of coil
d=0.005;	% depth of coil (see drawing in text)
r_x_13=0.04;	% Distance between parallel x-axis
r_y_13=0.04;	% Distance between parallel y-axis
r_z_13=0;	% Distance between parallel z-axis

$$I_{x_13_a}=(1/12)*M_{13}*(h^2) + (1/24)*M_{13}*(w^2) + (1/24)*M_{13}*(d^2) + M_{13}*(r_{x_13}^2);$$

$$I_{y_13_a}=(1/12)*M_{13}*(h^2) + (1/24)*M_{13}*(w^2) + (1/24)*M_{13}*(d^2) + M_{13}*(r_{y_13}^2);$$

$$I_{z_13_a}=(1/24)*M_{13}*(w^2) + (1/24)*M_{13}*(d^2) + M_{13}*(r_{z_13}^2);$$

% Coil in A-C-plane

$$I_{x_13_b}=(1/12)*M_{13}*(h^2) + (1/24)*M_{13}*(w^2) + (1/24)*M_{13}*(d^2) + M_{13}*(r_{x_13}^2);$$

$$I_{y_13_b}=(1/24)*M_{13}*(w^2) + (1/24)*M_{13}*(d^2) + M_{13}*(r_{y_13}^2);$$

$$I_{z_13_b}=(1/12)*M_{13}*(h^2) + (1/24)*M_{13}*(w^2) + (1/24)*M_{13}*(d^2) + M_{13}*(r_{z_13}^2);$$

% Coil in B-D-plane

$$I_{x_13_c}=(1/24)*M_{13}*(w^2) + (1/24)*M_{13}*(d^2) + M_{13}*(r_{x_13}^2);$$

$$I_{y_13_c}=(1/12)*M_{13}*(h^2) + (1/24)*M_{13}*(w^2) + (1/24)*M_{13}*(d^2) + M_{13}*(r_{y_13}^2);$$

$$I_{z_13_c}=(1/12)*M_{13}*(h^2) + (1/24)*M_{13}*(w^2) + (1/24)*M_{13}*(d^2) + M_{13}*(r_{z_13}^2);$$

% Walls
% Walls in A-C-plane

```

M_14=0.05;           % Mass of one wall
h_14=0.08;          % height of wall
w_14=0.10;          % width of wall
d_14=0.005;         % thickness of wall
r_x_14=0.04;        % Distance between parallel x-axis
r_y_14=0;           % Distance between parallel y-axis
r_z_14=0.04;        % Distance between parallel z-axis

I_x_14=(1/6)*M_14*(h_14^2) + (1/6)*M_14*(w_14^2) +
2*M_14*(r_x_14^2);
I_y_14=(1/6)*M_14*(h_14^2) + (1/6)*M_14*(d_14^2) +
2*M_14*(r_y_14^2);
I_z_14=(1/6)*M_14*(w_14^2) + (1/6)*M_14*(d_14^2) +
2*M_14*(r_z_14^2);

% Walls in B-D-plane

M_15=0.05;           % Mass of one wall
h_15=0.08;          % height of wall
w_15=0.10;          % width of wall
d_15=0.005;         % thickness of wall
r_x_15=0;           % Distance between parallel x-axis
r_y_15=0.04;        % Distance between parallel y-axis
r_z_15=0.04;        % Distance between parallel z-axis

I_x_15=(1/6)*M_15*(h_15^2) + (1/6)*M_15*(d_15^2) +
2*M_15*(r_x_15^2);
I_y_15=(1/6)*M_15*(h_15^2) + (1/6)*M_15*(w_15^2) +
2*M_15*(r_y_15^2);
I_z_15=(1/6)*M_15*(w_15^2) + (1/6)*M_15*(d_15^2) +
2*M_15*(r_z_15^2);

% Wall Zenith

M_16=0.05;           % Mass of one wall
h_16=0.08;          % height of wall
w_16=0.10;          % width of wall
d_16=0.005;         % thickness of wall
r_x_16=0.04;        % Distance between parallel x-axis
r_y_16=0.04;        % Distance between parallel y-axis
r_z_16=0;           % Distance between parallel z-axis

```

```

I_x_16=(1/12)*M_16*(h_16^2) +
(1/12)*M_16*(d_16^2) + M_16*(r_x_16^2);
I_y_16=(1/12)*M_16*(d_16^2) +
(1/12)*M_16*(w_16^2) + M_16*(r_y_16^2);
I_z_16=(1/12)*M_16*(w_16^2) +
(1/12)*M_16*(h_16^2) + M_16*(r_z_16^2);

```

```

% Circuit cards placed on side C
% Add one for each card.....
% Remember to add it to the total....

```

```

M_17_a=0;           % Mass of card
h_17_a=0;          % height of card
w_17_a=0;          % width of card
d_17_a=0;          % thickness of card
r_x_17_a=0;        % Distance between parallel x-axis
r_y_17_a=0;        % Distance between parallel y-axis
r_z_17_a=0;        % Distance between parallel z-axis

```

```

I_x_17_a=(1/12)*M_17_a*(w_17_a^2) +
(1/12)*M_17_a*(d_17_a^2) + M_17_a*(r_x_17_a^2);
I_y_17_a=(1/12)*M_17_a*(d_17_a^2) +
(1/12)*M_17_a*(h_17_a^2) + M_17_a*(r_y_17_a^2);
I_z_17_a=(1/12)*M_17_a*(w_17_a^2) +
(1/12)*M_17_a*(h_17_a^2) + M_17_a*(r_z_17_a^2);

```

```

% .....
% Aluminium structures (nadir wall and internal)
% Add one for each card.....
% Remember to add it to the total....

```

```

M_18_a=0;           % Mass of card
x_18_a=0;          % height of card
y_18_a=0;          % width of card
z_18_a=0;          % thickness of card
r_x_18_a=0;        % Distance between parallel x-axis
r_y_18_a=0;        % Distance between parallel y-axis
r_z_18_a=0;        % Distance between parallel z-axis
I_x_18_a=(1/12)*M_18_a*(y_18_a^2) +
(1/12)*M_18_a*(z_18_a^2) + M_18_a*(r_x_18_a^2);
I_y_18_a=(1/12)*M_18_a*(x_18_a^2) +
(1/12)*M_18_a*(z_18_a^2) + M_18_a*(r_y_18_a^2);

```

$$I_{z_18_a}=(1/12)*M_{18_a}*(x_{18_a}^2) + (1/12)*M_{18_a}*(y_{18_a}^2) + M_{18_a}*(r_{z_18_a}^2);$$

%

% Total

% Undeployed

$$I_{x_tot_u}=I_{x_1}+I_{x_2}+I_{x_3}+I_{x_4}+I_{x_6}+I_{x_12}+I_{x_13_a}+I_{x_13_b}+I_{x_13_c}+I_{x_14}+I_{x_15}+I_{x_16}+I_{x_17_a}+I_{x_18_a};$$

$$I_{y_tot_u}=I_{y_1}+I_{y_2}+I_{y_3}+I_{y_4}+I_{y_6}+I_{y_12}+I_{y_13_a}+I_{y_13_b}+I_{y_13_c}+I_{y_14}+I_{y_15}+I_{y_16}+I_{y_17_a}+I_{y_18_a};$$

$$I_{z_tot_u}=I_{z_1}+I_{z_2}+I_{z_3}+I_{z_4}+I_{z_6}+I_{z_12}+I_{z_13_a}+I_{z_13_b}+I_{z_13_c}+I_{z_14}+I_{z_15}+I_{z_16}+I_{z_17_a}+I_{z_18_a};$$

$$I_{x_tot_dep}=I_{x_3}+I_{x_7}+I_{x_8}+I_{x_9}+I_{x_10}+I_{x_11}+I_{x_12}+I_{x_13_a}+I_{x_13_b}+I_{x_13_c}+I_{x_14}+I_{x_15}+I_{x_16}+I_{x_17_a}+I_{x_18_a};$$

$$I_{y_tot_dep}=I_{y_3}+I_{y_7}+I_{y_8}+I_{y_9}+I_{y_10}+I_{y_11}+I_{y_12}+I_{y_13_a}+I_{y_13_b}+I_{y_13_c}+I_{y_14}+I_{y_15}+I_{y_16}+I_{y_17_a}+I_{y_18_a};$$

$$I_{z_tot_dep}=I_{z_3}+I_{z_7}+I_{z_8}+I_{z_9}+I_{z_10}+I_{z_11}+I_{z_12}+I_{z_13_a}+I_{z_13_b}+I_{z_13_c}+I_{z_14}+I_{z_15}+I_{z_16}+I_{z_17_a}+I_{z_18_a};$$

$$Moi=[I_{x_tot_u} \ I_{x_tot_dep}; \ I_{y_tot_u} \ I_{y_tot_dep}; \ I_{z_tot_u} \ I_{z_tot_dep}]$$

```

% gyrofilter.m
%Function who filters out most of the noise of the signals

function [y] = gyrofilter(data,t,x)

n = length(data);
s = 1/t; %samplingsrate
data=data/100; %gyrodata is in units of 100 m/s^2
y=[data(:,2), data(:,3), data(:,4)];

for j=2:n;
a=abs(y(j,1));
b=abs(y(j,2));
c=abs(y(j,3));

if (a<0.9 & b<0.9 & c<0.9)
y(j,1)=y(j,1);
y(j,2)=y(j,2);
y(j,3)=y(j,3);
else
y(j,1)=y(j-1,1);
y(j,2)=y(j-1,2);
y(j,3)=y(j-1,3);
end;
end;

for j=2:n;
a=abs(y(j,1) - y(j-1,1));
b=abs(y(j,2) - y(j-1,2));
c=abs(y(j,3) - y(j-1,3));

if (a+b)>0.9
y(j,1)=y(j-1,1);
y(j,2)=y(j-1,2);
y(j,3)=y(j-1,3);
end;
end;

tid=0:s:(n*s)-s;
figure
subplot(3,1,1), plot(tid(1:t*x),y(1:t*x,1),'-')
title('Boom 18, 130 cm long')
xlabel('time[s]')

```

```
ylabel('x-acc [m/s^2]')
subplot(3,1,2), plot(tid(1:t*x),y(1:t*x,2),'-')
xlabel('time[s]')
ylabel('y-acc [m/s^2]')
subplot(3,1,3), plot(tid(1:t*x),y(1:t*x,3),'-')
xlabel('time[s]')
ylabel('z-acc [m/s^2]')
```

```

% gyrofilter2.m
% Another filter. Does the job when the first one fails.

function [y ,tid]= testfilter(data,t, x)

n = length(data);
s = 1/t; %samplingsrate
data=data/100;
y=[data(:,2), data(:,3), data(:,4)];

for j=2:n;
a=abs(y(j,1));
b=abs(y(j,2));
c=abs(y(j,3));

if (a<0.9 & b<0.9 & c<0.9)
y(j,1)=y(j,1);
y(j,2)=y(j,2);
y(j,3)=y(j,3);
else
y(j,1)=y(j-1,1);
y(j,2)=y(j-1,2);
y(j,3)=y(j-1,3);
end;
end;

tid=0:s:(n*s)-s;
figure
subplot(3,1,1), plot(tid(1:t*x),y(1:t*x,1),'-')
title('Boom 14, 90 cm long')
xlabel('time[s]')
ylabel('x-acc [m/s^2]')
subplot(3,1,2), plot(tid(1:t*x),y(1:t*x,2),'-')
xlabel('time[s]')
ylabel('y-acc [m/s^2]')
subplot(3,1,3), plot(tid(1:t*x),y(1:t*x,3),'-')
xlabel('time[s]')
ylabel('z-acc [m/s^2]')

```

Appendix B

Application for parabolic campaign

B.1 Title of the experiment and Team name

Experiment: Gravity boom and antenna deployment for the Ncube satellite

Team name: Ncube

B.2 Experiment objectives

The goal of the experiment is to test the Ncube gravity boom and antenna deployment system in a controlled micro-g environment. This will confirm that the measuring tape is rigid enough to move the tip mass in space and also test the antenna deployment system under zero-g. NCube is a 10cm*10cm*10cm Pico satellite under construction by several Norwegian universities. The gravity boom is constructed of 1.5 meter measuring tape and a 40 gram lead tip-end. The movements of the satellite will be measured with 3-axis accelerometer and 3-axis gyros.

The gravity boom is part of NCubes attitude control system which goal is to achieve a accuracy of 20 b0 about nadir.

B.3 Experiment description

The measuring tape is coiled around the lead tip-mass and tightened with a fishing line. Nichrome wire is coiled around the fishing line. The boom is placed in a plastic box and mounted in the satellite. To deploy the boom, voltage is applied to the nichrome wire by a battery within the satellite and the fishing line is melted. The boom will then deploy due to the fact that the coiled measuring tape will act as a spring.

The experiment will be restrained be an Electromagnet and four ropes fastened to the satellite and anchored to the floor.

B.4 Technical description of the experiment set-up

Systems:

The main satellite consist of:

- Gravity boom system
- Antenna system
- 3-axis accelerometers and gyros
- Magnetic plate

The backup satellite consist of:

- Gravity boom system
- Antenna system
- Magnetic plate

The gravity boom system consist of:

- 1.5 meter Stanley measuring tape
- 40 gram lead tip-end
- fishing line
- nichrome wire
- plastic box (5cm*5cm*2cm)

The antenna system consist of:

- Antenna 1: 17 cm Stanley measuring tape
- Antenna 2: 40 cm Stanley measuring tape
- fishing line
- nichrome wire
- two plastic boxes (2cm*2cm*1cm)

The control panel consist of:

- Aluminium base plate
- Laptop
- Switch panel (Switch Electromagnet on/off, release boom/antennas)
- Emergency button
- Power supply

Satellite restraining system consist of:

- Aluminium base plate
- Electromagnet
- 4 ropes
- 3 nets (provided by Novespace (if not stated otherwise))

Two satellites will be constructed for redundancy. There will only be one measuring system in the main satellite so if that one fails there will only be visual results for the second satellite. 20 plastic boxes with measuring tape and tip-mass will be constructed. The boxes will be constructed in such a manner that it will be easy to change boxes. This will make it possible to replace a deployed boom with an undeployed boom between parabolas.

Design/Building/Testing

The design phase of the project was completed winter 2002 (for information and documents see www.rocketrange.no/ncube/) and the building is under way. The plastic boxes for the boom and antennas are constructed and are being mounted to the nadir side of the satellite. The satellite will undergo a balloon test at Andøya rocket range 13.06.03. Temperature and vibration tests will be completed before the balloon test.

B.5 Installation of the experiment in the aircraft

We request our experiment to be free floating because we need precise zero-g.

The satellite will be restrained by an electromagnet (EM) and 4 ropes to have control over it during the experiment. Our experiment will also be restrained by security

nets (see figure 4-7). The EM will be fastened to an aluminium plate between two rails (1006mm) with M10 screws.

The experiment will be controlled from the control board (see figure 2-4 for specification and location of the board). The control board will be made of aluminium and fastened to the rails with M10 screws.

During take-off the satellites and boom-boxes will be placed in 2 sportbags and strapped to the floor. Each sport bag will contain no more than 3 kg. (Each satellites mass is 1 kg and each boom-box mass is less than 100 gram. For two satellites and 20 boxes this gives at total max-mass of 4 kg).

B.6 Electrical

List of batteries (precise the type) and/or static converter (if applicable):

Danionics Li-ion polymer DLP485368

Confirm that the whole electrical circuits is fitted with one, and only one, emergency switch-off button (5 cm red pushbutton on yellow box, installed in a such way to be easily accessible by safety team) disconnecting all electrical equipment and 220V-AC and 28 V-DC power supply coming from aircraft electrical panel :

Yes

Confirm that the whole electrical circuit is protected by a fast fuse, adjusted to the experiment electrical consumption (8 A max for 220V-AC and 20 A max for 28 V-DC) :

Yes Fuse value(s) : 3A

Confirm that the whole electrical circuit is protected by ground fault interrupter adjusted at 30mA :

Yes

B.7 Mechanical resistance of the experiment

Demonstration of mechanical resistance for the restraining system

Part	Weight	Height of centre of gravity
Aluminium base plate	$m_1=4.3$ kg	$h_1=5$ mm
Electromagnet	$m_2=0.363$ kg	$h_2=27$ mm
Satellite	$m_3=1$ kg	$h_3=94$ mm

The plate is secured to the aircraft floor by 4 M10 screws

Total weight is then $m=5.663$ kg, and Total height of centre of gravity is $h=(4.3*5+0.363*27+1*94)/5.663=22.13$ mm

Shear force

on the attachment screws is then $F_c=(9*5.663*9.81)/4=125$

This gives a safety coefficient of $C=F_{max}/F_c=16250/176.6=130$

Traction force on the attachment screws

Distance between forward and rear attachment is; $d=101.6$ mm

Force on rear attachment, X is then: $X=(9*5.663*9.81*22.13)/101.6=108.9$ N

Then $X'=X/2=54.45$ N, and $F_t=54.45+14000=14054.45$ N

This gives a safety coefficient of $C=F_{tmax}/F_t=32940/14054.45=2.34$

Bending strength of uprights

$F_m=(9*5.663*9.81*22.13)/4=2766.2$ Nmm

Demonstration of mechanical resistance for the Control panel

Part	Weight	Height of centre of gravity
Aluminium base plate	$m_1=9.5$ kg	$h_1=5$ mm
Laptop	$m_2=3.2$ kg	$h_2=35$ mm
Power supply	$m_3=0.851$ kg	$h_3=37.5$ mm
Switch panel	$m_4=0.05$ kg	$h_4=15$ mm
Emergency stop	$m_5=0.130$ kg	$h_5=47.5$ mm

The plate is secured to the aircraft floor by 4 M10 screws

Total weight is then $m=13.01$ kg, and Total height of centre of gravity is $h=(9.5*5+3.2*35+0.851*37.5+0.05*15+0.130*47.5)/13.01=15.2$ mm

Shear force on the attachment screws

is then $F_c = (9 * 13.01 * 9.81) / 4 = 287.2$

This gives a safety coefficient of $C = F_{max} / F_c = 16250 / 287.2 = 56.6$

Traction force on the attachment screws

Distance between forward and rear attachment is; $d = 584.2 \text{ mm}$

Force on rear attachment, X is then: $X = (9 * 13.01 * 9.81 * 15.2) / 584.2 = 29.9 \text{ N}$

Then $X' = X / 2 = 14.95 \text{ N}$, and $F_t = 14.95 + 14000 = 14014.95 \text{ N}$

This gives a safety coefficient of $C = F_{tmax} / F_t = 32940 / 14014.95 = 2.35$

Bending strength of upright

$M_f = (9 * 13.01 * 9.81 * 15.2) / 4 = 4364.9 \text{ Nmm}$

B.8 In flight procedures and In flight personnel

The experiment will be conducted the following way: Before the first parabola the EM will be turned on and the satellite will be placed on it. In zero-g the EM will be turned off and the boom will be deployed. During the first deployment the antennas will also be deployed. Raw-data from the accelerometers and gyros will be logged to the laptop. The experiment will also be filmed (different boom-lengths will be used and the camera man will keep track of which boom is being recorded (either by voice or by a sheet with the boom length written on it)). Between parabolas the deployed boom is removed, stored in a sports bag, and a new box being connected to the satellite. The Em is then turned on and the satellite is placed on top if it. In the next zero-g phase the procedure is repeated. Since the boom should be deployed as close to zero-g as possible, the first parabolas should be used the “get familiar” with micro-g. This should give the “control officer” a better chance to deploy the boom at the right moment in the remaining parabolas.

	Executive control officer	Camera man
After take-off	Attach ropes to the satellite. Attach satellite to electromagnet.	
0-3 parabola	Familiarize with of micro/zero-g	
Zero-g (at each parabola)	Turn off electromagnet. Release gravity boom	Record deployment
Between parabolas	Change gravity boom. Turn on Em/connect satellite to Em. Store used boom in sportsbag	Log boom length
After last parabola	Store satellite in sportsbag	

B.9 Hazard analysis

- No dangerous products
- No pressure systems
- Nothing will happen in case of sudden depressurization
- No laser
- No motors
- Electrical wires shielded
- No electrostatic discharge
- If a power loss occurs the laptop will go blank and the electromagnet will be turned off. The satellite will be constrained by ropes and safety nets.
- Electro-magnetic fields will be generated by the electro magnet.
- The only hot part is the nichrome wire used to melt the fishing line
- The satellite include moving parts. The boom and the antennas. They are constrained by the Electromagnet, safety nets and ropes during deployment.
- No pump or oil

B.10 Pressure vessel certification (if applicable)

Any chamber, container, bottle with pressure should be proofed at 1.5 times the working pressure. Certificate by official authorities must be less than 5 years old.

Once selected :

Provide the pressure certificates of all pressure vessels/chambers, pressurized systems, manometers. For gas containers, indicate bottle (B1, B2, . . .) or chamber type and gas contained, working pressure and proofed pressure.

B.11 Vent line connection and other requests

Do you need to use the aircraft vent line (throwing experiments wastes out of aircraft)
No

Once selected please answer the following questions

What is the maximum temperature of exhausted products? :b0C

What is the maximum temperature of within the experiment? :b0C

Describe the way to control this temperature (automatic valves,):

What is the maximum resistance temperature of your exhaust pipe? :b0C

Tell if you have other specific requests:

B.12 Outreach section

During/After the campaign an article about the work will be published in the university paper (Under dusken).

After the campaign a news clip will most likely be showed on TV2 (one of three Norwegian commercial TV stations). The latter depends on whether our journalist gets the go ahead from his bosses.

B.13 Figures/Pictures

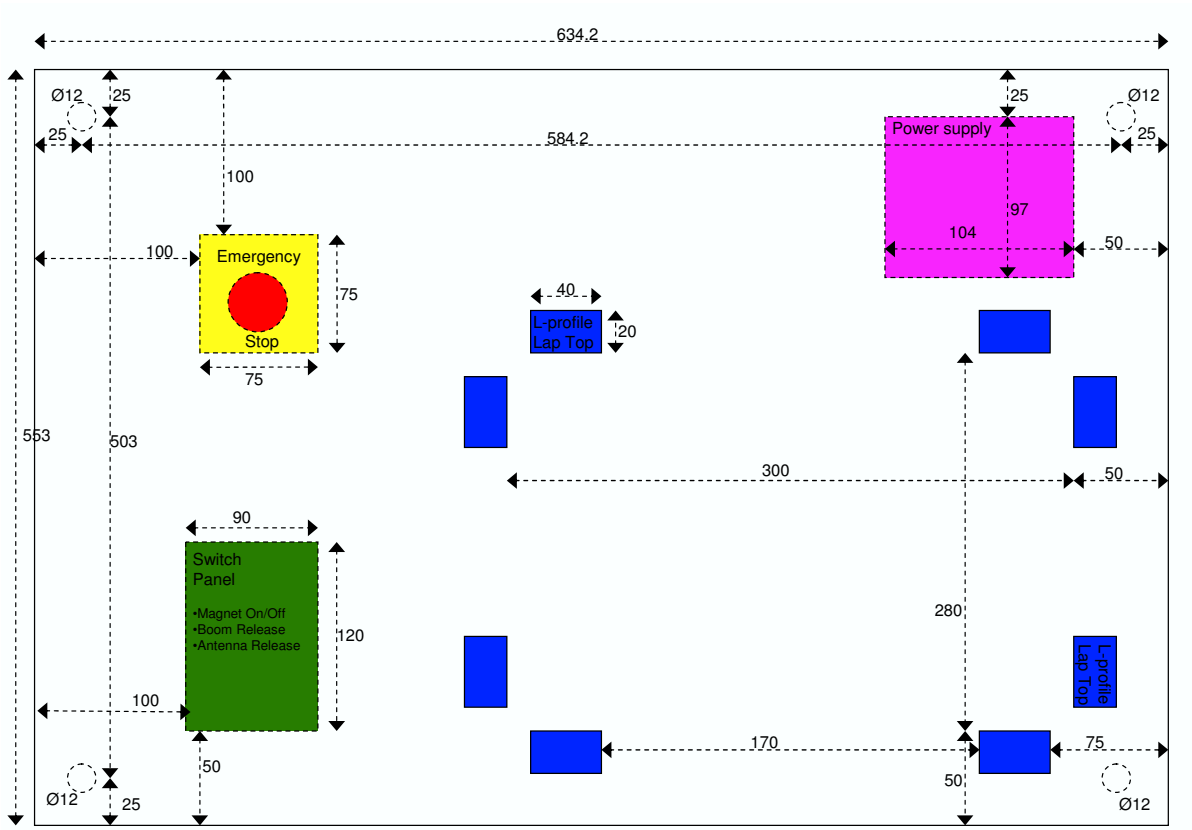


Figure B.1: Controlpanel

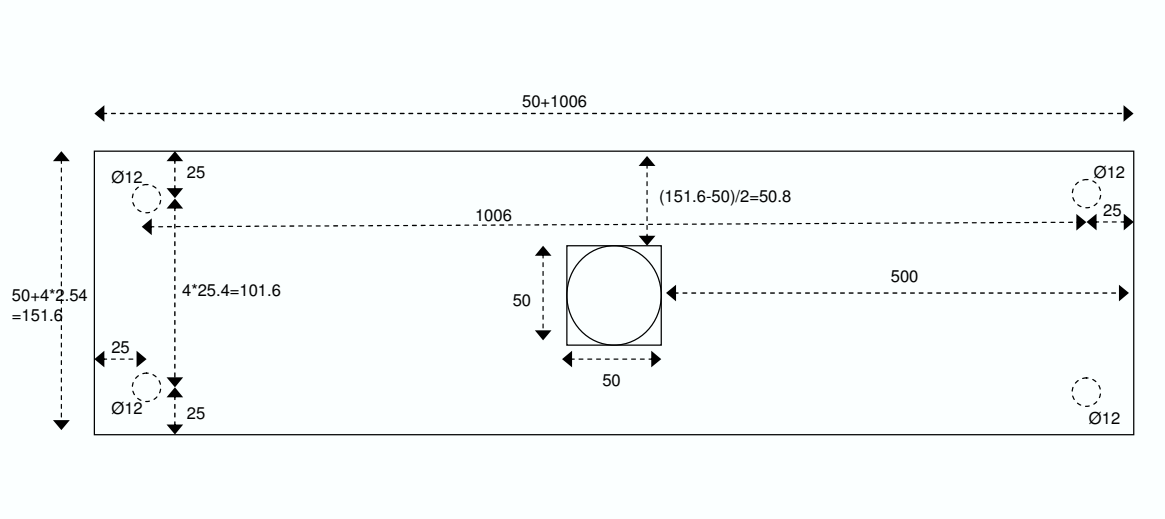
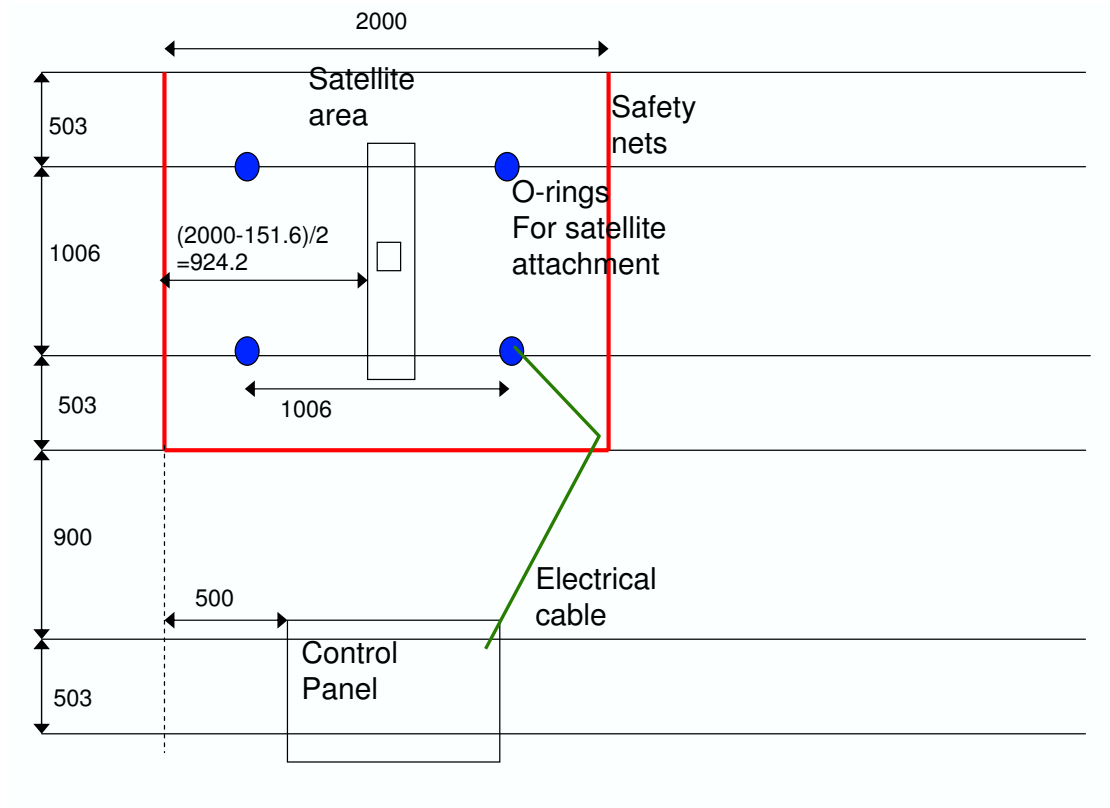


Figure B.2: Electromagnetpanel

Figure B.3: experiment area



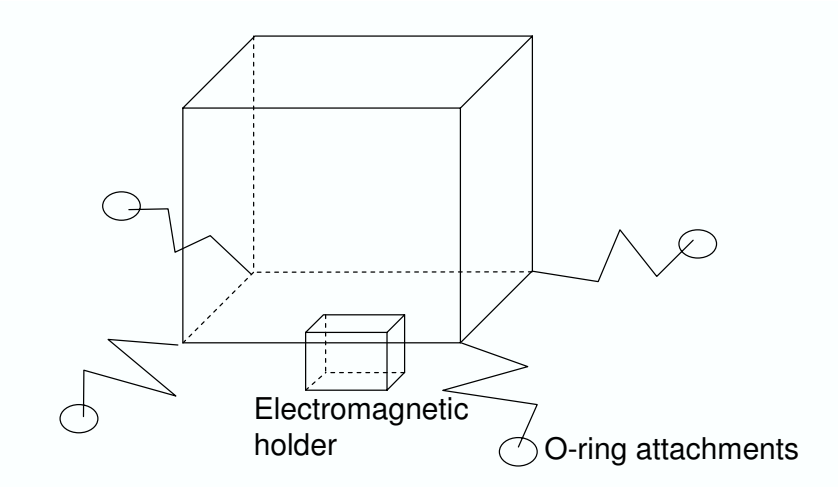


Figure B.4: satellite during 1.8g

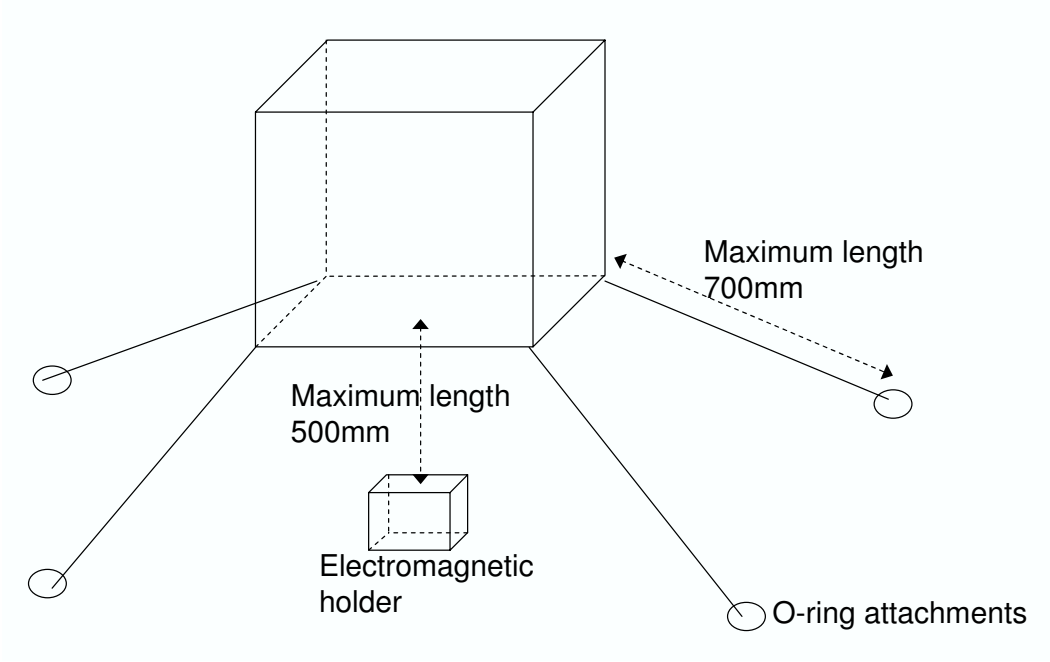


Figure B.5: satellite during zero-g

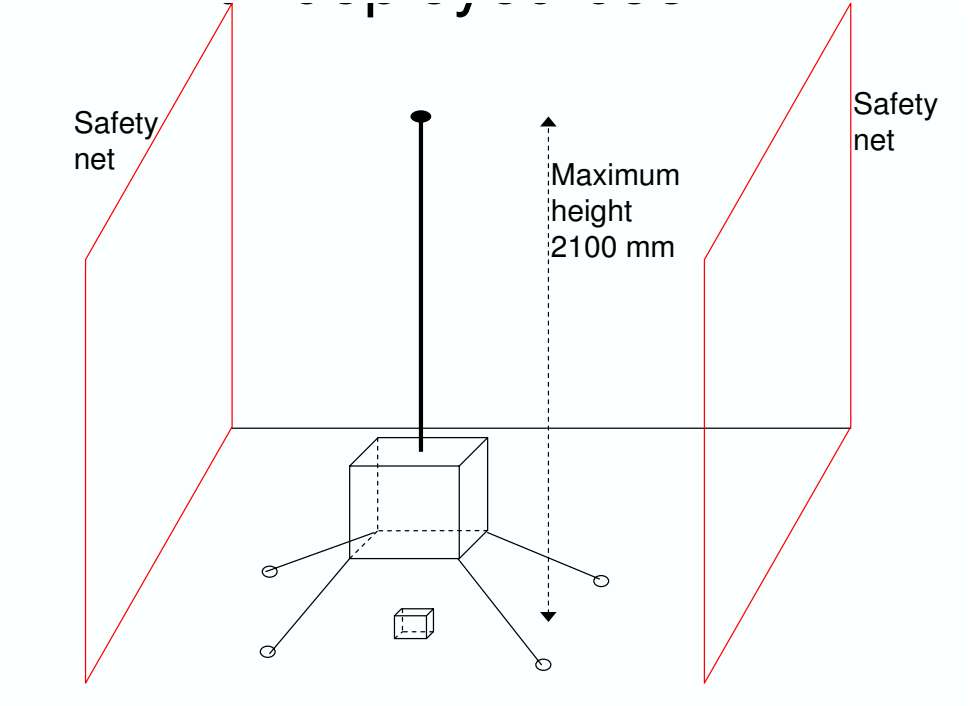


Figure B.6: satellite during zero-g with nets

Bibliography

[.]

- [1] Bergström, L. and A. Goobar (1999). *Cosmology and Particle Astrophysics*. Praxis Publishing Ltd, Chichester
- [2] Cederblad, H., Fasseland, J. and O. Nordin (2003). *Power supply*. Project report. HiN, Narvik.
- [3] Edwards, C. H. and D. E. Penny (1988). *Elementary Linear Algebra*. Prentice-Hall, Inc, New Jersey.
- [4] Edwards, C. H. and D. E. Penny (1994). *Calculus with Analytic Geometry. 4th ed.*. Prentice-Hall, Inc, New Jersey.
- [5] Edwards, C. H. and D. E. Penny (1996). *Differential Equations and Boundary Value Problems*. Prentice-Hall, Inc, New Jersey.
- [6] Egeland, O. (1993). *Servoteknikk*. Tapir Forlag, Trondheim.
- [7] Egeland, O. (1994). *NISSE Attitude Control and Determination System*. Project No 481757.00. SINTEF Automatic Control, Trondheim.
- [8] Egeland, O. and J. T. Gravdahl. (2001). *Modeling and Simulation for Control*. Department of Engineering Cybernetics, NTNU, Trondheim.
- [9] Farrell, J. A. and M. Barth (1999). *The Global Positioning System & Inertial Navigation*. McGraw-Hill Companies, Inc.
- [10] Fauske, K. M (2002). *Modeling and Control of Attitude for NCube*. Project report, Department of Engineering Cybernetics, NTNU, Trondheim.
- [11] Fossen, T. I. (1998). *Matematiske Modeller for Styring av Fly og Satelitter*. Report No 98-4-W. Department of Engineering Cybernetics, NTNU, Trondheim.
- [12] Fossen, T. I. (2001). *Matlab GNC Toolbox*. Marine Cybernetics, Trondheim.
- [13] Fossen, T. I. (2002). *Marine Control Systems*. Marine Cybernetics, Trondheim.
- [14] Furebotten, P.E. (2002). *AIS reciever as payload in NCube*. Project report, Department of telecommunications, NTNU, Trondheim.
- [15] Goldstein, H., C. Poole and J. Safko (2002). *Classical Mechanics. 3rd ed.*. Addison Westley.

- [16] Hughes, P. C. (1986). *Spacecraft Attitude Dynamics*. Jhon Wiley & Sons, Inc.
- [17] Indergaard, F. M. (2002). *Modeling and analysis/design of gravityboom for NCube*. Project report, Department of Engineering Cybernetics, NTNU, Trondheim.
- [18] Mansfield, M. and C O'Sullivan (1998). *Understanding Physics*. Praxis Publishing Ltd, Chichester.
- [19] Nilsson, J. W. and J. W. Nilsson (1996). *Electric Circuits. 5th ed.* Addison-Wesley, Reading, Massachusetts.
- [20] Ottestad, J. (2002). *Antenna system for NCUBE*. Project report, Department of telecommunications, NTNU, Trondheim.
- [21] Sciavicco, L. and B. Siciliano (2002). *Modelling and Control of Robot Manipulators*. Springer-Verlag, London.
- [22] Shepperd, S. W. (1978). Quaternion from Rotation Matrix. *Journal og Guidance and Control*. **Vol. 1(3)**, 223-224.
- [23] Slotine, J. E. and W. Li. (1991). *Applied Nonlinear Control*. Prentice-Hall, Inc, New Jersey.
- [24] Soglo, P. K. (1994). *3-axis Stabilization of Satellite Using Gravity Gradient and Magnetotorquers*. Doctor thesis, NTNU, Trondheim.
- [25] Svartveit, K. (2002). *Modeling, Sensors, Actuators and Attitude Determination for NCube*. Project report. Department of Engineering Cybernetics, NTNU, Trondheim,
- [26] Zeilik, M. and A. Gregory (1998). *Introductory Astronomy & Astrophysics*. 4th ed.. Saunders Collage Publishing, Orlando, Florida.